APPLIED COMPUTER SCIENCE

The Journal is a peer-reviewed, international, multidisciplinary journal covering a broad spectrum of topics of computer application in production engineering, technology, management and economy.

The main purpose of Applied Computer Science is to publish the results of cutting-edge research advancing the concepts, theories and implementation of novel solutions in computer technology. Papers presenting original research results related to applications of computer technology in production engineering, management, economy and technology are welcomed.

We welcome original papers written in English. The Journal also publishes technical briefs, discussions of previously published papers, book reviews, and editorials. Especially we welcome papers which deals with the problem of computer applications in such areas as:

- manufacturing,
- engineering,
- technology,
- designing,
- organization,
- management,
- economics,
- innovations,
- competitiveness,
- quality and costs.

The Journal is published quarterly and is indexed in: BazTech, Cabell's Directory, CNKI Scholar (China National Knowledge Infrastucture), ERIH PLUS, Google Scholar, Index Copernicus, J-Gate, Scopus, TEMA Technik und Management.

Letters to the Editor-in-Chief or Editorial Secretary are highly encouraged.

CONTENTS

Applied Computer Science, vol. 16, no. 3, pp. 5–15
doi:10.23743/acs-2020-17

Submitted: 2019-10-12
Revised: 2019-11-25
Accepted: 2020-09-07

Deep Neural Network, unlabeled dataset,
Just-In-Time defect prediction, unsupervised prediction

Saleh ALBAHLI[*]

A DEEP ENSEMBLE LEARNING METHOD FOR EFFORT-AWARE JUST-IN-TIME DEFECT PREDICTION

Abstract

Since the introduction of Just-in-Time effort aware defect prediction, many researchers are focusing on evaluating the different learning methods for defect prediction. To predict the changes that are defect-inducing, it is important for learning model to consider the nature of the dataset, its imbalance properties and the correlation between different attributes. In this paper, we evaluated the importance of dataset properties, and proposed a novel methodology for learning the effort aware just-in-time defect prediction model. We form an ensemble classifier, which consider the output of three individuals classifier i.e. Random forest, XGBoost and Deep Neural Network. Our proposed methodology shows better performance with 77% accuracy on sample dataset and 81% accuracy on different dataset.

1. INTRODUCTION

Reducing the number of failures in a software is important in order to produce the quality product. During software development, a software goes through many changes, and these changes are needed to be defect and error free. Since the introduction of Effort aware Just-in-Time (JIT) prediction by Mockus et al. (Mockus & Weiss, 2000), it is highly studied model for the better error detection mechanism. Mockus and Weiss used numerous change metrics for the prediction of the probability that the change will induce any defect in software instead of going through the lines of codes.

[*] Qassim University, College of Computer, Department of Information Technology, Saudi Arabia, 51452, Qassim, salbahli@qu.edu.sa

JIT defect prediction is of major practical value compared with conventional defect predictions at module. The JIT was coined by the Kamei et al. (Kamei et al., 2012) who put forward a method of checking the error based on raw metric which not only predicts the error out from the line of code under inspection, but also highlights the latent defect which can be detected at the check in time unlike other effort aware detection method (Zhou, Sun, Xia, Li & Chen, 2019). This method also reduces the tedious task of finding the author of the code as many people are involved over a module and doing the inspection at the check in time, where the change details are still being investigated, help make the debug very easy.

Much work is available on the JIT effort aware system using the file, package or method level for the defect prediction. However, there is still the need to accurately predict the defect using supervised, unsupervised and deep learning methods (Yu, Wen, Han & Hayes, 2018). In this paper, we proposed a novel methodology for the prediction of defects using the publicly available dataset for training few learning methods, and later we ensemble the output of each classifier to provide the final target prediction. In our proposed model, we used ensemble method classification utilizing random forest, XGBoost and deep neural network for model training. Therefore, our model try to take into account of the abstract features by using the deep ensemble technique, XGBoost and Random Forest, making it more robust and outperform the models available.

The rest of the paper is organized as follows. Section 2 review the existing techniques related to the effort aware JIT defect prediction. Proposed methodology is explained in detail in Section 3 followed by Experimental evaluation and result with discussion in section 4. Section 5 conclude the paper and state the possible future direction.

2. LITERATURE REVIEW

Effort-aware JIT defect prediction ranks the source code based on the probability of the defects and the effort to examine such variations. Effective and efficient defect prediction and detection algorithms help to find the defects accurately and, in less time with small effort. Such effort-aware models often help to allocate the software quality assurance tasks like code reviews and testing. Qiao et al., (Qiao & Wang, 2019) proposed a deep learning approach for the effort-aware JIT defect prediction. They used neural network and deep learning approach for the useful feature selection. They used ten numerical metrices of code changes and feed them to neural network to predict the presence of bug in the code change under review. They rank the code changes according to the benefit cost ratio, which is calculate beforehand by diving the likelihood of each code change by its size.

Yang et al. (Yang et al., 2016), state that many unsupervised effort aware JIT prediction models performs better than the state-of-the-art supervisor modes. They used only those prediction model that have a good scalability and low

application cost (i.e. metrices modelling cost and collection cost). It put forward the idea of using the unsupervised learning technique and highlighted that building the prediction models do not need defected data for unsupervised model, as a consequence, incur a low building cost and a high application range (Liu, Yang, Xia, Yan & Zhang, 2018). Therefore, it would be more fitting for users to use unsupervised models in effort-aware JIT defect prediction especially when defect-inducing changes can be predicted well. In general, unsupervised models aggregate similar data-points and performs the modelling. Thus, the model has to develop and train effectively to automatically identify on its own to figure out information. It primarily deals with the unlabeled data.

There are many bug prediction models built with the historical metrices. Many studies have targeted coarse-grained (file and packages level) prediction. Hata et al., (Hata, Mizuno & Kikuno, 2012) stated that fine-grained prediction is challenges because it needs method level histories of existing version control system. They tackle the mentioned problem and developed a fine-grained prediction version control system and proved that fine-grained performs better than the coarse-grained prediction. On the other hand, Kamei et al. (Kamei et al., 2012), claim that the common finding in literature say that package level prediction normally outperforms fine-level predictions, does not hold true when the effort is considered. They show that package level prediction can be improved when file level prediction is performed and then lifting them on the package level instead of just collecting all the metrices at the package level.

Kamie et al., (Kamei, Matsumoto, Monden, Matsumoto, Adams & Hassan, 2010) stated that defect detection from file or package level is very time consuming and it makes the approach very ineffective for large software systems. They proved that instead of using file and package level for defect prediction, we should identify defect-prone software changes. The conducted large-scale study on six open source projects and 6 open source projects, shows the 68% average accuracy with 64% average recall for the proposed system. Only 20% of effort is needed to review the changes, and 35% of all defect-inducing changes were identified. This proposed model provides effort-reducing way to handle the risky changes and minimize the cost for the development of high-quality software.

The existing literature mainly focuses effort-aware JIT prediction using the data extracted based on developer and using the unsupervised models that aggregated the similar data-point to perform the modelling. In contrast to previous work, we focus on using the deep learning ensembling techniques for the defect prediction. Later, implementing Deep ensembling using the XGboost, Random Forest and Deep neural network and then averaging their output.

3. PROPOSED METHODOLOGY

In this paper, we proposed a methodology for effort aware just-in-time prediction using the ensemble method. Instead of using only supervised or unsupervised method for classification, we proposed to use the combination of deep learning method, supervised methods for the classification task. As shown in Figure 1, for this task, we used various multiple learning algorithms including deep neural network, XGBoost and Random Forest. Deep neural network can map the input data to the given labelled dataset representing the non-linear relationship. Unlike most conventional machine learning algorithm, deep neural network can detect the feature automatically without the human intervention. For DNN optimization, we used ADAM (adaptive moment estimation) optimization algorithm. It updates model weight iteratively based on the training data. We used the following parameter setting for ADAM optimization:

- *Learning Rate* = 0.001,
- *Decay Rate* = 0.9,
- *Exponential Decay Rate* = 2.099.

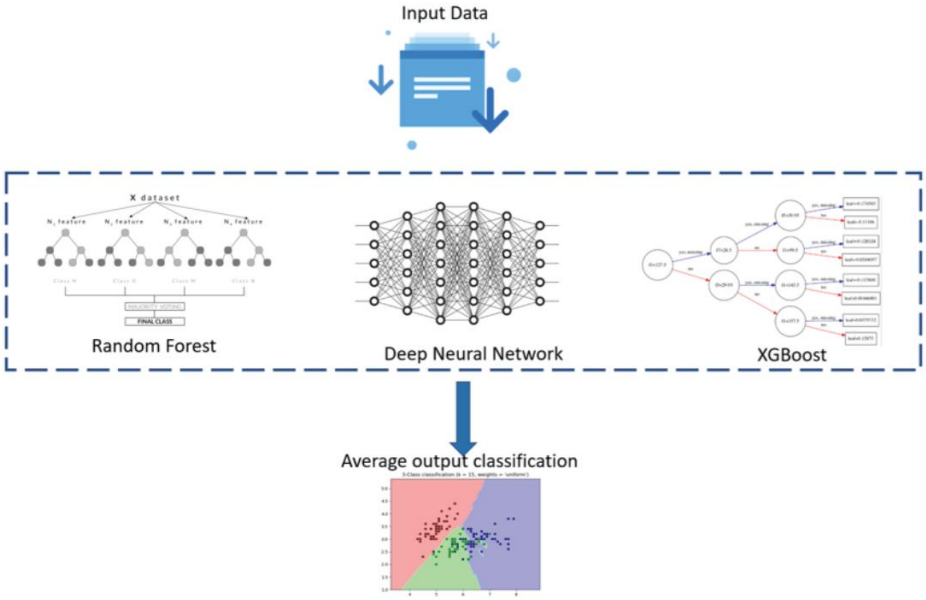

Fig. 1. Proposed Methodology: Effort aware just-in-time prediction using deep ensemble method

XGBoost (Chen & Guestrin, 2016) was initially developed with deep consideration of system optimization and principles in machine learning. The objective function *f* is:

$$\text{obj} = \sum_{i=1}^{n} l\left(y_i, \hat{y}_i^{(t)}\right) + \sum_{i=1}^{t} \Omega(f_i) \quad (1)$$

Note that this objective function should contain training loss and regularization. XGBoost complexity is defined as:

$$\Omega(f) = \gamma T + \frac{1}{2}\lambda \sum_{j=1}^{T} \omega_j^2 \quad (2)$$

Random forest contains many decision tree, and the prediction of each decision tree is considered and the class with the most votes is selected as the predicted class.

For the proposed methodology, we implemented deep ensembling used the above mentioned three classification mechanism, and later average the given output to get the final output.

4. EXPERIMENTAL EVALUATION

4.1. Dataset

The proposed methodology is evaluated on the publicly available dataset (Kamei et al., 2012) which was created by collecting information from the csv repositories with the corresponding bug reports of six large open source projects and five large commercial projects. Open source projects were Bugzilla, Mozilla, Eclipse JDT, Columba, PostgresSQL, Eclipse platform. The data for the Bugzilla and Mozilla were obtained from the MSR 2007 Mine Challenge. The data for Columba were gathered from the official CVS repository. Table 1 summarizes the statistic of dataset.

Tab. 1. Statistic of the projects included in the dataset (Kamei et al., 2012)

	Period	The total number of changes	Average LOC		# of modified files per change	# of changes per day	# dev. per file	
			File	Change			Max.	Avg.
Bugzilla	08/1998 – 12/2006	4.62 (36%)	389.8	37.5	2.3	1.5	37	8.4
Columba	11/2002 – 07/2006	4.46 (31%)	125.0	149.4	6.2	3.3	10	1.6
Eclipse JDT	05/2001 – 12/2007	35.38 (14%)	260.1	71.4	4.3	14.7	19	4.0
Eclipse Platform	05/2001 – 12/2007	64.25 (14%)	231.6	72.2	4.3	26.7	28	2.8
Mozilla	01/2000 – 10/2006	98.28 (5%)	360.2	106.5	5.3	38.9	155	6.4
PostgresSQL	07/1996 – 05/2010	20.43 (25%)	563.0	101.3	4.5	4.0	20	4.0
OSS-Median	–	27.91 20%	310.1	86.7	4.4	9.4	24	4.0
C-1	10/2020 – 12/2009	4.10	–	6.4	2.0	1.2	–	–
C-2	10/2020 – 12/2009	9.28	–	19.2	2.4	2.8	–	–
C-3	07/2002 – 12/2009	3.59	–	16.6	2.0	1.3	–	–
C-4	12/2003 – 12/2009	5.18	–	12.9	1.8	2.4	–	–
C-5	10/1982 – 12/1995	10.96	303.0	39.0	4.8	2.3	–	–
COM-Median	–	5.18	–	16.6	2.0	2.3	–	–

[*] *The percentage in brackets shows the percentage of defect-inducting changes to all changes*

This dataset is imbalanced hence it greatly affects the sensitivity of the model. The learning pattern is also distributed. If the imbalanced data is not dealt perfectly, then the model will only learn to distinguish one class with major number of instances. Hence, it makes the model to predict output for one class more over other class and in that case the biasedness will follow up. It will exhibit higher accuracy but will not be a right model. It may also be noted that accuracy metric does not help us get the right metric for the measure of the accuracy but F1 score, p score and recall followed by specificity and sensitivity are the right metric to measure the performance.

4.2. Result and Discussion

For evaluation we used the 10 cross fold validation for the performance testing of different unsupervised models. As shown in Figure 2, the correlation between different attributes is imbalanced, in order to handle the imbalanced data, we obtain the balance between two classes. The improved correlation between attributes is obtained by applying normalization on the attributes.

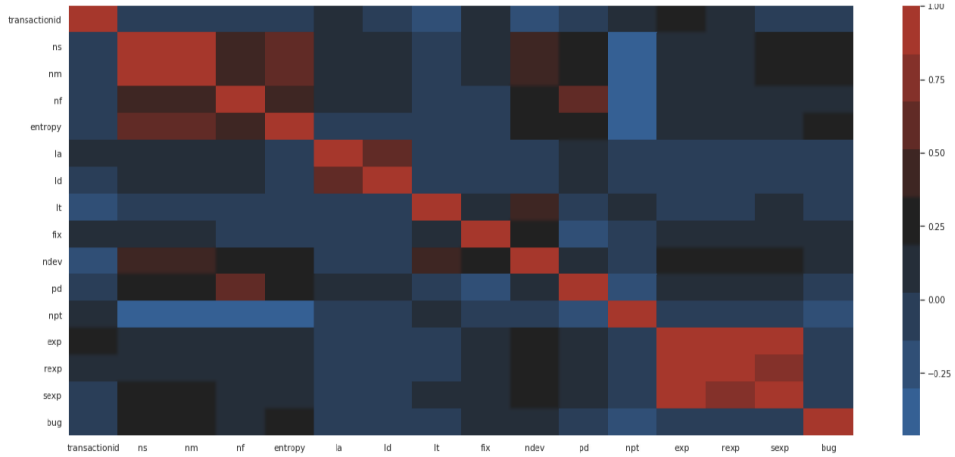

Fig. 2. Imbalance correlation matrix of attributes

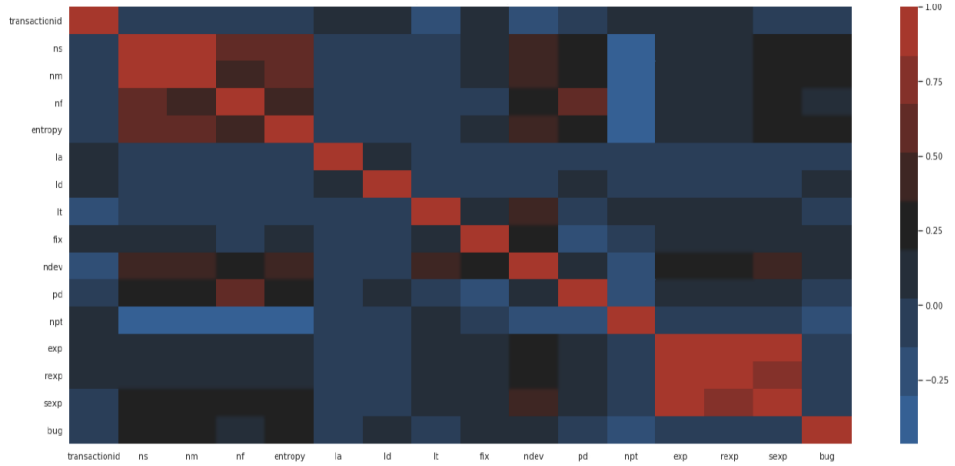

Fig. 3. Subsample correlation matrix of attributes

The current dataset which can create bottleneck at the time of learning. These outliers are needed to be dealt properly or we can discard them to make the distribution in the dataset even. Checking the dataset distribution with the target and we see that there are too many outliers and they can create a bottleneck when it comes to pattern learning. So, they must be dealt with properly else discarded.

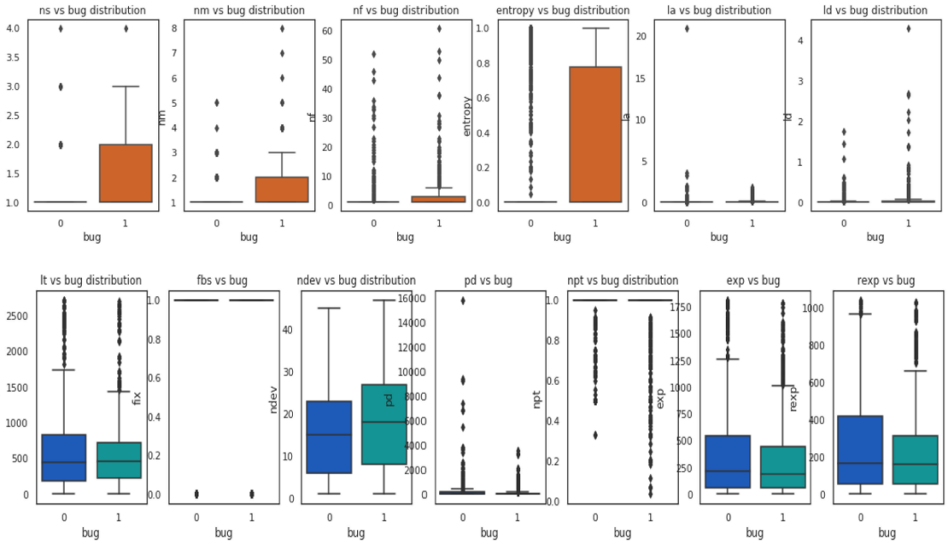

Fig. 4. Distribution of dataset

Figure 5 shows the distribution of three unsupervised model i.e. exp, rexp and sexp with the target. All these three attributes show maximum correlation with the target as compared to the rest of the attributes like npt, pd, ndev, fbs etc.

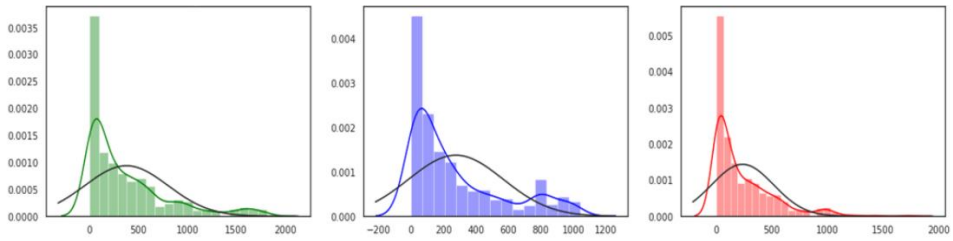

Fig. 5. Distribution of exp, rexp and sexp with the target

In Table 2, we report the performance of deep neural network along with other supervised and unsupervised learning methods. For performance reporting, we used the following measures: accuracy, p-score, f1-score, sensitivity and specificity. According to our evaluation, Random forest followed by XGBoost outperforms other classification methods and shows 71% accuracy. In general, supervised models outperforms unsupervised models when we have labelled data and the dataset is large for model training. This table also report results on across project cross validation using different dataset. In both cases high sensitivity and specificity is observed for all learning methods.

Tab. 2. Performance of different supervised, unsupervised and deep learning methods

MODEL	Acc	P-score	F1-score	Sensitivity	Specificity	Acc2	P-score2	F1-score2	Sensitivity2	Specificity2
Log. Reg.	0.6550	0.6714	0.6714	0.6368	0.6714	0.6303	0.4237	0.4911	0.7805	0.4237
SVM linear	0.6550	0.6551	0.6877	0.6547	0.6551	0.5833	0.3897	0.4768	0.7727	0.3897
SVM RBF	0.4725	0.4000	0.0186	0.4734	0.4000	0.6942	0.4000	0.0029	0.6946	0.4000
Naive Bayes	0.5775	0.5597	0.6943	0.6842	0.5597	0.6828	0.4726	0.3885	0.7398	0.4726
J48	0.6600	0.6813	0.6714	0.6377	0.6813	0.6823	0.4571	0.2893	0.7194	0.4571
Rand. Forest	0.7100	0.7701	0.6979	0.6637	0.7701	0.6754	0.4519	0.3561	0.7308	0.4519
AdaBoost	0.6900	0.7171	0.6633	0.6960	0.6633	0.6808	0.4760	0.4605	0.7628	0.4760
XGBoost	0.7000	0.7393	0.6984	0.6650	0.7393	0.6823	0.4571	0.2893	0.7194	0.4571
DNN	0.6275	0.6177	0.6823	0.6453	0.6177	0.5322	0.3289	0.4001	0.7156	0.3289
KMeans	0.4775	1.000	0.0094	0.4761	1.0000	0.6962	0.5178	0.1463	0.7057	0.5178

Yang et al. (Yang et al., 2016), state the importance of using unsupervised model instead of supervised model for learning. In their paper, they proposed the removal of highly correlated attributes by computing the reciprocal of raw metric and discarding the LA and LD, helps in ranking the values in descending order. However, considering the availability of enough training data and the presence of highly correlated attribute with target value supervised learning is the better option. On the other hand, when the labelled dataset is not available, choosing the unsupervised learning is the considerable option. In our proposed approach, we used abstract features in contrast to the use of LA and LD as proposed by Yang et al. (Yang et al., 2016), and the use of ensemble classification methods of three supervised learning method, deep Neural Network, XGBoost and Random forest performs better as compared to the stateof-the-art results. Table 3 shows the performance of our proposed methodology on sample and across different dataset. Our proposed methodology does not only perform better on the sample dataset but also shows better accuracy on different dataset with the accuracy of 81.85%.

Tab. 3. Performance on sample and different dataset

	Accuracy	P-score	F1-score	Sensitivity	Specificity
Sample Dataset	0.7739	0.7842	0.7546	0.7798	0.7842
Different Dataset	0.8185	0.7993	0.5860	0.8162	0.7993

Practically, there is no optimal approach which can meet all potential scenarios. Therefore, the unsupervised learning is a great way of learning when the labelled data is not applied but the Effort-aware JIT seems to be outperformed by the state of the art supervised model.

Yang et al. (Yang et al., 2016)model doesn't hold true for all the attributes as LA and LD had to be not taken into consideration. Our approach tries to take into account of the abstract features by using the deep ensemble technique and XGBoost and Random Forest, making it more robust and outperform all the models available. Yang paper (Yang et al., 2016) greatly highlights the use of unsupervised model and validates the importance of having the unsupervised model, their methodology of computing the reciprocal of raw metric and excluding the LA and LD and then removing the highly correlated help rank the values obtained in descending order (Huang, Xia & Lo, 2019). However, whilst observing the correlation with the target value and availability of sufficient data, it becomes obvious to opt for the supervised model. The supervised model XGBoost outperforms all the model in all aspects with high sensitive score.

Whilst using the model for Cross Validation Across Project, we observe the same trend for the classification model performance. The accuracy and all other metric performed well but XGBoost performed across all the models in both local and global models scenario.

5. CONCLUSIONS AND FUTURE WORK

Effort-aware Just-in-Time (JIT) defect prediction helps projects teams to allocate limited resources to the defect-prone software modules efficiently and accurately. Many machine learning and data mining approaches are used to detect and predict these defect inducing changes. However, the performance of these learning mechanism is highly dependent on the data that is used to train the model. In this paper, we proposed a novel methodology for effort aware just in time prediction for sample dataset and different dataset using different supervised and unsupervised learning methods. Our experiment concluded that unsupervised model have a very high degree of specificity and sensitivity both on current data and across project dataset. Unsupervised model are great but state of the art supervised model outperforms the unsupervised model on two context, when the data are labelled and the data is suffice enough. Specifically, Our results show that considering the performance of a single classifier, Random forest and XGBoost performs better than the other state-of-the-art methods. In addition, 77% accuracy is achieved by ensembling the output of three classifiers, i.e. Random Forest, XGBoost and Deep Neural Network for the sample dataset. We evaluate our proposed methodology only on the project that are publicly available, in future we can evaluate the result of our proposed methodology on closed source software projects.

Data Availability

The experiment uses public dataset shared by Kamei et al (Kamei et al., 2012), and they have already published the download address of the dataset in their paper.

REFERENCES

Chen, T., & Guestrin, C. (2016). Xgboost: A scalable tree boosting system. In *Proceedings of the 22nd acm sigkdd international conference on knowledge discovery and data mining* (pp. 785–794). ACM. https://doi.org/10.1145/2939672.2939785

Hata, H., Mizuno, O., & Kikuno, T. (2012). Bug prediction based on fine-grained module histories. In *Proceedings of the 34th International Conference on Software Engineering* (pp. 200–210). IEEE Press.

Huang, Q., Xia, X., & Lo, D. (2019). Revisiting supervised and unsupervised models for effort-aware just-in-time defect prediction. *Empirical Software Engineering*, *24*(5), 2823–2862. https://doi.org/10.1007/s10664-018-9661-2

Kamei, Y., Matsumoto, S., Monden, A., Matsumoto, K.I., Adams, B., & Hassan, A. E. (2010). Revisiting common bug prediction findings using effort-aware models. In *2010 IEEE International Conference on Software Maintenance* (pp. 1–10). IEEE. https://doi.org/10.1109/ICSM.2010.5609530

Kamei, Y., Shihab, E., Adams, B., Hassan, A.E., Mockus, A., Sinha, A., & Ubayashi, N. (2012). A large-scale empirical study of just-in-time quality assurance. *IEEE Transactions on Software Engineering*, *39*(6), 57–773. http://doi.org/10.1109/TSE.2012.70

Liu, C., Yang, D., Xia, X., Yan, M., & Zhang, X. (2018). Cross-Project Change-Proneness Prediction. In *2018 IEEE 42nd Annual Computer Software and Applications Conference (COMPSAC)* (Vol. 1, pp. 64–73). IEEE.

Mockus, A., & Weiss, D.M. (2000). Predicting risk of software changes. *Bell Labs Technical Journal*, *5*(2), 169–180.

Qiao, L., & Wang, Y. (2019). Effort-aware and just-in-time defect prediction with neural network. *PloS one*, *14*(2), e0211359. https://doi.org/10.1371/journal.pone.0211359

Yang, Y., Zhou, Y., Liu, J., Zhao, Y., Lu, H., Xu, L., ... & Leung, H. (2016). Effort-aware just-in-time defect prediction: simple unsupervised models could be better than supervised models. In *Proceedings of the 2016 24th ACM SIGSOFT International Symposium on Foundations of Software Engineering* (pp. 157–168). ACM. https://doi.org/10.1145/2950290.2950353

Yu, T., Wen, W., Han, X., & Hayes, J. (2018). ConPredictor: Concurrency Defect Prediction in Real-World Applications. *IEEE Transactions on Software Engineering*, *45*(6), 558–575. https://doi.org/10.1109/TSE.2018.2791521

Zhou, T., Sun, X., Xia, X., Li, B., & Chen, X. (2019). Improving defect prediction with deep forest. *Information and Software Technology*, *114*, 204–216. https://doi.org/10.1016/j.infsof.2019.07.003

Applied Computer Science, vol. 16, no. 3, pp. 16–29
doi:10.23743/acs-2020-18

Submitted: 2020-08-07
Revised: 2020-09-04
Accepted: 2020-09-21

Vibration Energy Harvesting, Impact Analysis, Diesel engine

Jacek CABAN [0000-0002-7546-8703]*, *Grzegorz LITAK* [0000-0002-9647-8345]*,
Bartłomiej AMBROŻKIEWICZ [0000-0002-8288-5230]*,
Leszek GARDYŃSKI [0000-0002-4162-179X]*,
Paweł STĄCZEK [0000-0003-0906-7917]*,
Piotr WOLSZCZAK [0000-0001-8603-4647]*

IMPACT-BASED PIEZOELECTRIC ENERGY HARVESTING SYSTEM EXCITED FROM DIESEL ENGINE SUSPENSION

Abstract

Vibration energy harvesting systems are using real ambient sources of vibration excitation. In our paper, we study the dynamical voltage response of the piezoelectric vibrational energy harvesting system (PVEHs) with a mechanical resonator possessing an amplitude limiter. The PVEHs consist of the cantilever beam with a piezoelectric patch. The proposed system was subjected to the inertial excitation from the engine suspension. Impacts of the beam resonator are useful to increase of system's frequency transition band. The suitable simulations of the resonator and piezoelectric transducer are performed by using measured signal from the engine suspension. Voltage outputs of linear (without amplitude limiter) and nonlinear harvesters were compared indicating better efficiency of the nonlinear design.

1. INTRODUCTION

In the last decade, the research interest in vibrational energy harvesting systems (VEHs) has been growing rapidly for applications with small power consumption, mainly in miniaturized electronics, wireless autonomous sensors used in medical and health monitoring, structural health monitoring, or smart buildings.

* Lublin University of Technology, Faculty of Mechanical Engineering, Nadbystrzycka 36, 20-618 Lublin, Poland, j.caban@pollub.pl, g.litak@pollub.pl, b.ambrozkiewicz@pollub.pl, l.gardynski@pollub.pl, p.staczek@pollub.pl, p.wolszczak@pollub.pl

In particular, self-powered sensors can use the information of any engineering or physical phenomena represented in the signal in the corresponding time series (Smutny, Nohal, Vukusicova & Seelmann, 2018). In the auto-motive sector, numerous methods can be applied to the measured signal in the time domain (Figlus, Szafraniec & Skrucany, 2019). Commercial solutions for energy harvesting from mechanical vibrations are offered in the frame of an intensively developing industrial Internet of Things (IoT). The electrical energy converted from ambient mechanical vibrations can be scavenged from different sources such as forced excitation in seismic and acoustic motions, random or periodic vibrations from sea waves, or vehicle motion. In order to obtain the highest voltage output of the system, the EH design should be adapted to the characteristic frequency of excitation causing operation at the resonant frequency. An alternative approach is to use the frequency broadband effect, namely the system can operate in a wider range of frequencies. At that time, the efficiency is admittedly lower, comparing to the peak resonance output, but the system operates constantly in variable conditions. The obtained output voltage provides a reasonable power supply for the autonomous sensor. On the other hand, the studied Diesel engine and its suspension are typically situated in an environment where energy is available for harvesting.

In the group of VEHs, we can specify electromagnetic (Tan, Dong & Wang, 2017; Ambrożkiewicz, Litak & Wolszczak, 2020), electrostatic (Zhang et al. 2018), and piezoelectric systems (Al-Yafeai, Darabseh & Mourad, 2020; Mieczkowski, Borawski & Szpica, 2019; Koszewnik, 2019, 2020) and their hybrid solutions. In our paper, we focus on the piezoelectric EHs, in which the piezoelectric effect is applied. In piezo-based EH systems obtained voltage output depends on the applied mechanical stress (direct piezoelectric effect). In Figure 1, the general scheme and functional principle of the piezoelectric VEH system are presented (Erturk, Hoffman & Inman, 2009; Litak, Friswell & Adhikari, 2010).

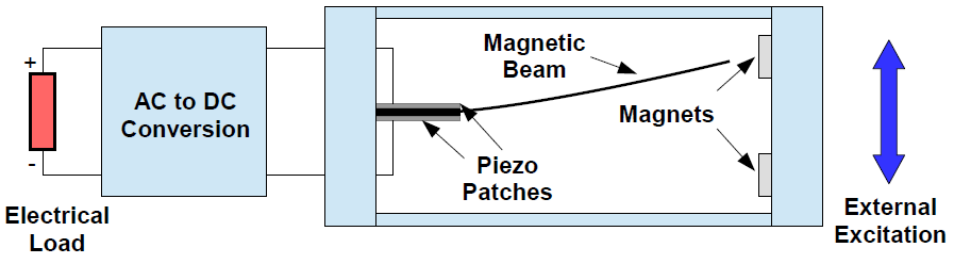

Fig. 1. Scheme of piezoelectric vibrational energy harvesting system based on cantilever beam

On the other hand, the rapid development of the automotive industry and changing into green technology in form of Electric Vehicles (EV) (Łukjanow & Zieliński, 2016; Skrucany, Kendra, Stopka, Milojevic, Figlus & Csiszar, 2019) or Plug-in Hybrids (Šarkan, Gnap & Kiktová, 2019), forces to apply autonomous sensors for condition monitoring systems in the car. The application of the energy harvesting systems seems to be the perfect solution for constant powering up of sensors placed in hardly accessible places such as tires, engine block or suspension column. The range of used sensors in the car is getting wider and wider and three main areas, where they are used can be defined:

- diagnostics,
- active safety,
- navigation & localization.

Tab. 1. The list of sensors in the car possible to power with the EH system

Position sensors	**Pressure sensors**	**Thermal sensors**	**Inertial measurement unit**	**Gas and chemical compositions sensors**
Fuel level, Engine throttle position, Steering wheel position, Chassis height	Tire pressure monitoring system, Engine manifold pressure sensing system, Cylinder pressure	Exhaust gas temperature, Engine coolant temperature	ABS, IMU-enabled GPS systems	Humidity detection, NO_x detection, CO and CO_2 emission, Hydrogen detection

Over the decade ago, Matsuzaki & Todoroki (2008) found energy harvesting as the future for powering up autonomous sensors in automotive applications. The paper of Askari et al. (Askari, Hashemi, Khajepour, Khamesee & Wang, 2018) provides wide and rich information on sensors to which the scavenged power from the EH system can be transferred to. In Table 1, the list of chosen sensors in the vehicles is presented.

So far, several solutions of piezoelectric energy harvesting systems based on cantilever beam have been proposed at real-, micro- and nanoscale in automotive applications. Many works are focused on powering up the tire pressure sensor as the tire manufacturers couple them with tire and in most cases they are irreplaceable. The application of piezoelectric energy harvester (PEH) in such solutions

seems to be a perfect solution as on car wheels act a different kinds of excitation coming from bumps, torsions, and accelerations. Bowen et al. (Bowen & Arafa, 2015) presented wide spectra of technologies for a tire pressure monitoring systems, mentioning piezoelectric solutions. Zhu et al. (Zhu, Han & Zhao, 2019) studied the acceleration and power response of the PEH mounted on the wheel by different speeds of the car. Xie et al. (Xie & Wang, 2015) provided a mathematical model for the piezoelectric ring energy harvesting system applied in vehicle tires comparing the power response by different thicknesses of PZT patches, class of road surface, and design of the system.

Another source of continuous vibrations in the car is its suspension. In the paper of Al-Yafeai et al. (Al-Yafeai, Darabseh & Mourad, 2020), the information on PEH implementations and harvested power in the car suspension is provided. Furthermore, Zhang et al. (Zhang, Zheng, Shimono, Kaizuka & Nakano, 2016) proposed the application of the stochastic resonance method for increasing the efficiency of PEH mounted in the suspension of the car.

In the present work, we are focusing on the application of random Diesel engine's vibrations as the source of excitation in the cantilever beam PEH system with an amplitude limiter. The application of impacts in the operating system provides a broadband effect, then the EH system can operate in a wider range of excitation frequencies (Borowiec, Litak & Lenci, 2014). Moreover, the different alignment of stoppers provides adjustable design and variable elastic properties of the system. A similar design was discussed in articles by Khalatkar et al. (Khalatkar & Gupta, 2017), Gatti et al. (Gatti, Ramirez, Febbo & Machado, 2018), and Chandru et al. (Chandru, Murugan & Keerthika, 2016) showing experimental results, Kim et al. (Kim, 2014) instead, proposed torsional vibrations in internal combustion engine as the source of vibration for PEH. The novelty of our research is to check how the impact phenomena will influence the power response of the EH system.

The rest of this paper is organized as follows. Section 2 presents solutions and advantages of impact-based energy harvesting systems. In Section 3, the experimental setup and proposed concept of the piezoelectric EH system with an amplitude limiter are described. Next, in Section 4, the results of numerical simulations in Matlab are shown. Section 5 summarizes the results obtained and the next steps in the development of the system are described.

2. IMPACT-BASED CANTILEVER BEAM PEH

In the case of real applications, the best choice is the nonlinear energy harvesting system as it can operate in a wider range of operational frequencies, than the linear oscillator only adapted to the resonant frequency. One of the approaches to obtain a positive broadband effect into EH is the introduction of impacts, which exploit the effects of non-linearity. In the paper of Vijayan et al., (Vijayan,

Friswell, Khodaparast & Adhikari, 2015) they proposed the model of cantilever beam PEH by which it was proved that contact stiffness and clearance have an influence on the output power. The advantage of the impact introduction into the system is the broadband effect caused by the achievement of bilinear stiffness characteristic resulting in energy harvesting in a wider range of frequencies (Borowiec, Litak & Lenci, 2014). The mentioned design of PEH led to the study of the physical system in the experimental and real environment. In the PhD thesis of Ye Zhang from Louisiana State University, the application of piezo-electric based EH systems in civil infrastructures is discussed (Zhang, 2014). In the papers of Zhao et al. (Zhao & Yang, 2018) and Jung et al. (Jung, Song, Hong, Yang, Hwang, Jeong & Sung, 2015) as the external excitation for PEH, the air stream is used, so such EH systems can have a utilitarian function. Based on related works, in our case, we propose a similar approach to the problem, but the excitation will be the random signal obtained from vibrations generated by the engine.

The PEH used for studying the dynamical response is based on the system proposed by Erturk et al. (Erturk, Hoffmann & Inman, 2009). The system consists of the ferromagnetic beam, two PZT-5A piezo-ceramic patches, and a mechanical amplitude limiter mounted on one side of the closed frame. The position of the mechanical stopper is adjustable, but the results of the response are presented for the only one showing the possibilities of the PEH. The considered system can be divided into the electrical part (piezo patches with the external electrical circuits) and the mechanical part (cantilever beam with amplitude limiter) presented in Figure 2.

The coupling of the two parts can be described by the electromechanical equations of motion with dimensionless parameters as following:

$$\ddot{x} + 2\zeta\dot{x} + x + F_r(x) - \chi v = F(t) \tag{1}$$

$$\dot{v} + \lambda v + \kappa\dot{x} = 0 \tag{2}$$

where: ζ – mechanical damping ratio,
$F_r(x) = F_0\,\Theta(-p-x)\,(x+p)$ – stopper restore force,
F_0 = 100– stopper stiffness ratio with respect to the effective normalized beam stiffness,
Θ – Heaviside step function,
p – the distance between the stopper stable position of the beam (equilibrium point x = 0),
χ – piezoelectric coupling term in the mechanical circuit equation,
v – voltage across the load resistance,
$F = A\omega^2 \cos(\omega t)$- excitation force,
A – amplitude of kinematic excitation,
ω – excitation frequency,

λ – reciprocal of the time constant ($\frac{1}{R_l C_p}$), R_l – load resistance,
C_p – capacitance of the piezoelectric layers,
κ – piezoelectric coupling term in the electrical circuit equation,
t – time.

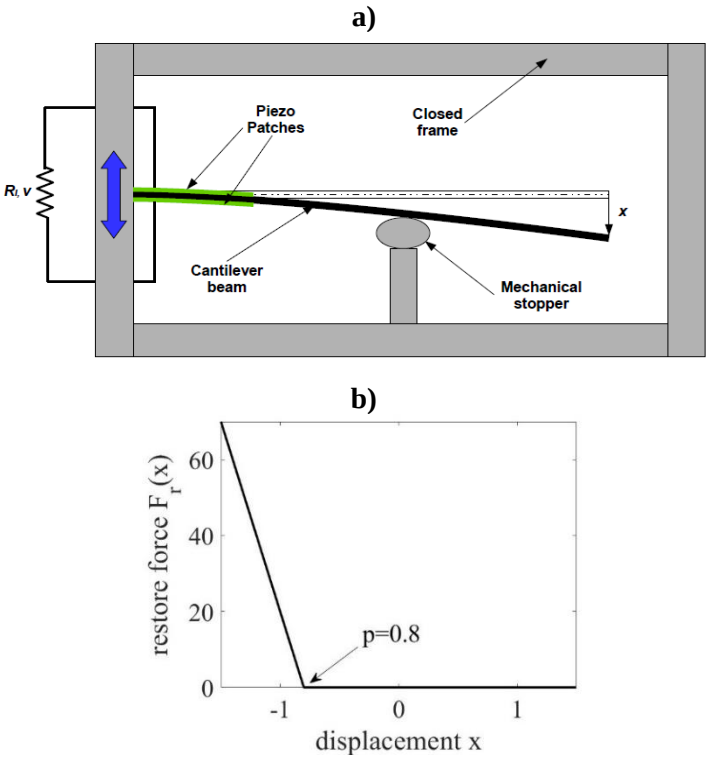

Fig. 2. a) Schematic plot of the piezoelectric energy harvesting system is based on a cantilever beam with mechanical stopper of amplitude – the blue arrows indicate the direction of excitation; b) The restoring force of the stopper with respect to the beam normalized effective stiffness – p = 0.8 indicated the distance of the stopper from the equilibrium fixed point (x = 0)

The impact was introduced into the system by the Heaviside function, we assumed that its influence will cause a sudden increase of the beam's stiffness by 100 times during contact with the mechanical stopper. Values of other terms used in Eq. 1 and Eq. 2 are collected in Table 2.

Tab. 2. Values of parameters used in electromechanical equations of motion (dimensionless units)

Parameter	Value
ζ	0.01
χ	0.05
λ	0.01
κ	0.50
p	0.80
A	0.183

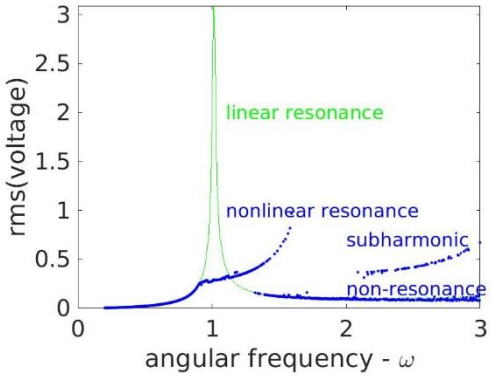

Fig. 3. The comparison of resonance curves for the linear (green line) and nonlinear (blue line) case for EH system. Namely, RMS (Root Mean Square) of voltage output is plotted versus excitation (angular) frequency. In the nonlinear problem, there are additional sub-harmonics (multiple solutions) arouse in result of impact. The calculations are done in such way that for each angular frequency different initial conditions are chosen $[x, \dot{x}, v] = [0, \sigma, 0]$, where σ is a random number uniformly distributed in the interval [-1,1]

Based on Eq. 1 and Eq. 2, we performed calculations of the voltage response. The results of calculations are presented in Figure 3. Interestingly, we observe a frequency broad band at the vicinity of the linear frequency resonance $\omega_0 = 1$ and additionally in the interval $\omega \in [2,3]$. Because the impact increases the stiffness of the nonlinear mechanical resonator the resonance curve is strongly inclined into the higher frequencies. Simultaneously, the total amplitude of the excitation is proportional to the square of excitation frequency causing increase of inertial force acting on the beam (Eq. 1). Note also that the width is much wider comparing to the linear resonance. On the other hand in the region of $\omega \in [1.2, 1.5]$ there two coexisting solutions including resonance and non-resonance ones. The non-resonance solution is a solution without impact. The situation is repeating for higher frequencies, $\omega \in [2, 3]$, where the corresponding resonance solutions is driven by the subharmonic resonance (Huang, Zhou & Litak, 2019; Huguet, Lallart & Badel 2019). Both resonance solutions, main andsubharmonic, are forming so called broad band effect in the studied harvester with impacts.

3. EXPERIMENTAL SETUP

For the research subject, the Diesel engine (2.5 Turbo Diesel – 4C90 Andoria) was chosen as in the case of this type of engine, we can expect the highest amplitudes of vibrations (Taghizadeh-Alisaraei, Ghobadian, Tavakoli-Hashjin |& Mohtasebi, 2012). The measurement system (Figure 4) used for recording vibrations was previously described in the article of Gardyński et al. (Gardyński, Caban & Droździel, 2015) consisting of 1) clamping arm, 2) potentiometer arm and 3) linear potentiometer. The measured displacement was converted into voltage and transferredto the oscilloscope DSO-2902 256K. The potentiometer applied to measurements is an A-linear type with 22 kΩ resistance and 0.5% linear tolerance and was mounted at 540 mm above the crankshaft. The scale of the potentiometer is the following: 1.6 mm displacement corresponds to a 1 V voltage response.

Fig. 4. The measuring system mounted on the engine block

The scheme of the measuring circuit is presented in Figure 5, the best place for mounting the EH system is the engine block, where are the pure vibrations of the operating engine. The potentiometer coupled with the oscilloscope and PC provides proper registration and visualization of the displacement signal. The measurements were performed for the operational velocity: n = 800 rpm (Figure 6).

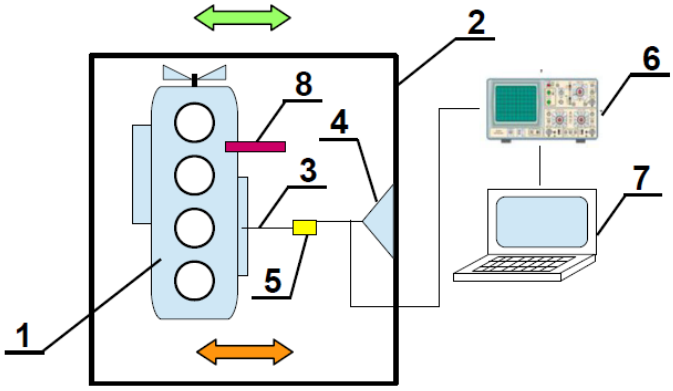

Fig. 5. The measuring circuit for engine displacement and mounted EH system on the engine block. The measuring circuit consists of the following equipment: 1 – Diesel Engine, 2 – Vehicle body, 3 – Potentiometer arm, 4 – Load-bearing structure, 5 – Linear potentiometer, 6 – Oscilloscope, 7 – Computer, 8 – Piezoelectric energy harvester (the orange arrow refers to the horizontal engine's vibrations and the green refers to vehicle's vibrations during driving)

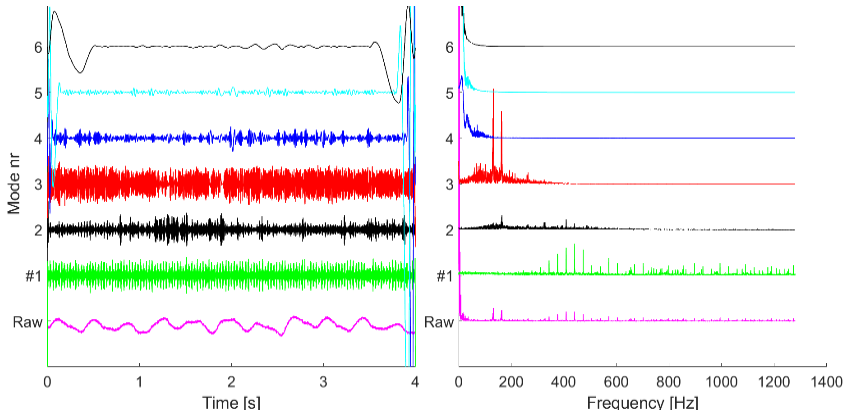

Fig. 6. Analysis of the frequency of engine vibration (displacement time series) signal components – left diagram: empirical mode decomposition, right diagram: Fast Fourier Transformation (FFT) of raw signal and empirical modes (for the analysis, the case 800 rpm was considered)

Usually, experimental signals have a strong nonlinear character, and the application of the Hilbert-Huang transform (HHT) allows separating characteristic modes of the raw signal. Additionally, Fast Fourier Transformation (FFT) helps to define the characteristic frequencies occurring in the spectra. In Figure 6, the results of HHT decomposition and its frequency analysis are presented. The raw signal consists of 6 modes and its number is defined by the period of signal recording (Feng, Liang & Chu, 2013). Based on the performed analysis, in the

experimental signal, there are many higher harmonics. However, some of them are affected by measurement errors, which cannot be used to estimation of the inertial force $F(t)$ as defined in Eq. 1. To overcome this difficulty, we used the FFT spectral low-pass filtering shown in Figure 7.

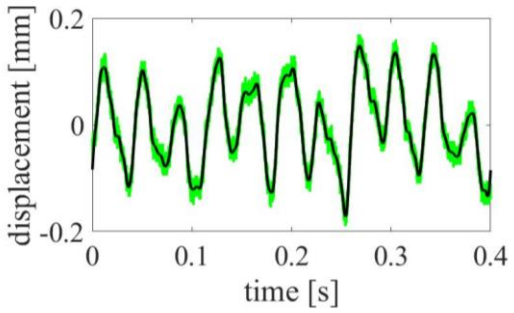

Fig. 7. Spectral low-pass filtering (the measured signal is plotted in green while the filtered one in black color)

4. MODEL FITTING RESULTS AND DISCUSSION

Using the repetition of the measured signal, we continued it for a longer time and adjusted to the non-dimensional model (Eq. 1 and Eq. 2). The course of the inertial force is calculated as the second-order derivative of the displacement signal (Figure 8).

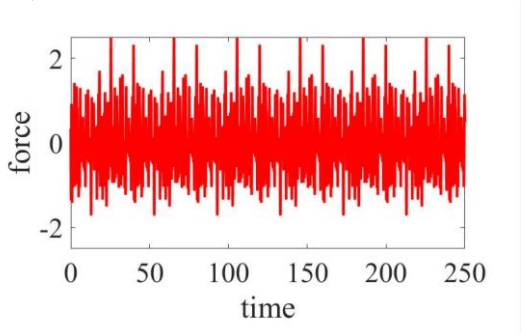

Fig. 8. Time course of inertial force for the case n = 800 rpm

In Figure 9, the results of the output voltage are presented. The worth noticing fact is that impacts support stable oscillations of the beam and its transient increase (a). In the linear case (b), there is constant damping of the beam's movement in time. To visualize the influence of the impact on the cantilever beam, the phase portraits are shown (Figure 10). The added dashed

vertical line on the plot represents the distance of set the amplitude limiter. If there is no limiter, the beam oscillates from peak to peak and around the stable point $x = 0$ (a). The contact with amplitude limiter shows a clear beam's reflection (b) and an increase of oscillations' amplitude on the side without the limiter.

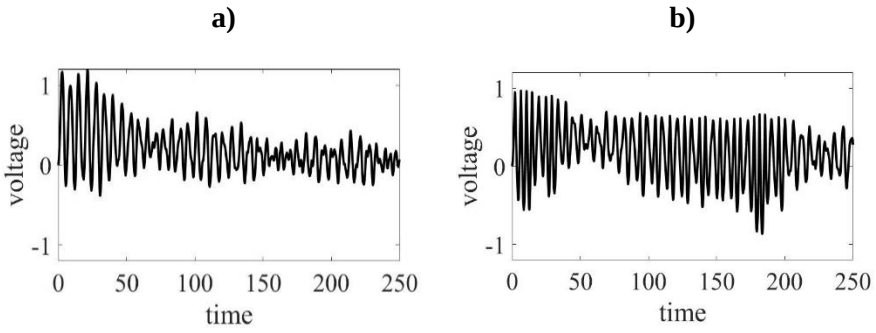

Fig. 9. The comparison results of output voltage for linear (a) and nonlinear (b) case – it is worth observing that by impacts there the damping effect is smaller; the corresponding Root Mean Square of the voltage output: RMS (voltage) is 0.1025 and 0.1330 for linear a) and nonlinear b) energy harvesters respectively

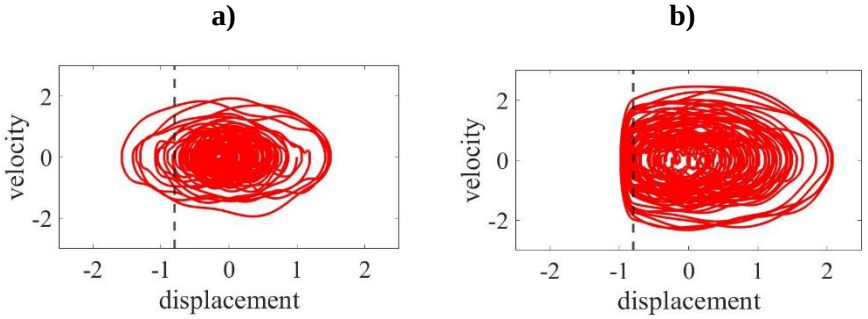

Fig. 10. Phase portraits of the energy harvesting resonator response – the limit of amplitude is set to $x = -0.8$ (black dashed line); picture (a) represents the case without amplitude limiter, (b) with impact

5. CONCLUSIONS

For the analysis, a vibrational piezoelectric energy harvesting system was used in which the experimental multi-frequency excitations coming from diesel engine were adopted. The introduction of the amplitude limiter to the system brought a positive effect on the dynamic response. Comparing linear (without impacts) with nonlinear (with impacts) cases, there is an effect of higher voltage output from the second. Impacts of the beam over the amplitude limiter cause

oscillations of the higher level, concerning the linear solution there is a dissipation of oscillations were present (see Figures 9 a and b). Additionally, the application of experimental multi-frequency vibrations improved the broadband effect of the system, as the occurrence of subharmonic branches can be induced easier in the resonance curve (Figure 3, blue line). The next steps in the planned investigations will be testing the performance of the physical system in the real environment and compare the output power with approaches including energy harvesting designed to moving rotating or swinging parts.

Acknowledgement

This work was supported by the program of the Ministry of Science and Higher Education in Poland under the project DIALOG *DIALOG 0019/DLG/2019/10 in the years 2019–2021.*

REFERENCES

Al-Yafeai, D., Darabseh, T., & Mourad, A.H.I. (2020). A state-of-the-art review of car suspension-based piezoelectric energy harvesting systems. *Energies*, *13*, 2336. https://doi.org/10.3390/en13092336

Ambrożkiewicz, B., Litak, G., & Wolszczak, P. (2020). Modelling of electromagnetic energy harvester with rotational pendulum using mechanical vibrations to scavenge electrical energy. *Applied Sciences*, *10*, 671. https://doi.org/10.3390/app10020671

Askari, H., Hashemi, E., Khajepour, A., Khamesee, M.B., & Wang, Z.L. (2018). Towards self-powered sensing using nanogenerators for automotive systems. *Nano Energy*, *53*, 1003–1019. https://doi.org/10.1016/j.nanoen.2018.09.032

Borowiec, M., Litak, G., & Lenci, S. (2014). Noise effected energy harvesting in a beam with stopper. *International Journal of Structural Stability and Dynamics*, *14*, 1440020. https://doi.org/10.1142/S0219455414400203

Bowen, C.R., & Arafa, M.H. (2015). Energy harvesting technologies for tire pressure monitoring systems. *Advanced Energy Materials*, *5*, 1401787. https://doi.org/10.1002/aenm.201401787

Chandru, A.A., Murugan, S.S., & Keerthika, V. (2016). Design and implementation of an energy harvester for Low-Power devices from vibration of automobile engine. *Advances in Intelligent Systems and Computing*, *397*, 1–8.

Erturk, A., Hoffmann, J., & Inman, D.J. (2009). A piezomagnetoelastic structure for broadband vibration energy harvesting. *Applied Physics Letters*, *94*, 254102. https://doi.org/10.1063/1.3159815

Feng, Z., Liang, M., & Chu, F. (2013). Recent advances in time-frequency analysis methods for machinery fault diagnosis: A review with application examples. *Mechanical Systems and Signal Processing*, *38*, 165-205. https://doi.org/10.1016/j.ymssp.2013.01.017

Figlus, T., Szafraniec, P., & Skrucany, T. (2019). Methods of measuring and processing signals during tests of the exposure of a motorcycle driver to vibration and noise. *International Journal of Environmental Research and Public Health*, *16*, 17, 3145. https://doi.org/10.3390/ijerph16173145

Gardyński, L., Caban, J., & Droździel, P. (2015). The impact of stiffness of engine suspension cushions in an all-terrain vehcile on its transverse displacement. *Journal of Science of the Military Academy of Land Forces*, *47*, 95–102.

Gatti, C.D., Ramirez, J.M., Febbo, M., & Machado, S.P. (2018). Multimodal piezoelectric device for energy harvesting from engine vibration. *Journal of Mechanics of Materials and Structures*, *13*, 17-34. https://doi.org/10.2140/jomms.2018.13.17

Huang, D., Zhou, S., & Litak, G. (2019). Theoretical analysis of multi-stable energy harvesters with high order stiffness terms. *Communications in Nonlinear Science and Numerical Simulation*, *69*, 270-286. https://doi.org/10.1016/j.cnsns.2018.09.025

Huguet, T., Lallart, M., & Badel, A. (2019). Orbit jump in bistable energy harvesters through buckling level modification. *Mechanical Systems and Signal Processing*, *128*, 202–215. https://doi.org/10.1016/j.ymssp.2019.03.051

Jung, H.J., Song, Y., Hong, S.K., Yang, C.H., Hwang, S.J., Jeong, S.Y., & Sung, T.H. (2015). Design and optimization of piezoelectric impact-based micro wind energy harvester for wireless sensor network. *Sensors and Actuators, A 222*, 314–321. https://doi.org/10.1016/j.sna.2014.12.010

Khalatkar, A.M., & Gupta, V.K. (2017). Piezoelectric energy harvester for low engine vibrations. *Journal of Renewable and Sustainable Energy, 9*, 024701. https://doi.org/10.1063/1.4979501

Kim, G.W. (2014). Piezoelectric energy harvesting from torsional vibration in internal combustion engines. *International Journal of Automotive Technology*, *16*, 645–651. https://doi.org/10.1007/s12239-015-0066-6

Koszewnik, A. (2019). Analytical modelling and experimental validation of an energy harvesting system for the smart plate with integrated piezo-harvester. *Sensors*, *19*, 812. https://doi.org/10.3390/s19040812

Koszewnik, A. (2020). Experimental validation of equivalent circuit modelling of the piezo-stripe harvester attached to SFSF rectangular plate. *Acta Mechanica et Automatica*, *14*, 8–15. https://doi.org/10.2478/ama-2020-0002

Litak, G, Friswell, M.I., & Adhikari, S. (2010) Magnetopiezoelastic energy harvesting driven by random excitations. *Applied Physics Letters*, *96*, 214103. https://doi.org/10.1063/1.3436553

Łukjanow, S., & Zieliński, W. (2016). Examination and assessment of electric vehicles' operational safety. *The Archives of Automotive Engineering – Archiwum Motoryzacji*, *74*, 4, 59–82. https://doi.org/10.14669/AM.VOL74.ART5

Matsuzaki, R., & Todoroki, A. (2008). Wireless Monitoring of Automobile Tires for Intelligent Tires. *Sensors*, *8*, 8123-8138. https://doi.org/10.3390/s8128123

Mieczkowski, G., Borawski, A., & Szpica, D. (2019). Static electromechanical characteristic of three-layer circular piezoelectric transducer. *Sensors*, *20*, 222. https://doi.org/10.3390/s20010222

Šarkan, B., Gnap, J., & Kiktová, M. (2019). The importance of hybrid vehicles in urban traffic in terms of environmental impact. *The Archives of Automotive Engineering – Archiwum Motoryzacji*, *85*, 3, 115–122. https://doi.org/10.14669/AM.VOL85.ART8

Skrucany, T., Kendra, M., Stopka, O., Milojevic, S., Figlus, T., & Csiszar, C. (2019). Impact of the electric mobility implementation on the Greenhouse Gases production in central European Countries. *Sustainability*, *11*(18), 4948. https://doi.org/10.3390/su11184948

Smutny, J., Nohal, V., Vukusicova, D., & Seelmann, H. (2018). Vibration analysis by the Wigner-Ville transformation method. *Communications – Scientific Letters of the University of Zilina*, *20*, 4, 24–28.

Taghizadeh-Alisaraei, A., Ghobadian, B., Tavakoli-Hashjin, T., & Mohtasebi, S.S. (2012). Vibration analysis of a diesel engine using biodiesel and petrodiesel fuel blends. *Fuel*, *102*, 414–422.

Tan, Y., Dong, Y., & Wang, X. (2017). Review of MEMS electromagnetic vibration energy harvester. *Journal of Microelectromechanical Systems*, *26*, 1–16.

Vijayan, K., Friswell, M.I., Khodaparast, H.H., & Adhikari, S. (2015). Non-linear energy harvesting from coupled impacting beams. *International Journal of Mechanical Sciences*, *96-97*, 101-109. https://doi.org/10.1016/j.ijmecsci.2015.03.001

Xie, X., & Wang, Q. (2015). A mathematical model for piezoelectric ring energy harvesting technology from vehicle tires. *International Journal of Engineering Science*, *94*, 113–127. https://doi.org/10.1016/j.ijengsci.2015.05.004

Zhang, Y. (2014). Piezoelectric based energy harvesting on low frequency vibrations of civil infrastructures. *LSU Doctoral Dissertations*, 1342.

Zhang, Y., Wang, T., Luo, A., Yushen, H., Li, X., & Wang, F. (2018). Micro electrostatic energy harvester with both broad bandwidth and high normalized power density. *Applied Energy*, *212*, 362–371. https://doi.org/10.1016/j.apenergy.2017.12.053

Zhang, Y., Zheng, R., Shimono, K., Kaizuka, T., & Nakano, K. (2016). Effectiveness testing of a piezoelectric energy harvester for an automobile wheel using stochastic resonance. *Sensors*, *16*(10), 1727. https://doi.org/10.3390/s16101727

Zhao, L., & Yang, Y. (2018). An impact-based broadband aeroelastic energy harvester for concurrent wind and base vibration energy harvesting. *Applied Energy*, *212*, 233–243. https://doi.org/10.1016/j.apenergy.2017.12.042

Zhu, B., Han, J., & Zhao, J. (2019). Study of Wheel Vibration Energy Harvesting for Intelligent Tires. *Lecture Notes in Electrical Engineering*, *486*, 971–978. https://doi.org/10.1007/978-981-10-8506-2_65

Applied Computer Science, vol. 16, no. 3, pp. 30–41
doi:10.23743/acs-2020-19

Submitted: 2020-08-11
Revised: 2020-09-04
Accepted: 2020-09-07

e-Commerce, AES, NDS,

Raphael Olufemi AKINYEDE [0000-0002-5544-8529]*,
Sulaiman Omolade ADEGBENRO [0000-0002-3432-0198]**,
Babatola Moses OMILODI [0000-0001-6999-7425]***

A SECURITY MODEL FOR PREVENTING E-COMMERCE RELATED CRIMES

Abstract

The major challenge being faced by the financial related institutions, such as e-Commerce has been insecurity. Therefore, there is urgent need to develop a scheme to protect transmitted financial information or messages from getting to the third party, intruder and/or unauthorized person(s). Such scheme will be based on Advanced Encryption Standard (AES) and Neural Data Security (NDS) Model. Based on this background, an AES using Time-based Dynamic Key Generation coupled with NDS model will be used to develop security model for preventing e-commerce related crimes. While AES will secure users' details in the database server and ensures login authentications, NDS model will fragment or partition sensitive data into High and Low levels of confidentiality. The sensitivity of the data will determine, which category of confidentiality the data will fall into. The fragmented data are saved into two different databases, on two different servers and on the same datacenter. In addition, an exploratory survey was carried out using different performance metrics with different classifications of algorithms. Out of the four algorithms considered, Naive Bayes performs better as it shows, out of a total of 105 instances that were observed, 85.71% were correctly classified while 14.29% were misclassified.

* The Federal University of Technology, School of Computing, Department of Computer Science, FUTA Rd, Akure, Nigeria, roakinyede@futa.edu.ng
** The Federal University of Technology, School of Computing, Department of Computer Science, FUTA Rd, Akure, Nigeria, adegbenrosulaiman@gmail.com
*** The Federal University of Technology, School of Computing, Department of Computer Science, FUTA Rd, Akure, Nigeria, omiloditola25@yahoo.com

1. INTRODUCTION

In recent times, our society is increasingly relying on the Internet and other Information Technology tools to engage in personal, public communication and conduct business activities among other several benefits (Berchane & Berchane, 2018). The cyber space creates boundless opportunities for commercial, business, economic, social and educational activities as well as a haven for societal miscreants to perpetrate their indiscriminate acts. Since the outbreak of coronavirus 2019 (COVID-19), Nigerian government, private sectors and mostly other establishment are increasingly depending on Internet to conduct business, manage industrial activities, and engage in personal communication among other numerous benefits within the reach of the country. While these developments allow for enormous gain in productivity, efficiency and communication that have changed the way in which data is managed, accessed and used commercially, they also create a loophole that criminals may take advantage of to destroy organization's image and reputation.

The Internet is a global network, which means, it contains several networks. Connecting a business to the Internet implies that such business can be reach globally. In other words, a company can reach anyone who has an access to the Internet such as customers, suppliers, on-line banks etc (Taroub, 2015). At the same time, the company can be reached by anyone both near and far. As mentioned above, the Internet creates vast opportunities for businesses, but at the same time poses some threats, which if they are not taken care of properly can lead to data thefts, diversion of funds and destroy businesses (Almunawar, 2012).

In Maitanmi *et al*. (2013) e-crime was defined as a type of crime committed by criminals who make use of computers through the Internet connections to perpetrate evils, such as illegal downloading of music files and films, piracy, spam mailing, data theft and the likes. E-crime evolves from the wrong application or abuse of Internet services. The core activities of e-commerce are business transactions between two parties or possibly mediated by a third party. In fact, the practice conducted by company before the term e-commerce appears is electronic data interchange (EDI), which is basically electronic transaction via computer networks (Yakasai, 2017). The major concern of electronic transactions is how to protect transactions from eavesdroppers (which can steal and modify the information in the transactions) and how to make sure those transactions are authenticated.

2. RELATED WORKS

In Hamilton and Gabriel (2012), a management system for dimensions of fraud in Nigeria selected firms was presented. The research was motivated by the need to examine the management of financial fraud in some selected companies in Nigeria. It involves the use of simple percentages and frequency distribution Tables. The purpose of the research is to provide a platform for the management of financial fraud in those companies and also minimize fraud through better internal control systems. The research work contributed a deep knowledge on the effect of fraud on business organizations and fraud reduction strategies. The method adopted is inappropriate and cannot be relied upon in combating cybercrimes because few firms were selected out of numerous companies facing same challenges.

In Jarupunphol & Buathong (2013), a secure electronic transactions (SET): a case of secure system project failures was presented. The research work was motivated by the need to enhance a security protocol for an electronic payment system that uses PKI to address e-commerce security and privacy concerns. It was designed to address security problems in e-payment systems and this involves the use of PKI for the architectural base of SET. Since the main purpose of securing e-commerce is to build a dependable system that addresses security requirements, as a result, this work appeared to be the most appropriate solution for it. The use of PKI for SET makes e-commerce end-users to reject SET because it has several usability issues. For example, e-commerce end-users are forced to comply with SET security requirements and this is unpleasant to them.

In Ogwueleka and Ocheme (2014), an RSA encryption/decryption algorithm for combating cybercrime using a case study of developing countries was presented. The research was to tackle cybercrime as anti-viruses and firewalls have been proved to be inadequate in minimizing the menace of cybercrime in cyber space. It provides a broader and specific approach for tackling cybercrime. It also involves the use of RSA encryption algorithm because hackers find it difficult to factor the large integers and this makes its deployment to be more secured. This research work established the efficiency of RSA encryption method which believed can never be cracked because it is computationally infeasible to permutated but is bound to be ineffective because RSA is vulnerable to Chosen Ciphertext Attack (CCA).

In Chinedu (2015), an e-commerce security using RSA cryptosystem was developed. This research was motivated by lack of adequate security on e-commerce information sent through the computer network and Internet. There is need for a security system that will protect e-commerce information transmitted via the Internet and computer networks. The developed system uses RSA Cryptosystem to secure e-commerce information sent. However, RSA encryption and decryption algorithm needs a lot of calculation and this slows down the speed of the system.

In Chauhan *et al.* (2015), an hybrid technique to secure e-commerce transaction was implemented. The developed system adopt parallel processing and multithreading on AES algorithm and steganography in Image. The system achieved time reduction in encryption and decryption with the use of multithreading and parallel processing. However, the use of steganography can aid illegitimate uses the system, such as in terrorism, pornography and data theft.

Rajeshree and Kirti (2018) developed a secured online transactions using biometrics in mobile phone. The research was motivated by the need to focus on the feature extraction from the runtime fingerprint image on an Android mobile and send to the server for authentication of an individual. The aim is to unravel the main security issues in online transaction with much safe, secure and very easy to use, also need not to remember passwords and secret codes system. The method adopted the use of a generic fingerprint authentication system which comprises of two parts: enrolment and verification. In enrolment, the raw fingerprint image is collected, pre-processed, and the features are extracted and stored. In verification the enrolled fingerprint features are compared with the features computed from the input fingerprint to find similarities between them. The limitation of the research work is based on the model used for fingerprint scanning embedded in a mobile phone that makes e-transactions very cost effective. In addition, the fingerprint scanner does not take into consideration users' finger that might change in either size or form/pattern over time.

3. SYSTEM ANALYSIS AND DESIGN

The proposed AES and NDS model for e-Commerce extracted and adapted some of the features of RasmiP and Paul (2011); Hamilton and Gabriel (2012); Akash and Bhonge (2013); Ogwueleka and Ocheme (2014); Kuppuswamy & Al-Khalidi (2014); and Rajeshree and Kirti (2018). From such systems, we can formally describe the security model for e-Commerce as a system that comprises of three modules, which are the customer side, server side and payment channel modules as shown in Figure 1.

The customer software is the front-end via web browser through which users can view, register and interact with the application. The web server (Apache) is the back-end that processes incoming network requests that are coming from customers to the merchant sites. MySQL is the database that works behind the scene to store data and deliver information to the users. The payment channel module includes functions designed to support ordinary types of payment services, the most common being credit/debit cards and mobile payments. Payment gateway such as Paypal, Stripe can be used.

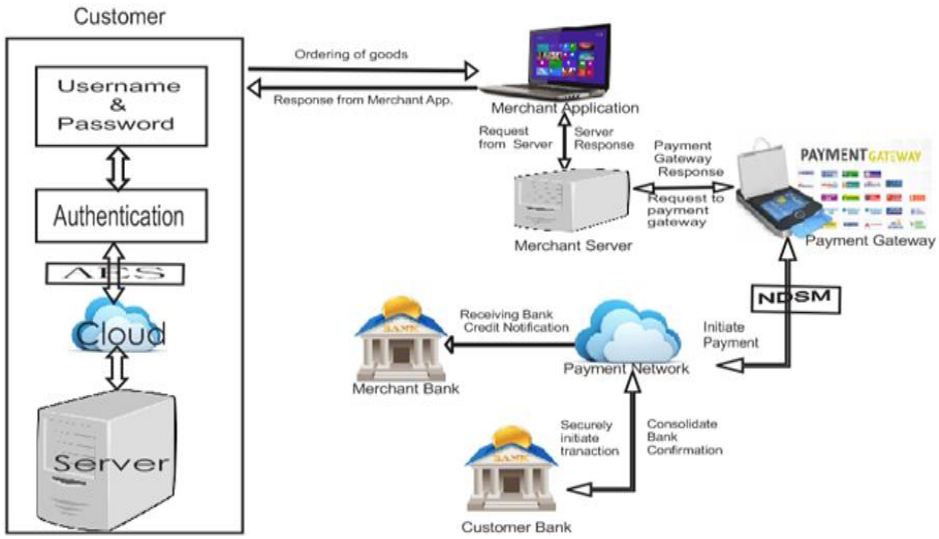

Fig. 1. Architectural design of the proposed System

Proposed algorithm execution steps are as follows:

A. Signup by entering details:
   - Securing of users credentials and credit card details using AES,
   - Login,
   - Input Credentials using Username and Password,
   - Authentication using AES.

B. Selection of desired products.

C. Payment with Credit Cards:
   - Securing of credit card details using NDS model.

D. Logout.

3.1. E-commerce performance metrics

For this analysis, performance metrics such as Confusion Matrix, Accuracy, and Kappa will be considered using some of the commonly used classification algorithm. The algorithms are Random Forest, J48, Naive Bayes Classifier, and Random Tree.

3.1.1. Confusion Matrix

Confusion Matrix, also referred to as Table of confusion, is made up of two rows and columns that project the number of True Positive (TP), False Positive (FP), False Negative (FN), and True Negative (TN). Table 1 shows the cross section of both Predicted and Actual Values which indicate whether the developed system is good for use or not, especially based on the number of True Positive Values.

Tab. 1. Confusion Matrix

		Predicted Class: Yes	Predicted Class: No
Actual Class	Yes	TP	FN
	No	FP	TN

I. **Accuracy:** This is the proportion of the total number of predictions that are corrected. The level of accuracy of each algorithm used are in Table 2:

$$Accuracy = \frac{\text{TP+TN}}{\text{TP+TN+FP+FN}} \quad (1)$$

II. **Recall:** This is the proportion of Positive cases that were identified correctly. High Recall indicates the class is correctly recognized (small number of FN). The Recall values for each of the algorithm used is as shown in Table 3:

$$Recall = \frac{\text{TP}}{\text{TP+FN}} \quad (2)$$

III. **F-Measure:** This is the harmonic mean of both precision and recall of the test. Since we have two measures (Precision and Recall) it helps to have a measurement that represents both of them. Values for each of the algorithm used can also be seen on Table 4:

$$F.Measure = 2 * \frac{\text{Precision*Recall}}{\text{Precision+Recall}} \quad (3)$$

IV. **Kappa Statistics**: The difference between the Observed Accuracy and the Expected Accuracy:

$$Kappa = \frac{O_A - E_A}{1 - E_A} \quad (4)$$

The value ranges from 0 to 1, the $Kappa$ value of 0 (zero) represents poor performance while value closer to 1 (one) represents good performance.

4. SYSTEM IMPLEMENTATION AND PERFORMANCE ANALYSIS

4.1. System Implementation

The layout of the user interface application is designed to be as user friendly as possible. When the user opens the system, e-Commerce Interface and Account Creation Page will appear as shown in Figures 2 and 3.

Click on anywhere on the Screen, then a User Sign-in Page form will appear. This will allow the registration of both the customer and merchant so that they can Login into the system. This is the first step for customer registration. The customer clicks on register new user and supplies his details including the payment information. System would process customer details for registration and send confirmation in form of cipher text. If the registration fails, an error messages would be displayed; and the system would prompt the customer to go through the process again. Then, CA checks that the credit card is valid and releases the signature certificate for customer who stores it for future use. All this information (such as credit card details) must be protected, but in case of merchant, he does not supply any credit card details as his form does not request for it. After that, when an OK button is clicked, a user sign-in page form will appear (Figure 4).

The user will log-in and the system will decrypt the encrypted user name and password from the http request and matches the details of user from database (e.g. validation). If authentication is successful, the system will display a message box with user session that informs the user that he can use the system. Otherwise, the system will display a message box that informs the user to go through the process again. Login authentication method of Akinyede *et al*. (2014) was adapted.

Login authentication.

When user (U), which can either be the customer or merchant wants to access the CA, he carries out the following steps.

a. U submits the computed ID, yId and Id and generates random number a, such that $a \in [1, n-1]$.
b. Calculates $Q_i = q_i P$ and then $p_i = h(Q_i)$, $X = q_i K_{pub\_ib}$ and $g = h(ID||Id||p_i||T_i)$.
c. Select random number a, calculates $Q_i = q_i P$ and then $p_i = h(Q_i)$, $X = q_i K_{pub\_ib}$ and $= h(ID||Id||p_i||T_i)$.
d. U computes the hashed password $Y = yId$, dynamic identity $dID = p_i H(ID_i)$ encrypted and sends message to CA server.
e. Decrypt $p_i H(ID_i)$.
f. Verify both certificate & signature.

Fig. 2. E-commerce Interface

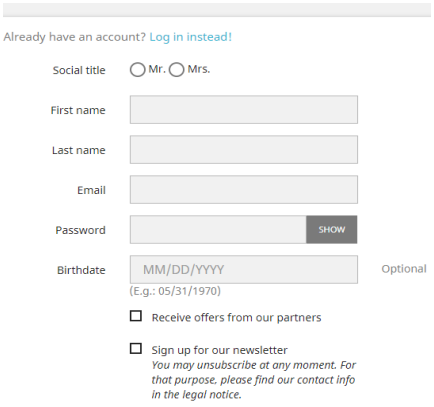

Fig. 3. Account Creation Page

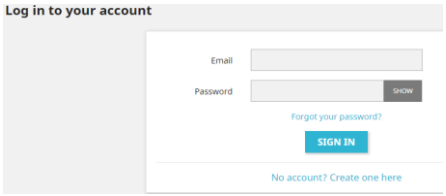

Fig. 4. User Sign-in Page

Fig. 5. List of Products

The system comprises of the merchant and customer interface. The merchant uses his interface to upload and display available items for shopping, while the customer chooses the desired merchant, the items that are available in his store at the customer's interface. Then, the customer can select the needed items from the list of products (Figure 5) and add them to the cart as shown in Figure 6. Having completed the ordering process, customers can checkout as shown in Figure 7. Shipping and payment can follows as shown in Figures 8 and 9: Here is the payment protocol.

Verify PIN

IF PIN is correct THEN

$$\{mp \;\; \text{A:} \left[[\text{PI}, \text{signed}], \text{C}\; ID\right]\}$$

ELSE $terminate$

$$\text{C} \rightarrow \text{M:}\; \{\{Ordered\ Items, Tr.ID, M_{ID}\}K^{-1}\}K^{secret}$$

$$\text{M} \rightarrow \text{C:}\; \{Item, M_{ID}, Tr.ID\ , ID_{\text{CA}}\}K^{secret}$$

$$\text{C} \rightarrow \text{M:}\; \{\{PaymentOrder, Tr.ID, M_{ID}\}K^{-1}\}K^{secret}$$

Merchant processes the order and starts the payment phase by forwarding the payment instructions to *payment Transaction Host*. Note that the *Transaction Host* will obtain transaction data via the network and processes the payment

transaction on behalf of a financial institution that holds the account of the customer for the payment method selected. This will be possible in the payment gateway (Figure 10).

Fig. 6. Shopping Cart

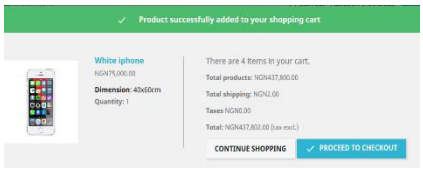

Fig. 7. Checkout

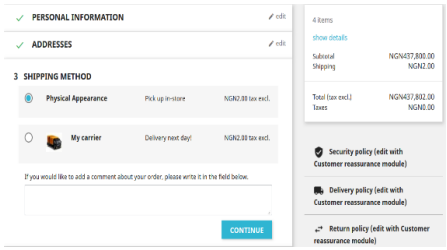

Fig. 8. Shipping Method

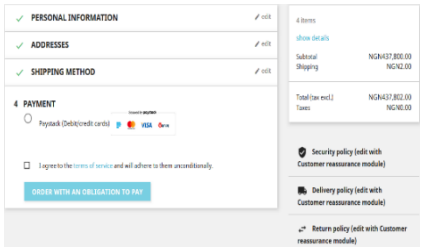

Fig. 9. Payment Method

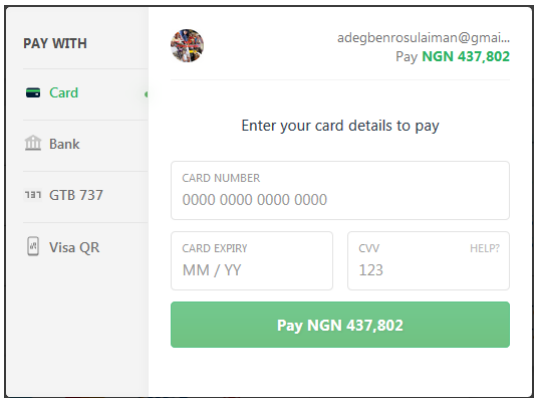

Fig. 10. Payment Gateway

4.2. Performance analysis using 10-fold cross validation technique

In order to investigate the performance of the classifiers, a 10-Fold cross validation was used to evaluate the classifiers. A 10-Fold cross validation is a technique to predictive models by partitioning the original sample into a training set to train the model, and a test set to evaluate it. Table 2 shows the performance analysis based on accuracy while Table 3 shows the results of both correct and incorrect classified data using different algorithms.

Tab. 2. Performance Result Based on Accuracy

Algorithm	TP Rate	FP Rate	Precision	Recall	F-Measure	RoC
Random Forest	0.838	0.244	0.853	0.838	0.830	0.909
J48	0.829	0.250	0.839	0.829	0.821	0.751
NaiveBayes	0.857	0.184	0.857	0.857	0.855	0.903
Random Tree	0.676	0.488	0.687	0.677	0.625	0.650

Tab. 3. Performance Result

	Random Forest	J48	NaiveBayes	Random Tree
Kappa	0.22	0.61	0.69	0.63
Correctly Classified (%)	67.62	82.86	85.71	83.81
Incorrectly Classified (%)	32.38	17.14	14.29	16.19
MAE	0.41	0.25	0.14	0.39
RAE(%)	5.75	77.96	69.87	82.41

Tab. 4. Confusion Matrix

	Random Forest		J48		NaiveBayes		Random Tree	
Class	**A**	**B**	**A**	**B**	**A**	**B**	**A**	**B**
CLASS A	62	2	62	3	60	5	61	4
CLASS B	15	25	15	25	10	30	30	10

Tables 2 to 4 gives all the details of the individual algorithm used. It shows the Accuracy Performance of each algorithm. Out of the four (4) algorithms, Naive Bayes seems to perform better but with little margin as against other algorithms. Explaining Naive Bayes performance result from Table 3, a total of 105 instances were observed out of which 85.71% were correctly classified while 14.29% were misclassified.

With Kappa value of 0.690 shows good performance classification of fraudulent and non-fraudulent cases of transaction.

Table 2 shows the TP, FP, Precision, Recall, F-Measure and RoC of the four algorithms used. The ranges from 0.676 to 0.857 signifies good performance index for the classifier.

As shown in Figure 11, it can be concluded that using AES and NDS Model improves the prevention of e-Commerce related crimes.

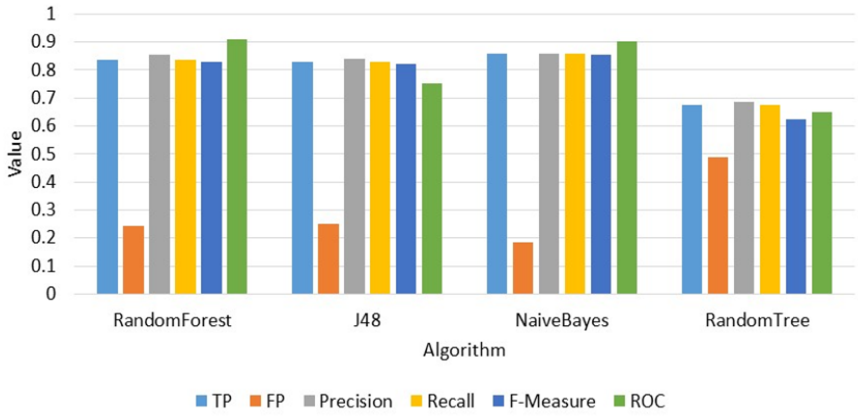

Fig. 11. Performance Result Based on Accuracy

5. CONCLUSIONS AND RECOMMENDATION

Despite the numbers of a security model for preventing e-commerce related crimes that have been proposed in the past, not many of them are practicable or implementable. As a result, in this work, an exploratory survey was carried out using different performance metrics with different classifications of algorithms. All the Tables show the Accuracy Performance of each algorithm. Out of the four algorithms, Naive Bayes seems to perform better but with little margin as against other algorithms. The scheme adopted the use of AES Dynamic key Generation for user authentication during login process and NDS model for fragmentation of customer's credit card detail into two different servers on the same data center. This paper also explained the user authentication and secured customers card details. User authentication provides the assurance that customer's details are secured and privacy is maintained. Merchant website provides vast security, thereby assuring the customers that the transaction is carried out without iota of doubt or fear of insecurity and also integrity, privacy and confidentiality is maintained.

REFERENCES

Akash, V. M., & Bhonge, S. P. (2013). Secure Information Transmission Based on Cryptography Fused with Steganography by using Metamorphic Video Encryption. *International Journal of Science and Research (IJSR)*, *4*(4), 16041503.

Akinyede, R. O., Alese, B. K, & Adewale, O. S. (2014). Building a Secure Environment for Client-Side Ecommerce Payment System Using Encryption System. *Proceedings of the World Congress on Engineering* (vol. 1). London.

Almunawar, M. N. (2012). *Securing electronic transactions to support e-commerce*. Arxiv.org. www.arxiv.org/ftp/arxiv/papers/1207/1207.4292.pdf

Berchane, N., & Berchane, N. (2018, March 21). Impacts of information technology (IT). Master Intelligence Economique et Stratégies Compétitives. https://master-iesc-angers.com/impacts-of-information-technology-it/

Chauhan, E. S., Datta, U., & Pratap, M. (2015). A Hybrid Technique to Secure E commerce Transaction with the Help of AES Encryption and Stenography in Image. *International Journal of Hybrid Information Technology*, *8*, 271–278.

Chinedu, J. N. (2015). Design and Development of an E-Commerce Security. *International Journal of Innovative Research in Information Security (IJIRIS)*, *6*(2), 5–17.

Hamilton, D. I., & Gabriel, J. M. (2012). Dimensions of fraud in Nigeria quoted firms. *American Journal of Social and Management Sciences*, *3*(3), 112–120. http://doi.org/10.5251/ajsms.2012.3.3.112.120

Jarupunphol, P., & Buathong, W. (2013). Secure Electronic Transactions (SET): A Case of Secure System Project Failures. *International Journal of Engineering and Technology*, *5*(2), 278–282. http://doi.org/10.7763/IJET.2013.V5.558

Kuppuswamy, P., & Al-Khalidi, S. Q. (2014). Securing E-Commerce Business Using Hybrid Combination Based on New Symmetric Key and RSA Algorithm. *MIS Rev. Int. J.*, *20*(1), 59–71.

Maitanmi, O., Ogunlere, S., & Ayinde, S. (2013). Impact of Cyber Crimes on Nigerian Economy. *The International Journal of Engineering and Science*, 2(4), 45–51.

Ogwueleka, F., & Ocheme, I. (2014). Review of RSA Algorithm Encryption for Combating Cybercrime: A Case Study of Developing Country. *International Journal of Emerging Technology and Advanced Engineering*, *4*(9), 538–548.

Rajeshree, S. T., & Kirti, K., (2018). Securing Online Transactions Using Biometrics in Mobile Phone. *International Research Journal of Engineering and Technology (IRJET)*, *5*(6), 848–851.

RasmiP, S., & Paul, V. (2011). A Hybrid Crypto System based on a new Circle- Symmetric key Algorithm and RSA with CRT Asymmetric key Algorithm for E-commerce Applications. *IJCA Proceedings on International Conference on VLSI, Communications and Instrumentation (ICVCI)*, *9*, 14–18.

Taroub, A. M. S. (2015). Privacy and Protection in Electronic Transaction: A Review of the e-Commerce Security Protocols. *The 7th International Conference on Information Technology* (pp. 421–429). http://doi.org/10.15849/icit.2015.0079

Yakasai, A. M. (2017). The Relevance of E-Commerce in Nigeria. In *Northwest Business and Entrepreneurship Development Review* (pp. 103–135). Faculty of Social and Management Sciences.

Applied Computer Science, vol. 16, no. 3, pp. 42–55
doi:10.23743/acs-2020-20

Submitted: 2020-09-15
Revised: 2020-09-21
Accepted: 2020-09-26

Decision Support Systems, material requirements planning, ERP, business intelligence

Wojciech DANILCZUK [0000-0002-4628-7620]*,
Arkadiusz GOLA [0000-0002-2935-50003]*

COMPUTER-AIDED MATERIAL DEMAND PLANNING USING ERP SYSTEMS AND BUSINESS INTELLIGENCE TECHNOLOGY

Abstract

Effective decision-making in industry conditions requires access and proper presentation of manufacturing data on the realised manufacturing process. Although the frequently applied ERP systems allow for recording economic events, their potential for decision support is limited. The article presents an original system for reporting manufacturing data based on Business Intelligence technology as a support for junior and middle management. As an example a possibility of utilising data from ERP systems to support decision-making in the field of purchases and logistics in small and medium enterprises.

1. INTRODUCTION

In order for a manufacturing enterprise to function effectively not only must it have an effectively functioning manufacturing system, but also (and above all) efficient information flow as well as fast and correct decision making (George, Schmitz & Storey, 2020; Gola, 2014; Świć & Gola 2013). One of the basic tools for planning and realisation of production utilized in Polish enterprises is ERP class. According to the data by GUS (Central Statistical Office in Poland) for 2019 over 90% of large companies and over 61% middle-sized companies (GUS, 2020) use ERP class software. The major aim of ERP systems is to record economic events – transactions – occurring in the company.

* Lublin University of Technology, Faculty of Mechanical Engineering, Department of Production Computerisation and Robotisation, Nadbystrzycka 36, 20-618 Lublin, Poland, danilczuk.wojciech@gmail.com, a.gola@pollub.pl

The functional area of the system may include all aspects of functioning of an enterprise, among others: finance-accounting, fixed assets, human resources, payroll, inventory management, sales, customer relationship management, purchases, production planning and control (Aremu, Shahzad & Hassan, 2019; Sobaszek, Gola & Kozłowski, 2018; Patalas-Maliszewska, 2012).

Since ERP systems play a significant role in ensuring uninterrupted business continuity planning and correct recording of transactions in databases (Huang, Chiu, Chao & Arniati, 2019). The aim of the ERP system is to ensure correct progression of the defined business process and recording all of the economic events (Rodriguez, Molina-Castillo & Svensson, 2020). Information systems may support the decision-making process and fulfil report needs – it is not, however, their major function (Chang, 2020; Cieśla & Gunia, 2019; Alsoub, Alrawashdeh, & Althunibat, 2018). Unfortunately, simply possessing data or basic reports is not sufficient to conduct a more in-depth analysis or answer information needs occurring in organisation and the ERP systems are not a tool SUFFICIENT for effective decision-making in industry conditions (Vargas & Comuzzi, 2020).

This article presents an example of utilizing the data stored in a manufacturing enterprise in ERP system and Business Intelligence technology to fulfil information needs in supply and logistics departments.

2. PLANNING MATERIAL PURCHASES USING ERP CLASS SYSTEMS

A closed control loop MRP system (Fig. 1) is one of the most significant elements of the ERP system in a manufacturing enterprise. The ERP system includes all areas of an enterprise, whereas the MRP area focuses on planning material needs in a closed control loop (Meilin, Xiangwei & Qingyun, 2010).

Contrary to primary Inventory Control systems . the MRP method utilizes the rule of dependent demand. Therefore inventory control (and production capacities) depend on the orders for ready product.

Algorithm for calculating material demand requires the following information:

- bill of material, BOM,
- information on the state of inventory and the cycle of production or purchase from the supplier,
- production schedules indicating when the product is finished (in which quantities too), during production and the date of the product being ready
- information on production orders, time norms and manufacturing routes (order limits).

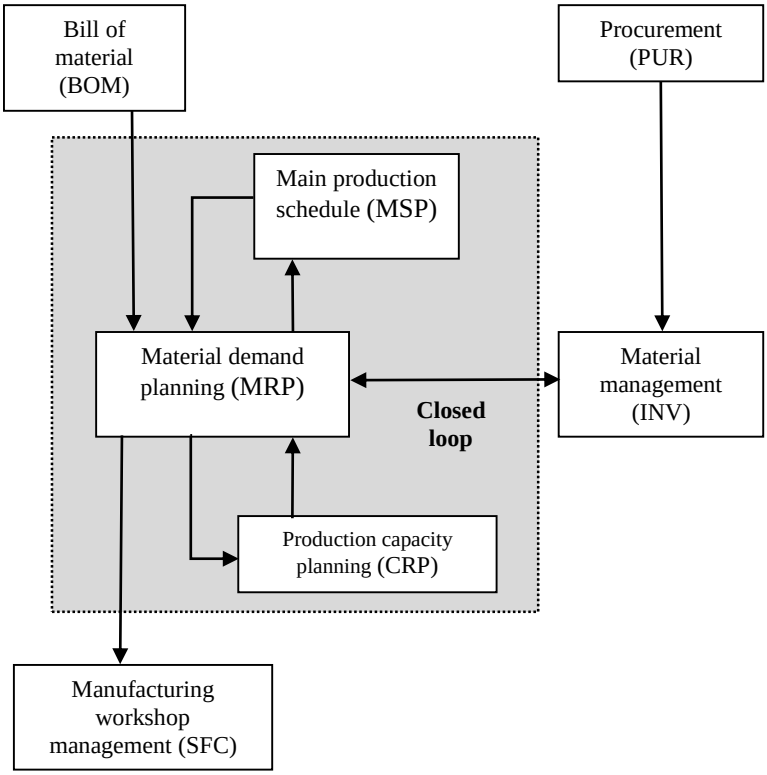

Fig. 1. Model of a closed control MRP loop (Januszewski, 2008)

At the moment of introducing a new order for a finished product and placing it in the schedule the system is able to:

- determine whether the material stock is sufficient to manufacture new product;
- determine when new purchase and delivery of materials ought to be planned in order to finish production at a given date.

The main objective of planning material demand is, based on the data recorded in the system, planning material deliveries at the time they are needed as far as production schedule is concerned as well as delivering the finished product to the customer.

Algorithm for calculating the material demand is as follows (Waters, 1996):

$$ZN = ZB - BB - ZZ, \tag{1}$$

where: ZN – net demand, ZB – gross demand, BB – in stock, ZZ – supply ordered.

Gross demand means all of the materials necessary to manufacture a certain amount of finished product. This information stems from BOM.

"In stock" informs about materials that are currently available in stock and can be immediately used for manufacturing the finished product. It is to be noted that the parts in stock may be in the manufacturing cycle or just in the manufacturing plans.

Supply ordered provides information on materials already ordered, which ought to be delivered to the enterprise at a certain moment. Contrary to the products currently in stock, ordered supply is not yet at the enterprise's disposal, since the materials are not located in the magazine and the enterprise cannot use it for production. At the moment of delivery and admittance to the magazine the products become "in stock" and can be expended. It is to be noted that delivery dates are planned and it is possible that the materials arrive earlier or, worse yet, later than planned.

On the basis of this data the department of supply and logistics receives an information on which materials and semi-finished products to order. Upon comparing information from schedules and production norms and the information on the time of delivery an important information can be obtained – the last moment to make the order so that it is delivered at the right moment and allows for the order to be made in a timely manner.

The algorithm for calculating the net demand is calculated in certain iterations (e.g. daily at night) for each manufacturing index. It can consider phenomena such as material reservations in the magazine, overseeing storage and logistic minima, including the multidimensional complexity of the product. Moreover, in many cases the information on what and when to purchase may not meet their information needs.

3. BUSINESS INTELLIGENCE SYSTEMS AND OLAP TECHNOLOGY

In the classical sense Business Intelligence (BI) is a user-oriented process of obtaining, exploring, interpreting and analysing data, which leads to expediting and rationalising the decision—making process (De Oliveira & De Almeida, 2019). These systems provide support to the management in the business decision-making process in order to increase the worth of the enterprise (You, Yeung & Jong, 2020).

One of the frequently used technologies in the BI systems is OLAP (*OnLine Analytical Processing*) (Queiroz-Sousa, & Salgado, 2020). It is based on multi-dimensional databases that can be described as cubes. Each dimension of the cube stores data aggregated according to presented criteria (Fig. 2).The dimensions can create hierarches – different levels may occur (e.g time dimension may be divided into years, months, days). OLAP cubes are supplemented by data from transaction systems.

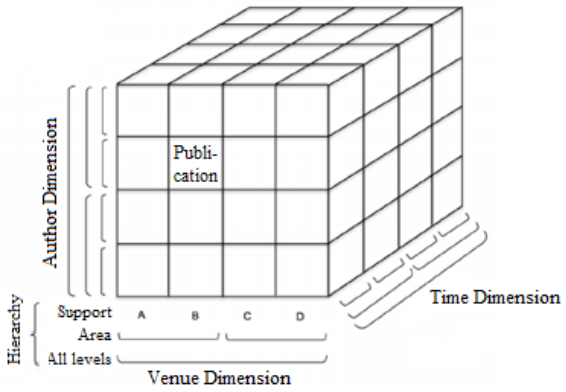

Fig. 2. An example of OLAP cube (Loudcher et al., 2015)

In terms of a multidimensional analysis the following operations may be performed on OLAP cubes (Djiroun, Boukhalfa & Alimazighi, 2019):

- drill down and drill up,
- rotation,
- slicing,
- rating,
- filtration,
- sorting.

Indubitably the data stored in ERP systems is a source of information on the processes occurring within the enterprise (Sobaszek, Gola & Świć, 2020; Zwolińska, Grzybowska & Kubica, 2017; Bocewicz, Nielsen & Banaszak, 2016; Terkaj, Tolio & Urgo, 2015). It is therefore natural to utilize this data as input data for the BI system in order to transform it into information useful business-wise that facilitates the process of analysing and decision-making for the management (Danilczuk, 2019).

4. DECISION-MAKING PROCESS AND THE RANGE OF THE NECESSARY SUPPORT IN THE PROCESS OF MATERIAL REQUIREMENTS PLANNING

One should consider an example of an enterprise with a small-lot production in make-to-order model – MTO. In the enterprise there is an implemented and efficient ERP IMPULS EVO system as well as a closed MRP loop. One of the elements of the system is the module "purchases", which generates purchase suggestions on the basis of the material requirements planning (Fig. 3). The algorithms creating purchase suggestions consider not only basic information stemming

from the rules of net demand estimating, but also logistic minimum of orders or the possibility of using replacements. On the basis of purchase suggestions the staff of the logistics department make purchases.

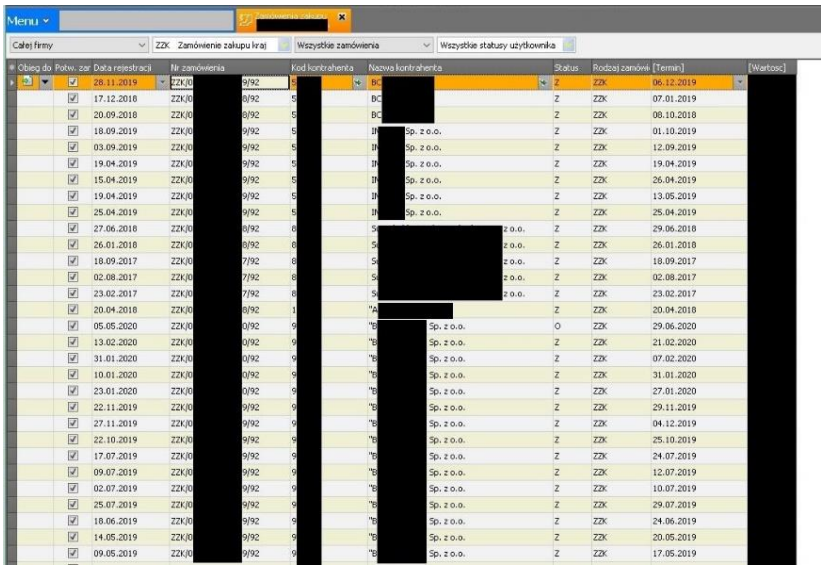

Fig. 3. View of the "Purchases" module in ERP IMPULS EVO

Effectiveness of purchase management is integrated with other areas of the ERP system. Within the purchases module data on orders is recorded (number and name of the order, status of the order, date of execution, time of production). Each order has an assigned status: "shipped", "completed", "partially completed", "cancelled". The first status informs one that the order was shipped to the contractor. Status "completed" informs that all parts of the order were admitted to the ware (instruments of acceptance were issued), partial completion means that at least one part of the order was admitted to the ware. Instruments of acceptance contain an information on indices, number of indices admitted, supplier and date of execution. Structure of the data and their linkage was shown in Fig. 4.

In order to effectively conduct the purchase process, the department of logistics and supply described additional information needs, apart from the basic information obtained from determining the demand. **A need for information on overdue supplies was issued.** Occurrence of overdue supplies may interfere with the MRP loop and falsely suggest a need for ordering a part that is not currently in stock. It is important to know that a certain part was already ordered and ought to be in stock already, but the supply is overdue. As far as production planning is concerned overdue supplies imply a delay in schedule realisation. Since information on planned supply dates and real admittance dates are stored in the system it is possible to determine the status of a supply in the ERP system.

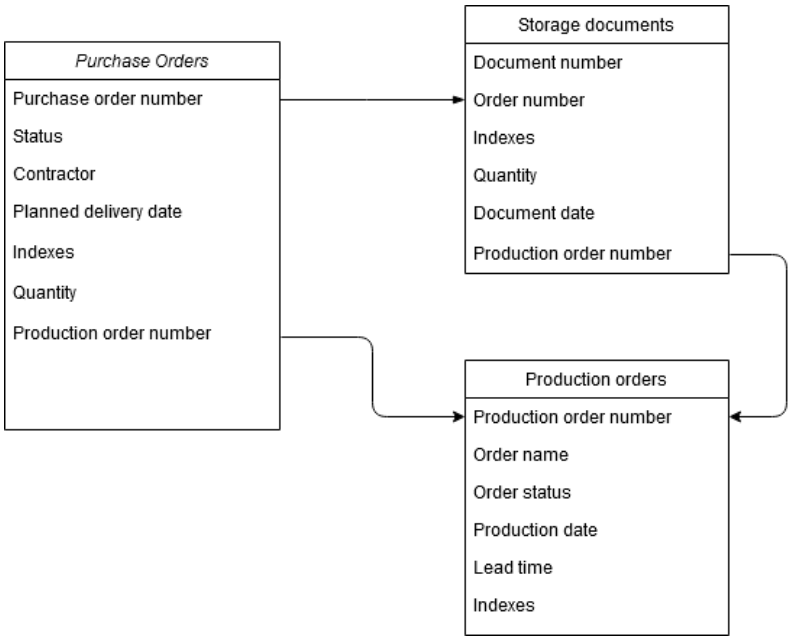

Fig. 4. Structure of data in ERP IMPULS EVO

Another report required by the purchase department was **a linkage of a production commission and orders and order statuses.** These information are logically linked in the ERP system, but there is not a single template which would combine the data and allow for its multidimensional analysis. The purchases department would gain a fast access to information on **what materials were already ordered and delivered to the analysed production commission.** This information is very important from the point of view of production manager. This report can be supplemented by adding information on planned dates (weeks) of supplies which would allow for a more effective operations management in manufacturing workshop. Since these structures are linked, it is possible to create such a compilation.

The last report is a **list of orders planned for the current week**. This information is valuable for the warehouse to know about the number of planned entries connected to new supplies. It would therefore be able to work more effectively.

5. DESIGNING A REPORT SYSTEM

As presented above, all data necessary for a set of reports to be presented is located in the ERP system. Moreover, logical linkages between the data exist and are shown in structures of the database. It is therefore theoretically possible to design a tool that would support information needs of the department of logistics

and purchases. Since those information are located in various modules of the ERP system it would be necessary to aggregate it on the level of the database. In order to achieve that a SQL query was generated to aggregate all data necessary for one database view (SQL 2010) (Fig. 5).

```
SELECT DISTINCT
PZZ.PURCHASE_ORDER_NUMBER,
V.DATE_OF_REGISTRATION,
V.COUNTERPARTY_NAME,
V.YEAR_NO,
V.PERIOD_NO,
V.PRODUCTION_ORDER_NUMBER,
PZZ.PART_INDEX,
I.PART_NAME,
PZZ.ORDERED_QTY,
PZZ.PURCHASE_UNIT_OF_MEASURE,
PZZ.DELIVERY_DATE,
PZZ.ORDER_STATUS,
SZ.ORDER_STATUS_NAME,
PZZ.AMOUNT_RECEIVED,
PZZ.AMOUNT_ORDERED,
PZZ.WAREHOUSE,
M.WAREHOUSE_SYMBOL,

FROM
```

Fig. 5. Fragment of the SQL query

Moreover, on the level of the database view necessary mathematical and logical operations in order to create additional dimensions necessary to fulfil all information needs. For example, upon comparing the delivery date with the current date (sysdate) it can be determined whether the delivery is overdue (and how many days overdue), determine the number of the week on the basis of the date etc.

Aggregating the necessary data into one structure is the first step to enabling a multidimensional analysis based on OLAP cubes. This analysis method allows one to base all reports, and therefore information, on one source of data.

Once data is aggregated in one structure, it is necessary to introduce the report in a tool enabling one to present and analyse the obtained data. Although it would seem natural to place such a compilation in the ERP system in defined reports, there are limitations to this operation. Not all staff requiring this data has access to the ERP system as well as the skill required for operating it. Moreover, IT systems offer a limited number of licences and the users allowed to use it. Purchasing additional licences to enable the access to several reports is economically unjustified.

Due to these limitations it was decided to employ MS Excel for report preparation. This software is widely used in the company, the program is accessible and well-known for every employee.

In order to transfer the data from database to a spreadsheet Online Data Base Connection technology was used. ODBC tool creates a direct connection between the spreadsheet and the database (in this case view of the database). Since it is a fixed connection instead of the data being exported whenever a modification

occurs in the source tables (new record in the form of a new order appears or a status of an order changes) the updates will be seen after refreshing the connection new/modified orders. The program refreshes every 10–20s, which is the time required for a ERP report of a similar volume to be created. Data in Excel is presented in form of a table (Fig. 6).

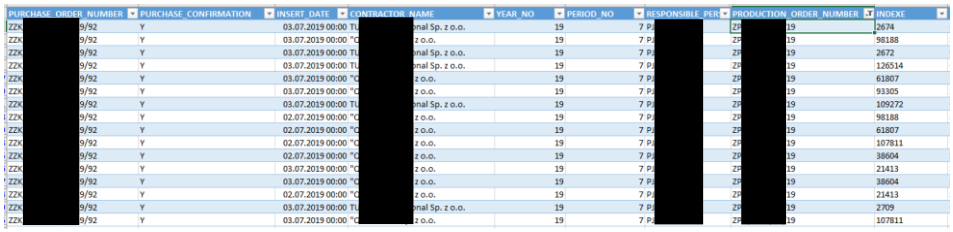

PURCHASE_ORDER_NUMBER	PURCHASE_CONFIRMATION	INSERT_DATE	CONTRACTOR_NAME	YEAR_NO	PERIOD_NO	RESPONSIBLE_PER	PRODUCTION_ORDER_NUMBER	INDEXE
ZZK [redacted]9/92	Y	03.07.2019 00:00 Tu	[redacted]nal Sp. z o.o.	19	7 P	[redacted]	ZP [redacted]19	2674
ZZK [redacted]9/92	Y	03.07.2019 00:00 "C	[redacted]z o.o.	19	7 P	[redacted]	ZP [redacted]19	98188
ZZK [redacted]9/92	Y	03.07.2019 00:00 Tu	[redacted]nal Sp. z o.o.	19	7 P	[redacted]	ZP [redacted]19	2672
ZZK [redacted]9/92	Y	03.07.2019 00:00 Tu	[redacted]nal Sp. z o.o.	19	7 P	[redacted]	ZP [redacted]19	126514
ZZK [redacted]9/92	Y	03.07.2019 00:00 "C	[redacted]z o.o.	19	7 P	[redacted]	ZP [redacted]19	61807
ZZK [redacted]9/92	Y	03.07.2019 00:00 "C	[redacted]z o.o.	19	7 P	[redacted]	ZP [redacted]19	93305
ZZK [redacted]9/92	Y	03.07.2019 00:00 Tu	[redacted]nal Sp. z o.o.	19	7 P	[redacted]	ZP [redacted]19	109272
ZZK [redacted]9/92	Y	02.07.2019 00:00 "C	[redacted]z o.o.	19	7 P	[redacted]	ZP [redacted]19	98188
ZZK [redacted]9/92	Y	02.07.2019 00:00 "C	[redacted]z o.o.	19	7 P	[redacted]	ZP [redacted]19	61807
ZZK [redacted]9/92	Y	02.07.2019 00:00 "C	[redacted]z o.o.	19	7 P	[redacted]	ZP [redacted]19	107811
ZZK [redacted]9/92	Y	02.07.2019 00:00 "C	[redacted]z o.o.	19	7 P	[redacted]	ZP [redacted]19	38604
ZZK [redacted]9/92	Y	03.07.2019 00:00 "C	[redacted]z o.o.	19	7 P	[redacted]	ZP [redacted]19	21413
ZZK [redacted]9/92	Y	03.07.2019 00:00 "C	[redacted]z o.o.	19	7 P	[redacted]	ZP [redacted]19	38604
ZZK [redacted]9/92	Y	02.07.2019 00:00 "C	[redacted]z o.o.	19	7 P	[redacted]	ZP [redacted]19	21413
ZZK [redacted]9/92	Y	03.07.2019 00:00 Tu	[redacted]nal Sp. z o.o.	19	7 P	[redacted]	ZP [redacted]19	2709
ZZK [redacted]9/92	Y	03.07.2019 00:00 "C	[redacted]z o.o.	19	7 P	[redacted]	ZP [redacted]19	107811

Fig. 6. Table with data on an Excel spreadsheet

In order to visualise reports mechanism of pivot tables was employed. On the basis of data in the table an OLAP (online analytic process) cube is created. Presenting data in a pivot table allows one to conduct all operations typical for multidimensional analysis on OLAP cubes, such as drill-up and drill-down, select, sort, filter etc. Tool of pivot tables allows one to freely "rotate" the cube.

„Rotating" selected dimensions of the cube allows one to prepare a proper view of data fulfilling information needs. The first report was a compilation of orders divided into overdue and not overdue. Status of the delivery was set as a report filter. The rows were number of days overdue, order status, contractor, number of the order and name of the part (Fig. 7).

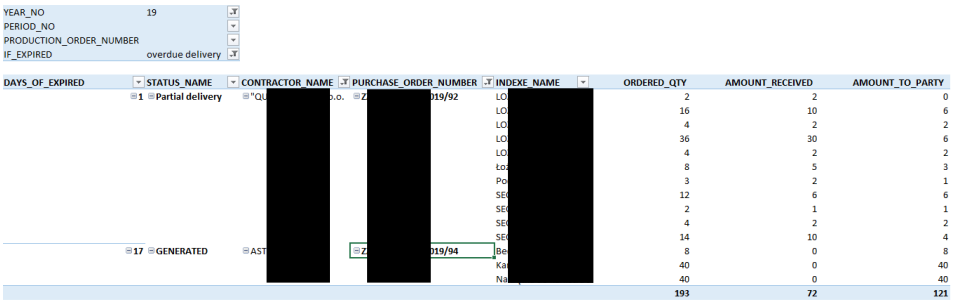

YEAR_NO	19
PERIOD_NO	
PRODUCTION_ORDER_NUMBER	
IF_EXPIRED	overdue delivery

DAYS_OF_EXPIRED	STATUS_NAME	CONTRACTOR_NAME	PURCHASE_ORDER_NUMBER	INDEXE_NAME	ORDERED_QTY	AMOUNT_RECEIVED	AMOUNT_TO_PARTY
1	Partial delivery	"QU [redacted]o.o.	Z [redacted]019/92	LO [redacted]	2	2	0
				LO	16	10	6
				LO	4	2	2
				LO	36	30	6
				LO	4	2	2
				to	8	5	3
				Po	3	2	1
				SE	12	6	6
				SE	2	1	1
				SE	4	2	2
				SE	14	10	4
17	GENERATED	AST	Z [redacted]019/94	Be	8	0	8
				Ka	40	0	40
				Na	40	0	40
					193	72	121

Fig. 7. Report of overdue deliveries

The second report (Fig. 8) informs one on deliveries of parts to a certain order planned for selected weeks. The dimensions of the OLAP cube ought to be "rotated". The main filter will be the number of the order and the following elements will be removed from the rows: number of days overdue, number of the order. Columns of the report will be the numbers of weeks for which the deliveries are planned.

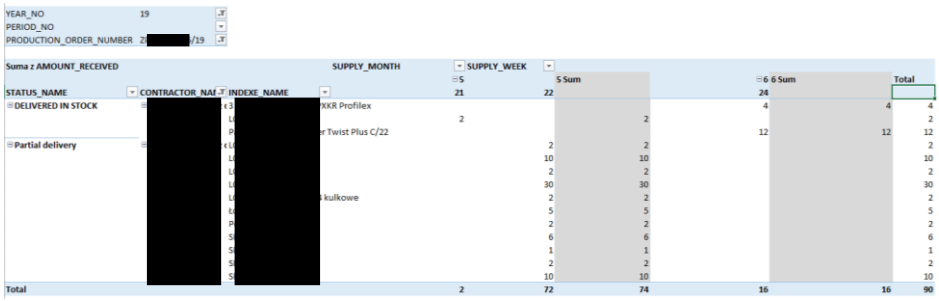

YEAR_NO	19						
PERIOD_NO							
PRODUCTION_ORDER_NUMBER	[redacted]						
Suma z AMOUNT_RECEIVED		SUPPLY_MONTH		SUPPLY_WEEK			
				5	5 Sum	6 6 Sum	Total
STATUS_NAME	CONTRACTOR_NAM	INDEXE_NAME		21	22	24	
DELIVERED IN STOCK	[redacted]	[redacted]	XKR Profilex			4	4 4
				2	2		2
			r Twist Plus C/22			12	12 12
Partial delivery				2	2		2
				10	10		10
				2	2		2
				30	30		30
			kulkowe	2	2		2
				5	5		5
				2	2		2
				6	6		6
				1	1		1
				2	2		2
				10	10		10
Total				2	72	74	16 16 90

Fig. 8. Delivery report until the production order

Report of deliveries planned for the current week (Fig. 9) was also created on the basis of the same data as the remaining compilations. The data was presented by properly selecting the dimensions in such a way that the created perspective answers the information need.

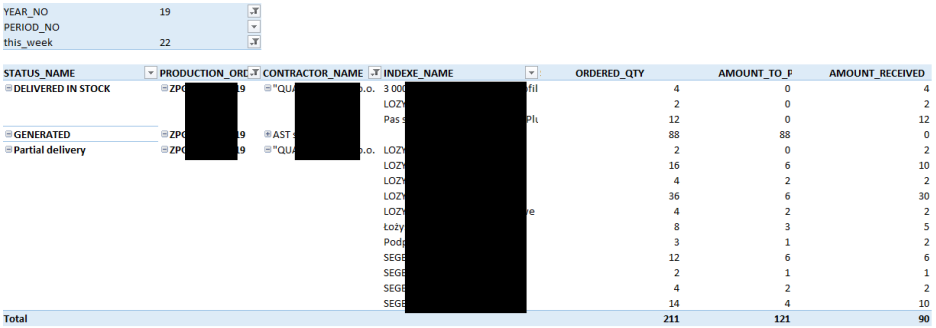

YEAR_NO	19						
PERIOD_NO							
this_week	22						
STATUS_NAME	PRODUCTION_ORD	CONTRACTOR_NAME	INDEXE_NAME		ORDERED_QTY	AMOUNT_TO_F	AMOUNT_RECEIVED
DELIVERED IN STOCK	ZP[redacted]19	"QU[redacted]o.	3 000[redacted]	fil	4	0	4
			LOZ		2	0	2
			Pas	Pl	12	0	12
GENERATED	ZP[redacted]19	AST			88	88	0
Partial delivery	ZP[redacted]19	"QU[redacted]o.	LOZ		2	0	2
			LOZ		16	6	10
			LOZ		4	2	2
			LOZ		36	6	30
			LOZ	e	4	2	2
			Łoży		8	3	5
			Podp		3	1	2
			SEGE		12	6	6
			SEGE		2	1	1
			SEGE		4	2	2
			SEGE		14	4	10
Total					211	121	90

Fig. 9. Report of deliveries planned for the current week

The data was presented in MS Excel, which is well-known to the employees. After a while of working with the report system a new information need was observed – **percent of order realisation for each index group for a certain order.** Since all the required data was already available within the structures of the OLAP cube the staff was able to create such a report (Fig. 10). Employing this solution allowed the company not only to avoid purchasing licences for the ERP system and its report module (as well as creating a new report), but also to gain a tool for the employees to independently fulfil their information needs.

The report system was implemented in a manufacturing enterprise from the sector of small and medium-sized enterprises. The main users were the staff from the department of logistics and purchases, production manager with the department of production planning and warehouse workers. Implementing a solution available for all those users enhanced communication between those units. Should a query about a certain delivery or project arise, the user was able to search the report system first and in the case of lack of information, contact the purchase department.

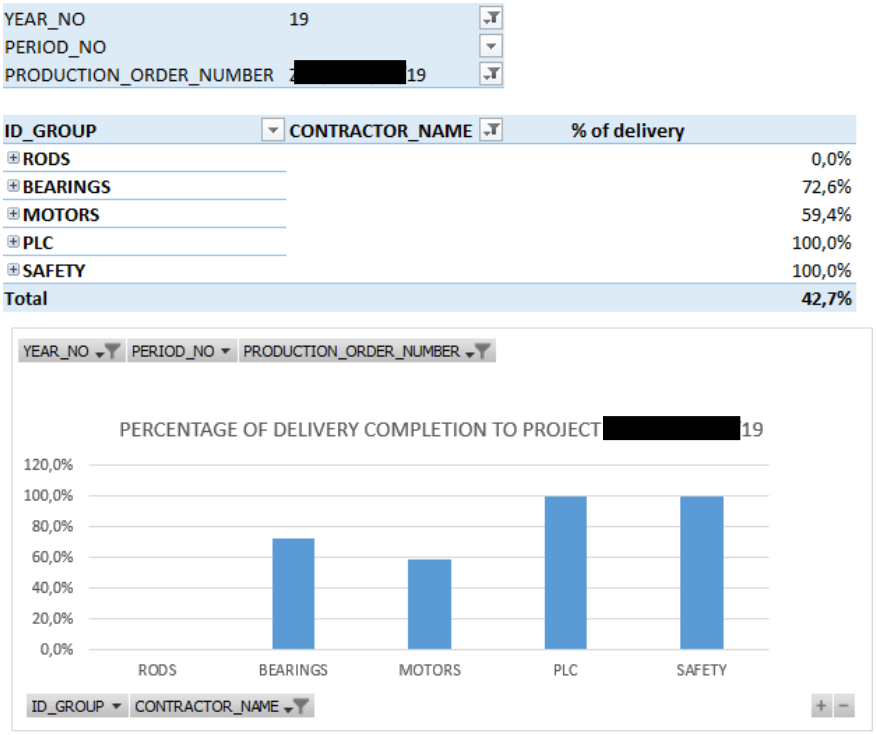

Fig. 10. View of the report for selected production orders

Moreover, communication with the purchase department was based on a given number of order. Previously the workers asked about the status of a part X in project A. Now, using numbers of orders (previously not available to the production department, since the data was stored in other modules of the ERP systems) facilitates searching the information in the purchase department. Apart from communication, operational planning was also enhanced. Production manager was able to plan the tasks for the upcoming week more efficiently and in-detail.

5. SUMMARY AND CONCLUSIONS

An efficiently functioning procurement department is one of the key elements of efficacy and low-cost of any production enterprise. Lack of timely delivery of elements results in production being stopped, which implicates high cost as well as loss of customers. On the other hand, purchasing too much too soon results in an increase of upkeep and stock depreciation.

Correct decision-making in terms of purchases requires access to aggregated data, which poses a serious problem in non-repetitive and multi-product manufacturing. Although the majority of manufacturing enterprises in developed

countries have access to more or less advanced ERP systems, it is often impossible access present information in a fast and aggregated manner, which is a key element in the decision-making process in a dynamic environment.

To address this problem in one of enterprises realising small-lot make-to-order production a report system based on business intelligence technology was implemented. OLAP cube technology allowed for multi-dimensional data analysis. On the basis of data in the ERP system it is possible to:

- Quickly generate a compilation of overdue deliveries,
- Generate information on the type of material ordered and delivered to the analysed production order,
- Preparing a compilation of orders planned for the current week.

In order to make this solution available for small and medium-sized enterprises it was decided to implement this report system to the widely known MS Excel. The solution presented in this study was implemented in the analysed enterprise.

REFERENCES

Alsoub, R.K., Alrawashdeh, T.A., & Althunibat, A. (2018). User acceptance for Enterprise Resource Planning Software Systems. *International Journal of Innovative Computing Information and Control*, *14*(1), 297–307. http://doi.org/10.24507/ijicic.14.01.297

Aremu, A.Y., Shahzad, A., & Hassan, S. (2019). The Empirical Evidence of Enterprise Resource Planning System Adoption and Implementation on Firm's Performance Among Medium-sized Enterprises. *Global Business Review*, UNSP 0972150919849751. http://doi.org/10.1177/0972150919849751

Bocewicz, G., Nielsen, I., & Banaszak, Z. (2016). Production Flows Scheduling Subject to Fuzzy Processing Time Constraints. *International Journal of Computer Integrated Manufacturing*, *29*(10), 1105–1127. http://doi.org/10.1080/0951192X.2016.1145739

Chang, Y.W. (2020). What drives organizations to switch to cloud ERP systems? The impacts of enablers and inhibitors. *Journal of Enterprise Information Management*, *33*(3), 600–626. http://doi.org/10.1108/JEIM-06-2019-0148

Cieśla, B., & Gunia, G. (2019). Development of integrated management information systems in the context of Industry 4.0. *Applied Computer Science*, *15*(4), 37–48. http://doi.org/10.23743/acs-2019-28

Danilczuk, W. (2019). Analiza danych produkcyjnych na podstawie transakcji w systemie ERP z wykorzystaniem technologii Business Intelligence. *Autobusy – Technika, Eksploatacja, Systemy transportowe*, *232*(7/8), 62–65. http://doi.org/10.24136/attest.2019.192

De Oliveira, A., & De Almeida, J.R. (2019). Business Intelligence Application for Multidimensional Analysis Risks in Complex Projects. *IT Professional*, *21*(6), 33–39. http://doi.org/10.1109/MITP.2018.2876931

Djiroun, R., Boukhalfa, K., & Alimazighi, Z. (2019). Designing data cubes in OLAP systems: a decision makers' requirements-based approach. *Cluster Computing* –

The Journal of Networks Software Tools and Applications, *22*(3), 783–803. http://doi.org/10.1007/s10586-018-2883-7

George, A., Schmitz, K., & Storey, V.C. (2020). A Framework for Building Mature Business Intelligence and Analytics in Organizations. *Journal of Database Management*, *31*(3), 14-39. http://doi.org/10.4018/JDM.2020070102

Gola, A. (2014). Economic aspects of manufacturing systems design. *Actual Problems of Economics*, *156*(6), 205–212.

GUS (2020, August 7). Wykorzystanie technologii informacyjno-komunikacyjnych w jednostkach administracji publicznej, przedsiębiorstwach i gospodarstwach domowych w 2019 roku. Retrieved from https://stat.gov.pl/obszary-tematyczne/nauka-i-technika-spoleczenstwo-informacyjne/spoleczenstwo-informacyjne/wykorzystanie-technologii-informacyjno-komunikacyjnych-w-jednostkach-administracji-publicznej-przedsiebiorstwach-i-gospodarstwach-domowych-w-2019-roku,3,18.html

Huang, S.Y., Chiu, A.A., Chao, P.C., & Arniati, A. (2019). Critical Success Factors in Implementing Enterprise Resource Planning Systems for Sustainable Corporations. *Sustainability*, *11*(23), 6785. http://doi.org/10.3390/su11236785

Januszewski, A. (2008). *Funkcjonalność informatycznych systemów zarządzania: Tom 1 Zintegrowane systemy transakcyjne*. Wydawnictwo Naukowe PWN.

Loudcher, S., Jakawat, W., Soriano Morales, E.P., & Favre, C. (2015). Combining OLAP and information networks for bibliographic data analysis: a survey. *Scientometrics*, *103*, 471–487. http://doi.org/10.1007/s11192-015-1539-0

Meilin, W., Xiangwei, Z., & Qingyun, D. (2010). An Integration Methodology Based on SOA to Enable Real-Time Closed-Loop MRP between MES and ERP. *2010 International Conference on Computing, Control and Industrial Engineering*, *1*, 101–105. http://doi.org/10.1109/CCIE.2010.33

Patalas-Maliszewska, J. (2012). Assessing the Impact of ERP Implementation in the Small Enterprises. *Foundations of Management*, *4*(2), 51–62. http://doi.org/10.2478/fman-2013-0010

Queiroz-Sousa, P.O., & Salgado, A.C. (2020). A review on OLAP Technologies Applied to Information Networks. *ACM Transactions on Knowledge Discovery from Data*, *14*(1), 8. http://doi.org/10.1145/3370912

Rodriguez, R., Molina-Castillo, F.J., & Svensson, G. (2020). Enterprise resource planning and business model innovation: process, evolution and outcome. *European Journal of Innovation Management*, *23*(4), 728–752. http://doi.org/10.1108/IJIM-04-2019-0092

Sobaszek, Ł., Gola, A., & Kozłowski, E. (2018). Job-shop scheduling with machine breakdown prediction under completion time constraint. *Annals of Computer Science and Information Systems*, *15*, 437–440. http://doi.org/10.15439/2018F83

Sobaszek, Ł., Gola, A., & Świć, A. (2020). Time-based machine failure prediction in multi-machine manufacturing systems. *Eksploatacja i Niezawodnosc – Maintenance and Reliability*, *22*(1), 52–62. http://doi.org/10.17531/ein.2020.1.7

Świć, A., & Gola, A. (2013). Economic analysis of casing parts production in a flexible manufacturing system. *Actual Problems of Economics*, *141*(3), 526–533.

Terkaj, W., Tolio, T., & Urgo, M. (2015). A virtual factory approach for in situ simulation to support production and maintenance planning. *CIRP Annals Manufacturing Technology*, *64*(1), 451–454. http://doi.org/10.1016/j.cirp.2015.04.121

Vargas, M.A., & Comuzzi, M. (2020). A multi-dimensional model of Enterprise Resource Planning critical successes factors. *Enterprise Information Systems*, *14*(1), 38–57. http://doi.org/10.1080/17517575.2019.1678072

Waters, D. (1996). *Operations Mangement: Producing Goods and Services*. Addison Wesley Longman Limited.

Yiu, L.M.D., Yeung, A.C.L., & Jong, A.P.L. (2020). Business intelligence systems and operational capability: an empirical analysis of high-tech sectors. *Industrial Management & Data Systems*, *120*(6), 1195–1215. http://doi.org/10.1108/IMDS-12-2019-0659

Zwolińska, B., Grzybowska, K., & Kubica, Ł. (2017). Shaping production change variability in relation to the utilized technology. *24th International Conference on Production Research, ICPR 2017*, 155812, 51–56.

Applied Computer Science, vol. 16, no. 3, pp. 56–68
doi:10.23743/acs-2020-21

Submitted: 2020-06-18
Revised: 2020-09-03
Accepted: 2020-09-21

Spoken Language Recognition, Computer Vision, Image Recognition, CNN

Nancy WOODS [0000-0001-8396-3467]*, *Gideon BABATUNDE**

A ROBUST ENSEMBLE MODEL FOR SPOKEN LANGUAGE RECOGNITION

Abstract

The identity of a language being spoken has been tackled over the years via statistical models on audio samples. A drawback of these approaches is the unavailability of phonetically transcribed data for all languages. This work proposes an approach based on image classification that utilized image representations of audio samples. Our model used Neural Networks and deep learning algorithms to analyse and classify three languages. The input to our network is a Spectrogram that was processed through the networks to extract local visual and temporal features for language prediction. From the model, we achieved 95.56 % accuracy on the test samples from the 3 languages.

1. INTRODUCTION

Speech is an important means of human communication. Recently, speech serves a means of interaction between machines and humans as seen in voice control and commands, map navigation/guide, robotics, intelligent assistants like "Siri", "Alexa","Bixby" e.t.c. Thoughts and ideas are exchanged through speech and statistics shows that there exist over 7,111 unique languages of the world (Eberhard, Simons & Fennig, 2020).

There are several attributes contained in speech utterance which can be extracted via machines, and over the years, efforts have been made by researchers to create methods for extracting the fundamental information which a speech utterance conveys. This led to the development of various extraction modules such as 'Speech to Text', Speaker Recognition, Topic Identification, Spoken Language Recognition and many ways to understand the semantic meaning which speech utterance coveys via machines. (Li, Ma & Lee, 2013).

* University of Ibadan, Faculty of Science, Department of Computer Science, Oyo State Ibadan, Nigeria, chyn.woods@gmail.com, gideonbabs2@yahoo.com

Spoken Language Recognition (SLR), also known as Automatic Language Identification, is the process by which the identity of a language in a given speech sample is detected. Spoken language recognition task is perceived as a pre-processing step for Speech technologies such as Automatic Speech Recognition. SLR can also be applied as a standalone task. (Zissman, 1993; Muthusamy, Cole & Oshika, 1992)

In the area of Spoken Language Recognition, studies have shown that it is part of human intelligence to distinguish between languages, and this is a natural ability we are born with (Zhao et al., 2008). It was also discovered that with minimal exposure to a language, humans can detect the identity of the language being spoken in a conversation with reference to languages they have heard or languages they know. Although these judgments may be less precise when hard decisions need to be made for an identification task, they show that human listeners can apply auditory perception with linguistic knowledge at different levels to distinguish between broad language groups (Li, Ma & Lee, 2013). Most SLR systems are based on high level features such as Frequency, Phonotactics, Prosodic and Acoustic-Phonetic Modelling. Such systems have an inherent problem: tokenizing the features accurately.

In this study we developed a model for Automatic Spoken Language Recognition Systems (ASLRs) from a Computer-vision perspective, using deep learning algorithms, similar to that proposed by (Bartz, Herold, Yang & Meinel, 2017). We proposed an ensemble of Convolutional Neural Network (CNN)-Recurrent Neural Network (RNN) algorithm. The system adopts existing algorithms, with a variant in network architecture on the deep learning techniques. Furthermore, training and testing of the system was carried out on 3 Spoken Nigerian Languages (English, Yoruba and Igbo). The research does not consider full development of a SLRs, nor the other aspects of Speech information extraction such as Automatic Speech Recognition (Speech to text transcription), Language Translation, Machine hearing/ Language understanding, linguistic analysis etc. Our approach is restricted to the computer vision perspective and not the advanced signal processing techniques or statistical modelling approach.

2. REVIEW OF RELATED LITERATURE

Language recognition systems are usually categorized by the features they use, such as the acoustic–phonetic approach, the phonotactic approach, the prosodic approach, and the lexical approach. More recently, newer features for identification have surfaced which do not fall into any of these categories thanks to deep learning. These are lower level features like ‘Spectrogram images extracted from sounds. The mainstream research on spoken language recognition adopts techniques utilizing these higher level features (Torres-Carrasquillo et al., 2002).

Acoustic Phonetics refers to the wide range of sounds that the human speech apparatus is capable of producing. Speech sounds as concrete acoustic events are referred to as phones. Whereas speech sounds as entities in a linguistic system are termed as phonemes (Kirchhoff, 2006). The phonotactic constraints dictate the permissible phone sequences. Each language has its unique set of lexical–phonological rules that govern the combinations of different phonemes. Phonemes can be shared considerably across languages, but the statistics of their sequential patterns differ very much from one language to another. Prosody refers to supra-segmental features in running speech, such as stress, duration, rhythm, and intonation (Ashby & Maidment, 2005). The set of interrelated prosodic features are all important characteristics of spoken languages. Prosody appears to be useful for distinguishing between broad language classes (e.g., tonal versus non-tonal languages). However, human listening experiments reported in (Navratil, 2001), and (Ramus & Mehler, 1999) show that prosodic cues are less informative than the phonotactic one. In the past few decades, researchers have explored many speech and language knowledge sources, including articulatory parameters, acoustic features (Sugiyama, 1991), prosody (Adami & Hermansky, 2003), phonotactic (Zissman, 1996), and lexical knowledge (Adami & Hermansky, 2003).

(Safitri, Zahra & Adriani, 2016) carried out a study involving the identification of spoken data in three local Indonesian languages: Minangkabau, Sundanese and Javanese. In their study, two phonotactic methods were used, namely Phone Recognition followed by Language Modelling (PRLM) and Parallel Phone Recognition followed by Language Modelling (PPRLM). PRLM method showed the highest accuracy using the phone recognizer trained for English and Russian with the average of 77.42% and 75.94% respectively. From their study, observation was made that accuracy of Spoken LID system with PRLM and PPRLM methods are affected more by the performance of phone recognizer that is used.

In the study carried out by (Boussard, Deveau & Pyron, 2017), several machine learning techniques for classifying spoken language were explored. They applied algorithms which utilized various spectral features derived from English and Mandarin Chinese phone call audio to predict the language of conversation. They assert that to a large extent, a language is not distinguished by the presence of certain sound waves, but rather by the patterns they form and the sequence in which they are produced. The information was incorporated explicitly via Shifted Delta Cepstrum (SDC) features and using Gaussian Mixture Method (GMM) and neural network models, they were able to effectively capture this crucial information, leading to improved predictive power. The modelling assumptions of the GMM ultimately turned out to be vital since they had only limited data.

According to (Abdel-Hamid et al., 2014) exploration of Deep Neural Networks (DNN) revealed that the hybrid deep neural network (DNN)-hidden Markov model (HMM) showed significant improved speech recognition performance over the conventional Gaussian mixture model (GMM)-HMM. This improvement is attributed to the inherent ability of DNN's to model complex correlations

in speech features. Their study attempted to further reduce error rate in the underlying model by using Convolutional Neural Networks (CNNs).

These studies, among several others, have shown that high accuracies in language recognition can be achieved, depending on the adopted model for development of the SLRs. To this effect, we undertook our study exploring a different approach that was motivated by the recent successes in the area of deep learning and Computer Vision.

3. METHODOLOGY

The field of Computer vision deals with utilization of techniques to help machines understand the content of digital images. It involves the extraction of information from images to infer something about a real world problem. The application of computer vision techniques to this problem domain, meant audio samples had to be represented with images for further processing. We applied Convolutional Neural Network-Recurrent Neural Network (CNN-RNN) in an ensemble, to the development of our model for SLRs thus, the approach is image processing based. More specifically, these Deep Neural Networks were adapted to the problem of identifying the language of a given spoken utterance from short-term spectral features.

3.1. Dataset

Our model was trained and tested using the three languages: Yoruba (Ibadan dialect), Igbo, and English. Audio recordings of conversations in all the three languages were acquired from various sources such as Radio streams, Video Streams and other available online corpus for research purposes (Kaggle, Librovox). These audio samples served as the dataset. The total data set consists of over 2100 wav and mp3 files, with an average of 700 samples per language.

Tab. 1. Size of the Dataset

Language	Length of Files (secs)	Average Time (secs)
English	$2 < X < 5$	3
Igbo	$4 < X < 10$	5
Yoruba	$2 < X < 8$	5

From these 2100 files, we separated 80% of the sample files for training and the rest for validation and testing. The recordings had varying length of approximately 10 seconds. Some of the audio files contained background noise, intermittent laughter, music and other unwanted properties while some samples were noise free.

3.2. Pre Processing

As part of our pre-processing step, all the mp3 format files were first converted to a lossless wav format at a 22050 kHz/16bit sampling rate. We investigated audio specific techniques to denoise and remove unwanted properties of our audio samples and resorted to manually denoising each file thereby utilizing an audio engineering tool called FL Studio (Fig. 1). We removed unnecessary silences between sentences, intermittent jingles or unwanted background sounds and we removed noise stemming from recording apparatus (mic and general audio recording setup), while maintaining characterizing features of the Samples. This process produced clean versions of the audio samples as wav files.

Fig. 1. Wav Sample Pre-processing

In other to adopt an image processing approach to the Language recognition problem rather than the conventional audio processing approach, an image representation of the audio sample was utilized. We discovered that spectrograms (Fig. 2) are the standard ways to represent audio for deep learning systems from our investigations and also according to recent studies (Park et al., 2019; Amodei et al., 2015). Spectrograms are 2D visual representations of audio frequency spectra over time. The image depicts the intensity of sound around certain frequencies as time varies. A major point about speech is that the sounds generated by humans are filtered by the shape of the vocal tract including tongue, teeth, etc. This shape determines what comes out, and it gives an accurate representation of the phoneme being produced. More specifically, the shape of the vocal tract manifests itself in the envelope of short term power spectrum, and the job of the Mel-scepstrum is to accurately represent this envelope. Mel-Spectrogram images of our training files were created, and these mel-spectrogram images serve as the input to our DNN-based model.

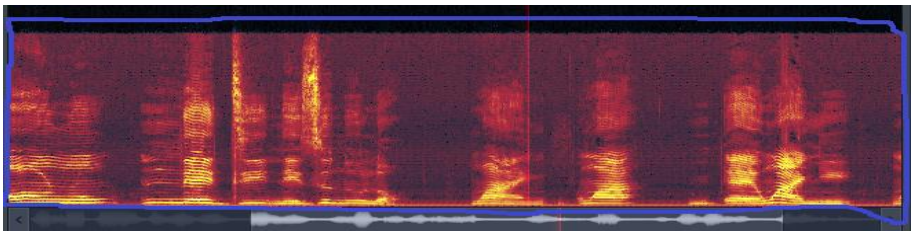

Fig. 2. Sample of Spectrogram Image of an Audio file

The mel-spectrogram can be viewed as a sequence of column vectors that consist of 256 (or 128, if only <5.5 KHz frequencies are used) numbers. We considered only frequencies of less than 5.5 KHz.

3.3. Network Architecture (CNN-RNN Ensemble)

As illustrated in Figure 3, the overall architecture of our model comprised of 3 stages. In the first stage, a convolutional feature extractor was utilized. The convolutional feature extractor transformed our input (Spectrogram image of recordings) into a feature map through several series of processing. This CNN algorithm was used in the model because they can transform high level information in images with great capacity thereby improving predictive power of our model. The output of the convolutional neural network (feature map) was then fed into a variant of the Recurrent Neural Network (RNN) architecture known as the Bi-directional Long-short term memory (having two LSTM layers). This Bi-LSTM was introduced in the model due to their ability to store information of both past and future sequences at the same time, such that at every point in time large, information is available to the model thereby improving chances of obtaining higher classification accuracy. The data sequence (RNN's Output) is further passed to a fully connected layer in order to solidify training efficiency of our model. Finally, a Softmax layer was introduced for classification purpose. The output of the model is the detected language.

20% dropout was factored in our model in order to reduce overfitting in the network. The Activation function, Rectified Linear Units activation function (ReLU) was used in this model to increase non linearity of the CNN. We also utilized batch normalization in the model to increase the stability of the neural network. This model used Adam optimization algorithm instead of the classical stochastic gradient descent procedure to update the network weights.

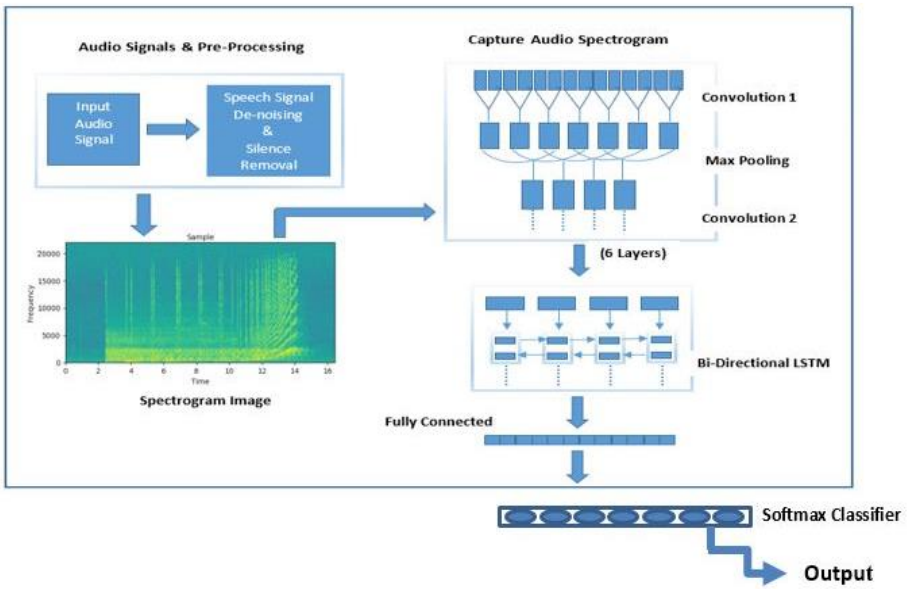

Fig. 3. Model for Spoken Language Recognition

3.3.1. Convolutional Neural Network

CNN's have the ability to capture and transform high level images with great capacity and our model leveraged on this property to explore its performance on the input features (Spectrogram images). As shown in Figure 4, the network had 6 convolutional layers thus a deep convolutional network. It consisted 6 blocks of 2D convolution, ReLU nonlinearity, 2D max pooling between each layer and batch normalization. 3x3 filters was used for all the convolutional layers with a stride 1. Pooling size was always 3x3 with a stride 2. The network used "Same" padding throughout. Learning rates were set to be higher for the first convolutional layers and lower for the top convolutional layers. We trained the CNN on Keras framework with Python with 32 images in a batch. This significantly increased the training speed.

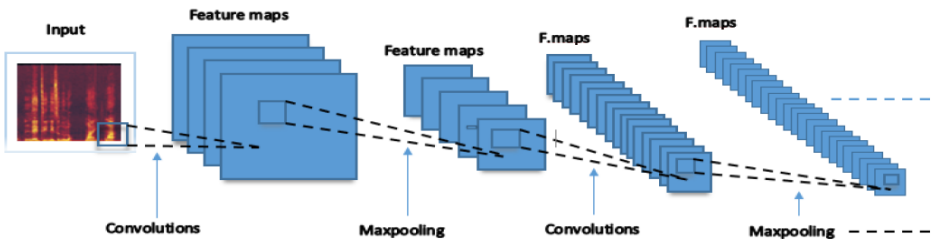

Fig. 4. Convolutional Neural Network Architecture

3.3.2. Recurrent Neural Network

The RNN accounts for the sequential characteristic of the audio data; therefore we applied a Bi-directional long short term memory (BLSTM). As shown in Figure 5, the output of the CNN were sets of several channels (*feature maps*). These feature maps were then reshaped to the RNN input dimension (which takes 3dimensional input). Two layers of LSTM in opposite directions captured and stored information on sequences from the past and future set. These units then combine and were fed to a fully connected layer. The Bi-directional LSTM makes large amount of information available in the network.

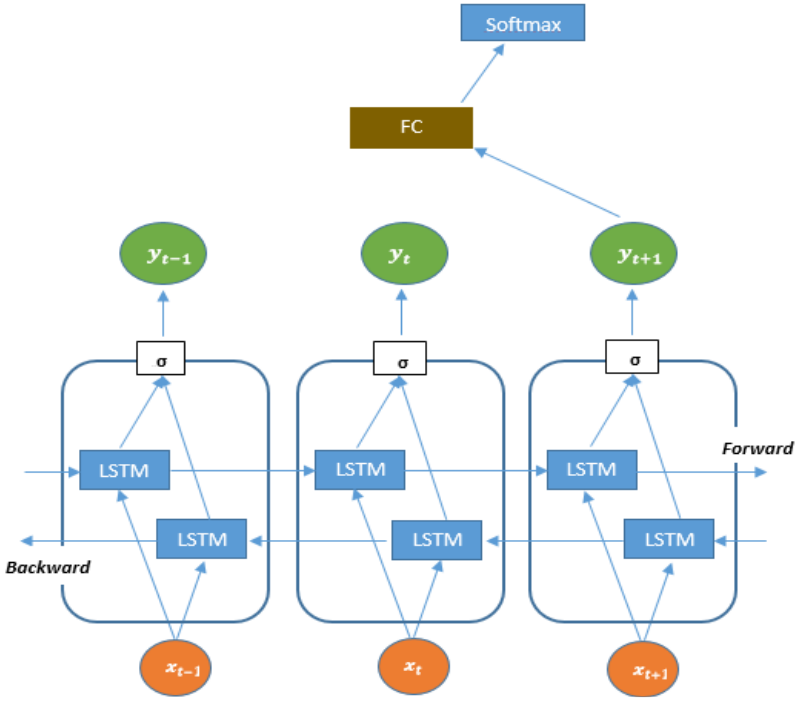

Fig. 5. Bi-directional Long Short Term Memory–RNN

Finally we used only 1 fully connected layer between the RNN (Bi-directional LSTM) and the Softmax layer, and apply 20% dropout on that. The fully connected layer had 64 neurons and was trained using a Softmax loss. The output of the Softmax layer is the predicted language. We utilized Keras framework for Model implementation.

4. RESULT

Our system was trained on 1,437 samples and tested with 360 samples all comprising the 3 languages. Although we had over 2100 files in our dataset, some samples were discarded during the processing stage, because we wanted a uniform dimension (128 x 128) for all our spectrogram images for less than 3secs of spoken utterance (~3s). The CNN algorithm which was used required uniformity for all training set, as such, all samples that did not meet this shape were discarded. For over 100 Epochs, the accuracy of the model was given at 95.56%

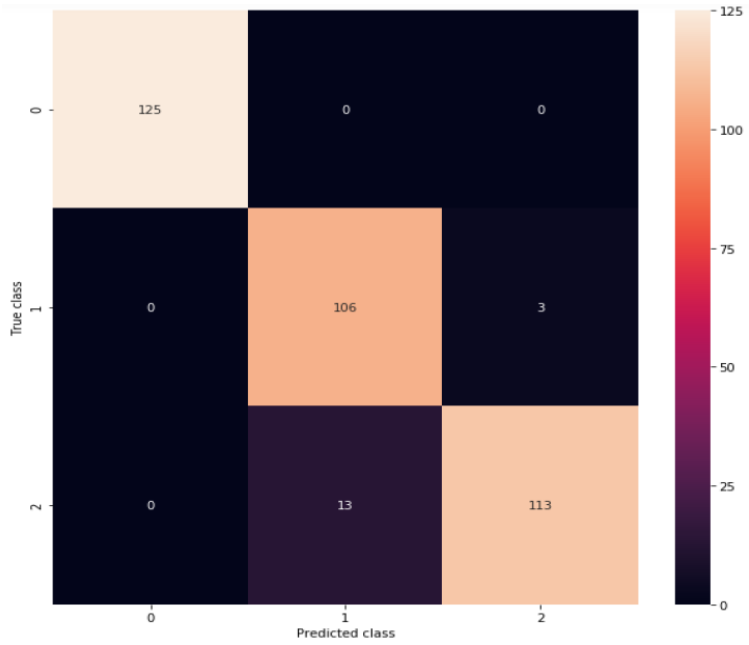

Fig. 6. Confusion Matrix

Shown in Figure 6 is the confusion matrix which depicts the classification correctness of the model. It shows the predicted class and the true class and shows where the classification lies for every input. We worked on 3 Languages (English, Yoruba, and Igbo) therefore an audio sample having an utterance or conversation in any of the languages should be detected by the model by correctly classifying it in one of the 3 classes. The English language was labelled with index 0, Yoruba was labelled with index 1 and Igbo language was labelled with index 2. We tested 125 English samples with the model, and it classified all 125 samples correctly (as belonging to English class-index 0). From observation, there was no mis-classification, hence the predicted class and the true class match. For Yoruba language, 109 audio samples were tested on the model, and from that, 106 were

accurately classified while 3 samples were misclassified as Igbo. And finally, for the Igbo language, 126 test samples were tested on the model, 113 were classified correctly, while 13 samples were misclassified as Yoruba language.

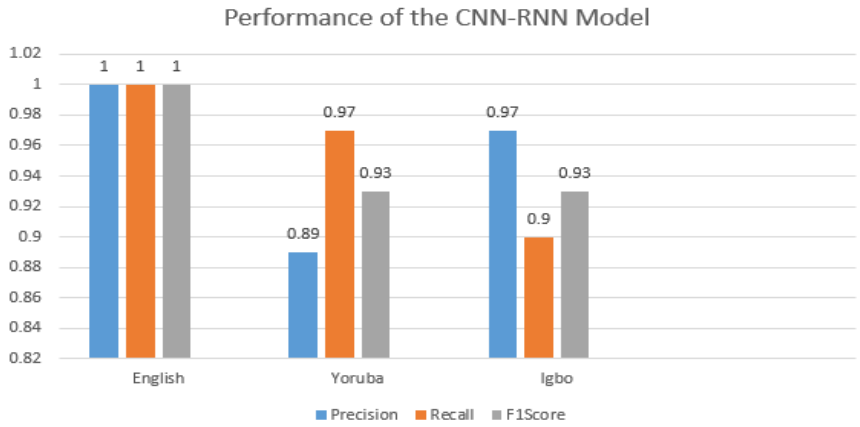

Fig. 7. Model evaluation using Precision, recall, and F1 Score as metrics

Figure 7 depicts the performance of the model in terms of precision, accuracy, and the F1 score. The precision values show the extent to which the model captures the true classes of a sample out of the total. It is a ratio of correctly predicted positive observations to the total predicted positive observations. And from the chart, we see that English has the highest precision value followed by that of the Igbo language and then the precision of the Yoruba classification is fair in relative terms. The recall value depicts that given the total test samples, how many elements were captured.it is the ratio of correctly predicted positive observations to the all observations in actual class.

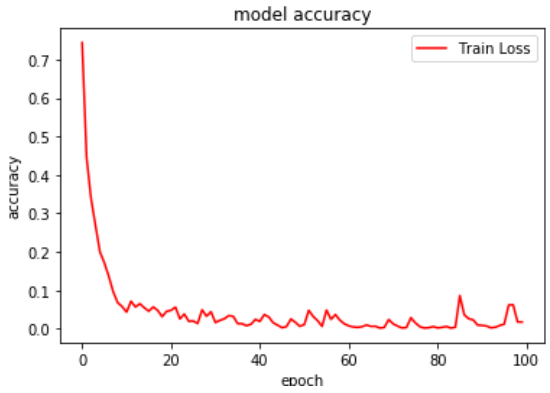

Fig. 8. Training Loss of the Model

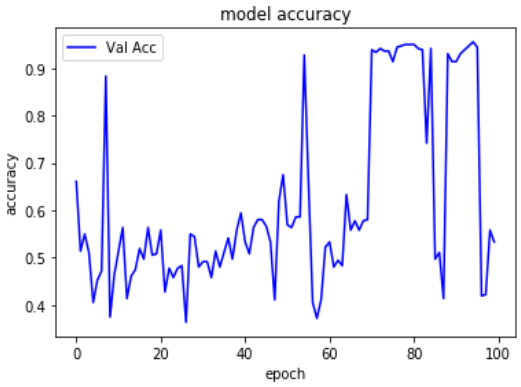

Fig. 9. Validation Accuracy of the Model

From Figure 8, it is observed that over 100 epochs of training the loss (which is the degree of error) is actually minimized. This shows that the level of accuracy of the model after training is very near optimum, which is a desired property in every model. From figure 9, it is observed that validation accuracy fluctuates but becomes stable towards last few epochs. This is also a desired property which shows that the model can be functional.

5. CONCLUSION

The high performance of our CNN-RNN deep learning algorithm based model for SLR shows that approaching the Language recognition problem domain from an Image classification perspective yields comparable optimal performance to the mainstream phonological computational and statistical modelling approach. This observation also shows that using intermediate features such as a Spectrogram is adequate enough to obtain improved performance for SLRs, thereby eliminating the need for large corpus bearing phonetically transcribed data.

Based on the performance of the system on short speech excerpts, we infer that the system can classify even short speech utterances of less than 3s (~3s) thus, it is a long enough interval to classify a spoken language correctly with this model. Noises in speech samples affect SLR performance considerably as observed in our experiments. The observation made was that the English samples were properly classified due to the very minimal noise contained in the training sample. The English dataset had far less noise because it was created specifically for training purposes (Kaggle, Librovox), while the Yoruba and Igbo language testset had some misclassifications stemming from the noise contained in the Training set. Although these samples went through series of denoising, they were not as clean as that of the English because they contained white-noise which is almost impossible to completely remove. The white-noise was from the recording apparatus in the radio station.

We observed that the architecture of the deep learning model used for developing SLR's is pertinent to the performance of a model, therefore we recommend the exploration of deeper architectures for future works. Google's Inception v3 is one of such networks which has much more layers in its architecture and is considered deeper than ours. We believe a deeper network should be able to extract more general features thus leading to increase in accuracy although they come with an increase of computational cost, as the Inception-v3 model uses up to six times more parameters, than a regular CNN. We also suggest utilizing completely noise free samples as dataset for training models.

REFERENCES

Abdel-Hamid, O., Mohamed, A. R., Jiang, H., Deng, L., Penn, G., & Yu, D. (2014). Convolutional neural networks for speech recognition. *IEEE Transactions on Audio, Speech and Language Processing*, *22*(10), 1533–1545. https://doi.org/10.1109/taslp.2014.2339736

Adami, A., & Hermansky, H. (2003). Segmentation of speech for speaker and language recognition. *EUROSPEECH-2003* (pp. 841–844). Geneva. Retrieved from https://www.academia.edu/32317887/Segmentation_of_speech_for_speaker_and_language_recognition

Amodei, D., Anubhai, R., Battenberg, E., Case, C., Casper, J., Catanzaro, B., ... Narang, S. (2015). Deep Speech 2: End-to-End Speech Recognition in English and Mandarin. *CoRR, abs/1512.02595*. Retrieved from https://arxiv.org/abs/1512.02595v1

Ashby, M., & Maidment, J. (2005). *Introducing phonetic science*. Cambridge University Press.

Bartz, C., Herold, T., Yang, H., & Meinel, C. (2017). Language Identification Using Deep Convolutional Recurrent Neural Networks. In D. Liu, S. Xie, Y. Li, D. Zhao, & E. El-Alfy (Eds.), *Neural Information Processing ICONIP 2017. Lecture Notes in Computer Science* (vol. 10639). Springer. https://doi.org/10.1007/978-3-319-70136-3_93

Boussard, J., Deveau, A., & Pyron, J. (2017). *Methods for Spoken Language Identification*. Retrieved from http://cs229.stanford.edu/proj2017/final-reports/5239784.pdf

Eberhard, D. M., Simons, G. F., & Fennig, C. D. (Eds.). (2020). *Ethnologue: Languages of the World*. Retrieved from http://www.ethnologue.com

Kirchhoff, K. (2006). Language characteristics. In T. Schultz, & K. Kirchhoff (Eds.), *Multilingual Speech Processing* (pp. 5–33). Elsevier.

Li, H., Ma, B., & Lee, K. A. (2013). Spoken Language Recognition: From Fundamentals to Practice. *Proceedings of the IEEE, 101*(5), 1136–1159. https://doi.org/10.1109/JPROC.2012.2237151

Muthusamy, Y. K., Cole, R., & Oshika, B. (1992). The OGI multi-language telephone speech corpus. *Int. Conf. Spoken Lang. Process*, 895-898. Retrieved from https://pdfs.semanticscholar.org/aad7/274fdd57191e89f9df2880a50ec14581d671.pdf

Navratil, J. (2001). Spoken language recognition A step toward multilinguality in speech processing. *IEEE Trans. Speech Audio Process*, *9*(6), 678–685. https://doi.org/10.1109/89.943345

Park, D. S., Chan, W., Zhang, Y., Chiu, C.-C., Zoph, B., Cubuk, E. D., & Le, Q. V. (2019). SpecAugment: A Simple Data Augmentation Method for Automatic Speech Recognition. *Proc. Interspeech 2019* (pp. 2613–2617). https://doi.org/10.21437/interspeech.2019-2680

Ramus, F., & Mehler, J. (1999). Language identification with suprasegmental cues: A study based on speech re-synthesis. *Journal of Acoustical Society of America*, *105*(1), 512–521. https://doi.org/10.1121/1.424522

Safitri, N. E., Zahra, A., & Adriani, M. (2016). Spoken Language Identification with Phonotactics Methods on Minangkabau, Sundanese, and Javanese Languages. *Procedia Computer Science 81* (pp. 182–187). Elsevier. https://doi.org/10.1016/j.procs.2016.04.047

Sugiyama, M. (1991). Automatic language recognition using acoustic features. *International Conference on Acoustics, Speech, and Signal Processing* (pp. 813–816). Toronto. https://doi.org/10.1109/icassp.1991.150461

Torres-Carrasquillo, P., Singer, E., Kohler, M., Greene, R., Reynolds, D., & Deller, J. (2002). Approaches to language identification using Gaussian mixture models and shifted delta cepstral features. In *ICSLP-2002* (pp. 89–92). Denver. https://doi.org/10.1109/icassp.2002.5743828

Zhao, J., Shu, H., Zhang, L., Wang, X., Gong, Q., & Li, P. (2008). Cortical competition during language discrimination. *NeuroImage*, *43*(3), 624–633. https://doi.org/10.1016/j.neuroimage.2008.07.025

Zissman, M. (1996). Comparison of four approaches to automatic language identification of telephone speech. *IEEE Transactions on Speech and Audio Processing*, *4*(1), 31–44. https://doi.org/10.1109/icassp.1993.319323

Zissman, M. A. (1993). Automatic language identification using Gaussian mixture and hidden Markov models. *IEEE International Conference on Acoustics, Speech and Signal Processing* (Vol. 2, pp. 399–402). IEEE. https://doi.org/10.1109/tsa.1996.481450

Applied Computer Science, vol. 16, no. 3, pp. 69–79
doi:10.23743/acs-2020-22

Submitted: 2020-09-18
Revised: 2020-09-24
Accepted: 2020-09-25

*wavelength, hue angle, chroma, CIE (L*a*b*)*

Karolina FERYSIUK[*[0000-0002-5246-0207]],
Karolina M. WÓJCIAK[*[0000-0002-4202-433X]],
Paulina KĘSKA[*[0000-0002-2668-2025]],
Dariusz M. STASIAK[*[0000-0002-6172-3013]]

INSTRUMENTAL COLOR MEASUREMENT OF MEAT AND MEAT PRODUCTS IN X-RITECOLOR® MASTER

Abstract

The aim of the study was to evaluate the influence of lyophilized plant extract on color of canned meat with reduced amount of sodium (III) nitrite measured by spectrophotometric methods. The results were collected through the X-RiteColor® Master software. The results of the experiment show that reduction of nitrite salt is possible but additional fortification is required: the best results were obtained when the extract was added in the amount of 0.015%.

1. INTRODUCTION

Color of meat is one of the most important factors which influence the consumer's decision about purchase (Suman & Joseph, 2013; Mancini & Hunt, 2005; León et al. 2006; Trinderupet, Dahl, Jensen, Carstensen & Conradsen, 2015). Color criteria is used to select or reject products and generally depends on myoglobin, the primary red pigment in meat. Evaluation of meat color is an essential part of product development and identification of roots of processing problems. Instrumental measure of color parameters is powerful laboratory method used by meat scientists. However, properly designed procedures are especially important. A lot of scientific publications present inconsistent and incomplete information especially regarding the aperture size, angle of observation, kind of illuminant (Tapp, Yancey & Apple, 2011).

[*]Department of Animals Raw Materials Technology, Faculty of Food Science and Biotechnology, University of Life Sciences in Lublin, Skromna 8 Street, 20-704 Lublin, Poland, karolina.ferysiuk@student.up.edu.pl, karolina.wojciak@up.lublin.pl

Barkley et al. (2018) reported weak influence of the kind of used apparatus and number of replications on color value. Therefore, the location of measurements is more important when performing color evaluations, assuming the settings are the same. Especially, the parameters of meat color strongly depend on oxygenation level and storage conditions of meat. Highly oxygenated beef steaks are redder than steaks in air and they show significant detrimental effects when frozen storage is extended (Henriott et al., 2020).

Basic standards and procedures of metrology in the fields of light and lighting are published by CIE (Commission Internationale de l'Eclairage) with Central Bureau in Vienna, Austria. The CIELAB color space (also known as CIE L*a*b*) describes all the colors visible to the human eye, defines colors independently of how they are created or displayed and is device-independent. It was defined in 1976. The color of sample is expressed as three values: L* for the lightness from black (0) to white (100), a* from green (−) to red (+), and b* from blue (−) to yellow (+). This model is perhaps the most frequently mentioned in scientific publications (Mancini & Hunt, 2005). It can be transferred to other spaces such as CIEXYZ, CIELCh, CIELUV, Hunter Lab.

The protein responsible for meat color is myoglobin (Mb) – a sarcoplasmic heme protein. In muscle of living animals, Mb is also responsible for, among others, oxygen transportation. Depending on iron atom's structure, Mb can exist in oxidized (Fe^{3+}) or reduced (Fe^{2+}) forms. Thanks to various forms of Mb meat and meat products can present different palette of colors: bright-red, purplish-pink or dull brown (Suman & Joseph, 2013; Danijela et al., 2013). The forms of Mb in reduced state are: deoxymyoglobin (DeoxyMb) – related with meat freshness and is characterized by purplish-red/purplish-pink color, oxymyoglobin (OxyMb) and carboxymyoglobin (COMb) - characterized by bright cherry-red color (Suman & Joseph, 2013; Danijela et al., 2013; Mancini & Hunt, 2005). The discoloration of Mb – the change from OxyMb to MetMb (metmyoglobin) – is associated with the oxidation of the heme group central iron atom. MetMb has gray-red/brownish color (Faustman, Sun, Mancini & Suman, 2010; Suman & Joseph, 2013; Danijela et al., 2013). This color of meat can also be formed as a result of pathogenic bacteria growth (Danijela et al., 2013).

The color of meat is possible to control – in case of fresh meat various packaging methods are applied: e.g. MAP (Modified Atmosphere Packaging) when different ratio of gases (the most common are CO_2, CO, O_2 and N_2) are applied or vacuum packaging through the removal of all the air from the package (Danijela et al., 2013). In the processed meat products, the characteristic pink color is an effect of reaction between sodium nitrite salt ($NaNO_2$) and metmyoglobin. During complicated reaction steps, nitric oxide (NO) formed from $NaNO_2$, reacts with Mb and creates NO-Mb (unstable) which, under the heat treatment, is converted into stable, pink nitrosylhemochrome (Suman & Joseph, 2013).

Oxidation process leads to deterioration of smell, taste, nutritional value of the product and it negatively influences its color. All these factors deteriorate the quality of the product which becomes unsafe for consumption (Ribeira et al., 2019). Additive E 250 – sodium III nitrite – plays a crucial role in meat industry. It not only allows to generate desirable color of meat products but also presents strong protecting (antioxidant, antibacterial) properties. And these properties also translate into, among others, maintaining the characteristic color (Gassara, Kouassi, Brar & Belkacemi, 2016; Alahakoona, Jayasena, Ramachandra & Jo, 2015).

Unfortunately, nitrite addition contributes to the formation of N-nitrosamines – cancerogenic, genotoxic substances (European Food Safety Authority, 2017). N-nitrosamines can occur in final products due to heat treatment or in specific conditions (low pH) such as in human gastrointestinal tract (Food Chain Evaluation Consortium, 2016).

For this reason, the amount of sodium (III) nitrite must be limited. The amount of 0–15 mg/kg of nitrite salt allows the nitrosylomioglobin formation but the amounts of 55–70 mg/kg allow to create proper color in meat products (other than dry fermented ones) (Rivera, Bunning & Marti, 2019; Food Chain Evaluation Consortium, 2016). However, apart from the appearance, product must be safe for consumption. Therefore, the Food Chain Evaluation Consortium (2016) concluded that lowering the nitrite addition, to the amount of 80–100 mg/kg (for most types of meat products) is possible but with additional measures to ensure safe consumption.

Color, like other factors such as antioxidant value, are important parameters for determining the quality, durability and safety of food (Ferysiuk & Wójciak, 2019).

The aim of the research was to determine the color of the canned meat containing reduced by half amount of nitrite and fortified with the addition of plant extract contrary to the control sample.

2. MATERIAL AND METHODS

2.1. Preparation of canned pork

Canned pork was prepared from pork dewlap and pork shoulder obtained from an organic farm (Zakład Mięsny Wasąg SP. J.). The recipe for all variants was: 5% of water, 2% of salt and alternatively: control sample – 100 mg/kg or sample fortified with herb extract – 50 mg/kg of sodium (III) nitrite. Meat was then cut with knife, grinded (KU2-3E – Mesko-AGD, Poland) on 5 mm mesh and mechanically mixed with above mentioned components. Each steel can was next filled with 300 g of meat, closed with lid and treated in temperature 120°C in a vertical steam sterilizer (AS2, Poland) and lastly cooled with fresh cold water. The obtained sterilizing value (F0) measured with TrackSense® wireless temperature logger (Ellab A/S, Denmark) placed in one of cans was 7,1. Products were then chilled at 4°C and stored for 60 days.

2.2. Color attributes

The samples intended for color testing were prepared as follows: the meat was removed from the can, cleaned of jelly and sliced (30 mm thickness). Measurement was taken after 10 min of product stabilization at normal laboratory conditions (air temperature 20°C, daylight app. 700 lx). The color was determined using the CIELAB color space (Hunt, 1987).

The X-Rite Color 8200 series spectrophotometer (X-Rite Inc., MI, USA) was used. The aperture size was 13 mm, standard observer 10˚ and illuminant D65 (daylight 6500K) was used. The measurement was taken in extended wavelength range from 360 to 740 nm. The color was measured at three different places of each slice surface.

2.3. Color parameters

Amount of MetMb – metmyoglobin was calculated according to Wójciak & Dolatowski (2015) from the reflectance measured at 580 nm and expressed as the percentage. The color difference was calculated according to Mokrzycki & Tatol (2011) using formula CIE76 (1)

$$\Delta E = \sqrt{(\Delta L)^2 + (\Delta a)^2 + (\Delta b)^2} \quad (1)$$

where: ΔE – color distance between two colors,
ΔL – difference of lightens of two colors,
Δa – difference of redness of two colors,
Δb – difference of yellowness of two colors.

3. THE CIELAB METHOD MEASUREMENT

Color measurement is possible thanks to the spectrophotometer (Fig. 1). The device must be connected to the computer unit; the recommended software for X-Rite Color 8200 series spectrophotometer is X-RiteColor® Master. This type of devices includes transmittance chamber, port reducer, sample holder hook and power switch.

In general, color can be expressed by a various system applied for measurement using spectrophotometer and colorimeters. Those instruments allow to choose apparatus sizes, observers, solo systems and illuminates (Mancini & Hunt, 2005). CIELAB space takes into account the lighteness/luminance (L*), color space from green to red (a*), and color space from blue to yellow (b*). The lightness values range from 0 (dark) to 100 (white). The a* and b* parameters range from -120 to 120 (León, Mery, Pedreschi & León, 2006).

Except for the lightness, redness and yellowness measurements it is also possible to define other parameters by calculating selected reflectance in their wavelengths (Khatri et al., 2012). The various form of Mb is possible to identify by applying spectrophotometric method at the wavelength between 500 and 600 nm (Suman & Joseph, 2013). It is also possible to calculate the differences between samples (ΔE (total color differences), hue angle (h°) and chroma (C).

The ΔE present the change in color over a selected period of time (AMSA, 2012), the differences can be described as small differences (1.5 < ΔE), distinctive (1.5 < ΔE < 3) or very distinctive (ΔE < 3) (Pathare, Opara & Al-Said, 2013). Mokrzycki & Tatol (2011) suggest another classification: 0 < ΔE < 1 – no differences are noted by observer, 1 < ΔE < 2 – differences are noted only by experienced observer, 2 < ΔE < 3.5 – differences are noted by unexperienced observer, 3.5 < ΔE < 5 – clear differences are noted, 5 < ΔE – two different colors are noted by observer.

For calculating the h° parameter, which represents the whole color spectrum and which takes values from 0° to 360°, this equation should be applied (2):

$$h° = arctan\frac{b^*}{a^*} \tag{2}$$

According to Yancey & Kropf (2008), the combination of those two color parameters is vital when the result of the equation has a positive value (h° is between 0° and 90°). When result of the equation is a close to number 0, the value of red parameter (a*) decreases, h° increases and its value is closer to 90°. When the red color becomes stronger, the situation is reverse.

Chroma (saturation index) is calculated from (3):

$$C = (a^{*2} + b^{*2})^{1/2} \tag{3}$$

More options for parameter calculation can be found in the guidelines created by American Meat Science Association (2012).

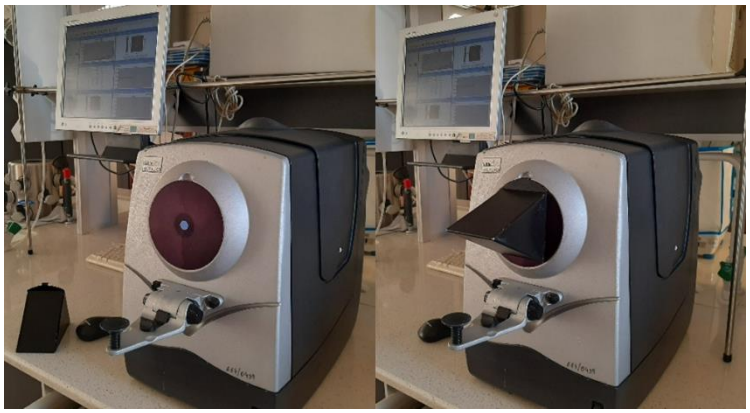

Fig. 1. The spectrophotometer before (left photo) and during calibration process (right photo)

Spectrophotometer must be calibrated before each use through calibration standards applied (Fig. 2) via computer program (Fig. 3). The light trap standard is used for zero reflectance measurement, the SRM is a white standard. X-RiteColor® Master program allows the calibration and configuration of the instrument and also the sample measurements (Fig. 4).

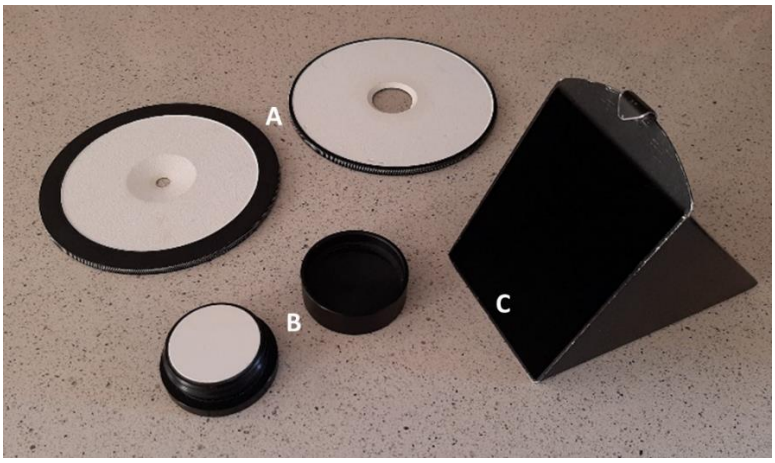

Fig. 2. Port redactors (A), calibrations standards: Standard Reflection Material – SRM (B), light trap (C)

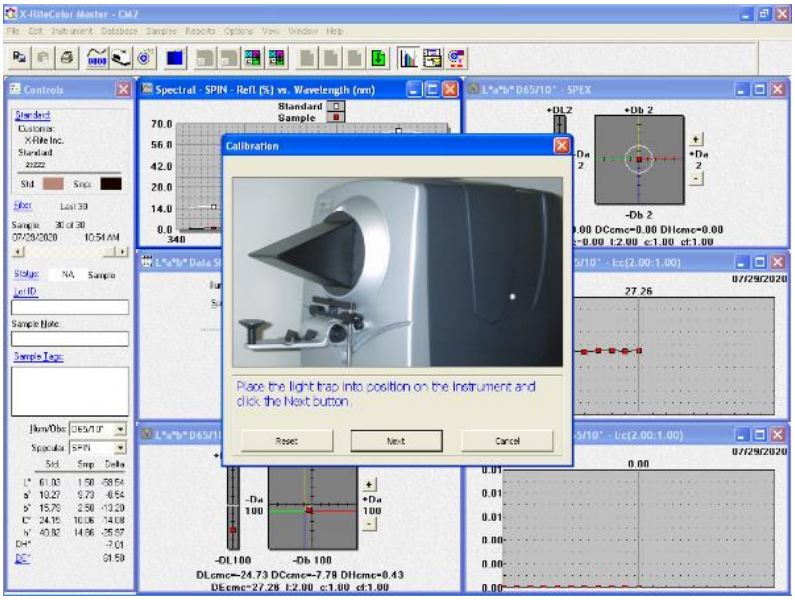

Fig. 3. Main menu of X-RiteColor® Master program – calibration process

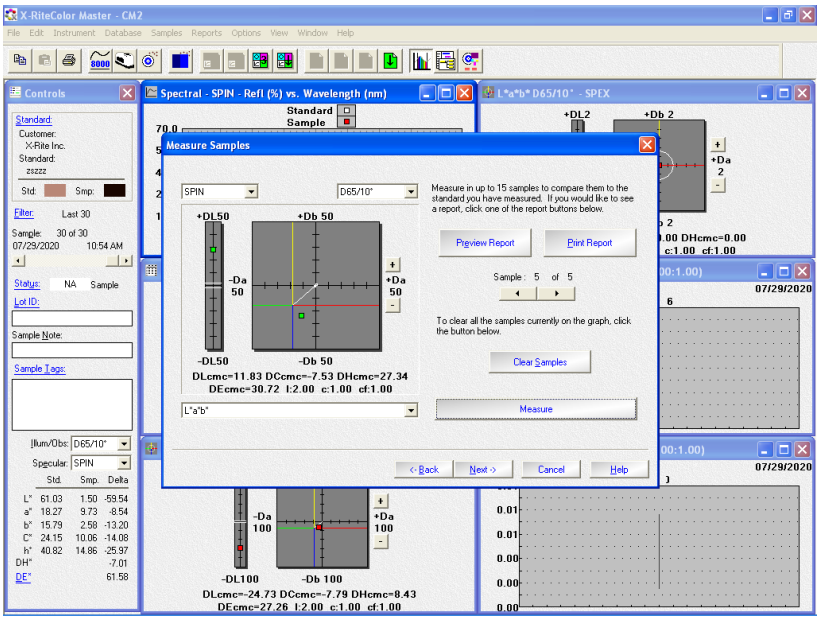

Fig. 4. Sample analyses

The data collected by software can be imported by another program e.g. Excel® – then the calculated values for parameters L*, a*, b* and parameters C and h° are obtained. X-RiteColor® Master allows to select the results from a specific time period (e.g. data from last month, week or the last 20 samples).

The instrument measures the wavelength in the range from 340 nm to 780 nm (in 10 nm intervals). Knowing the isobestic wavelengths of selected color traits it is possible to calculate other parameters (ΔE, nitrosating index, Mb content etc.) from the reflectance values, as it was mentioned earlier.

4. RESULTS AND DISCUSSION

The differences between samples with various amount of sodium (III) nitrite are presented in Fig. 5. As it could be noted, the greatest differences are between samples N_0 and with the nitrite addition. However, after 60 days of storage the change in total color of canned meat decreased for samples N_0 and N_50 and increased for samples N_0 and N_100. Differences between samples with various amount of sodium (III) nitrite were at the low level (3.07) at the day after production. Yet after 60 days it was observed that the differences started to increase slowly (3.37). This situation allows the conclusion that canned meat without the addition of nitrite salt clearly differs from the others, so it may not be purchased by a potential consumer. The decrease of the differences between samples

without nitrite and with reduced amount of nitrite were getting smaller after two months of storage. It may indicate the insufficient addition of nitrite salt to keep the stable color. Therefore, it may be necessary to fortify this sample.

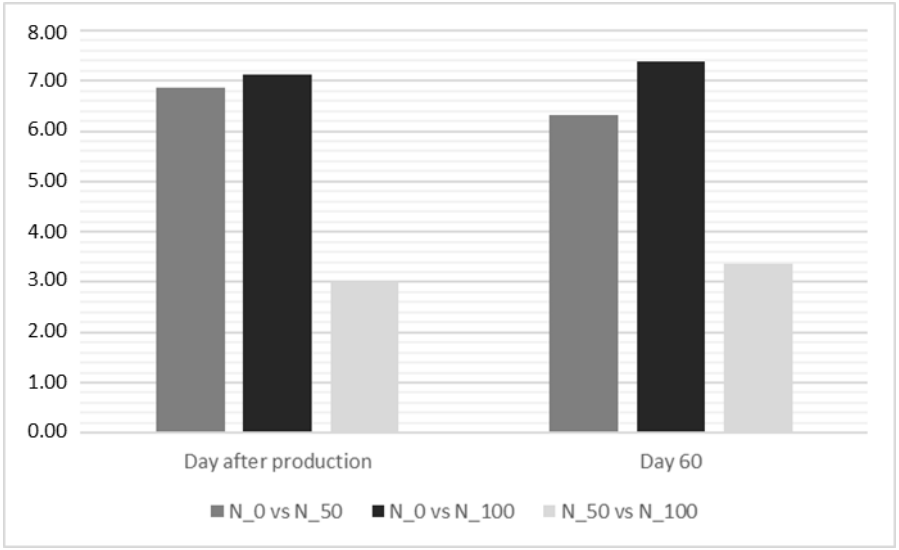

Fig. 5. Differences in color between canned meat with various amount of nitrite addition: N_0 - nitrite free, N_50 – 50 mg/kg of sodium (III) nitrite addition, N_100 – 100 mg/kg of sodium (III) nitrite addition

The percentage amount of MetMb and color intensity of cured canned pork are presented in Fig. 6. As it was mentioned earlier, MetMb is responsible for unattractive, gray-brownish meat color. The addition of nitrite counteracts this process. As it can be noted, nitrite-free sample (N_0) presented higher percentage amount of MetMb (36.5%) compared to samples with nitrite addition (29.9% and 29.4% respectively). According to the Regulation No 1333/2008 (2008) the maximum amount of sodium (III) nitrite which can be added to the canned meat is 100 mg/kg. In our experiment, this amount was reduced by half and did not cause negative effects. However, to maintain the consumer safety lyophilized plant extracts were added. The addition of red pepper and black currant leaf extracts in the amount of 0.005% contributed to the increased amount of MetMb where in the sample with higher amount of these extracts, the percentage value was similar to the samples with nitrite salt.

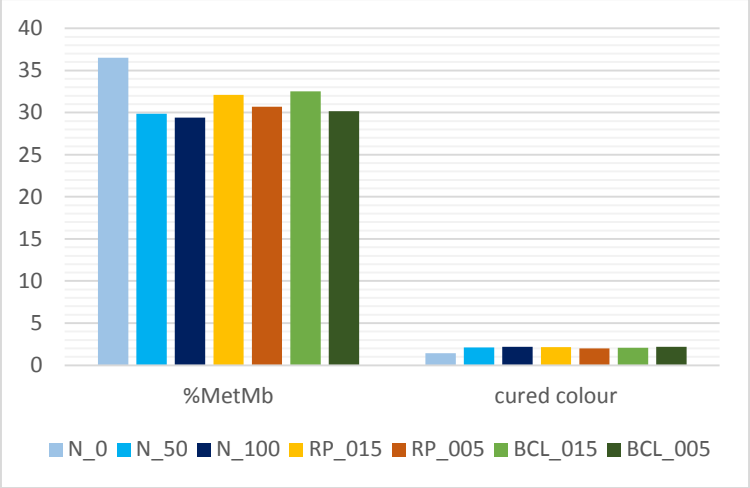

Fig. 6. Percentage amount of metmyoglobin and cured color parameter of canned meat after 60 days of storage: N_0 – nitrite free, N_50 – 50 mg/kg of sodium (III) nitrite addition, N_100 – 100 mg/kg of sodium (III) nitrite addition, RP_015 – red pepper extract addition (0.015%), RP_005 – red pepper extract addition (0.005%), BCL_015 – black currant leaves extract (0.015%), BCL_005 – black currant leaf extract (0.005%)

5. CONCLUSIONS

The data collected through the X-RiteColor® Master software via spectrophotometer instrument measurement allows to state that sharp reduction of sodium (III) nitrite in canned pork is possible. However, for better color results additional fortification with lyophilized herb extract is needed – addition of red pepper and blackcurrant leaf extracts in the amount of 0.015 allows to get greater results than the addition of these herbs in lower amount.

Acknowledgment

This project was financed by the program of the Minister of Science and Higher Education under the name "Regional Initiative of Excellence" in 2019–2022 (project number: 029/RID/2018/19, funding amount: 11,927,330.00 PLN).

REFERENCES

Alahakoon, A.U., Jayasena, D.D., Ramachandra, S., & Jo, Ch. (2015) Alternatives to nitrite in processed meat: Up to date. *Trends in Food Science & Technology*, *45*, 37–49. https://doi.org/10.1016/j.tifs.2015.05.008

American Meat Science Association (2012). Meat color measurements guidelines. Champaign, Illinois, USA: AMSA. 43–49.

Barkley, K.E., Fields, B., Dilger ,A.C., & Boler, D.D. (2018). Rapid Communication: Effect of machine, anatomical location, and replication on instrumental color of boneless pork loins. *Journal of Animal Science*, *96*(7), 2747–2752. https://doi.org/10.1093/jas/sky223

Danijela, Š.Z., Vera, L.L., Ljubinko, L.B., Lato, P.L., Vladimir, T.M., & Nevena, H.M. (2013). Effect of specific packaging conditions on myoglobin and meat color. *Food and Feed Research*, *40*(1), 1–10.

European Food Safety Authority. (2017). Re-evaluation of potassium nitrite (E 249) and sodium nitrite (E 250) as food additives. https://doi.org/10.2903/j.efsa.2017.4786

Faustman, C., Sun, Q., Mancini, R., & Suman, S.P. (2010). Myoglobin and lipid oxidation interactions: Mechanistic bases and control. *Meat Science*, *86*, 86–94. https://doi.org/10.1016/j.meatsci.2010.04.025

Ferysiuk, K., & Wójciak, K.M. (2019). The spectrophotometric analysis of antioxidant properties of selected herbs Invision-Pro™ UV-VIS. *Applied Computer Science*, *15*(4), 49–62. https://doi.org/10.23743/acs-2019-29

Food Chain Evaluation Consortium. (2016). Study on the monitoring of the implementation of Directive 2006/52/EC as regards the use of nitrites by industry in different categories of meat products.

Gassara, F., Kouassi, A.P., Brar, S.K., & Belkacemi, K. (2016). Green Alternatives to Nitrates and Nitrites in Meat-based Products – A Review. *Critical Reviews in Food Science and Nutrition*, *56*(13), 2133–2148. https://doi.org/10.1080/10408398.2013.812610

Henriott, M.L., Herrera, N.J., Ribeiro, F.A., Hart, K.B., Bland, N.A., & Calkins, C.R. (2020). Impact of myoglobin oxygenation level on color stability of frozen beef steaks. *Journal of Animal Science*, *98*(7), skaa193. https://doi.org/10.1093/jas/skaa193

Hunt, R.W.G. (1987). A model of colour vision for predicting colour appearance in various viewing conditions. *Color Research & Application*, *12*(6), 297–314. https://doi.org/10.1002/col.5080120605

Khatri, M., Phung, V.T., Isaksson, T., Sørheim, O., Slinde, E., & Egelandsdal, B. (2012). New procedure for improving precision and accuracy of instrumental color measurements of beef. *Meat Science*, *91*, 223–231. https://doi.org/10.1016/j.meatsci.2012.01.012

León, K., Mery, D., Pedreschi, F., & León, J. (2006). Color measurement in L*a*b* units from RGB digital images. *Food Research International*, *39*, 1084–1091. https://doi.org/10.1016/j.foodres.2006.03.006

Mancini, R.A., & Hunt, M.C. (2005). Current research in meat color. *Meat Science*, *71*, 100–121. https://doi.org/10.1016/j.meatsci.2005.03.003

Mokrzycki, W., & Tatol, M. (2011). Colour difference ΔE – A survey. *Machine Graphics and Vision*, *20*(4), 383–411.

Pathare, P.P., Opara, U.L., & Al-Said, F.A. (2013). Colour Measurement and Analysis in Fresh and Processed Foods: A Review. *Food Bioprocess Technology*, *6*, 36–60. https://doi.org/10.1007/s11947-012-0867-9

Ribeiroa, J.S., Santosb, M.J.M.C., Silvac, L.K.R., Pereirab, L.C.L., Santosb, I.A., da Silva Lannesd, S.C., & da Silva, M.V. (2019). Natural antioxidants used in meat products: A brief review. *Meat Science*, *148*, 181–188. https://doi.org/10.1016/j.meatsci.2018.10.016

Rivera, N., Bunning, M., Marti, J. (2019). Uncured-Labeled Meat Products Produced Using Plant-Derived Nitrates and Nitrites: Chemistry, Safety, and Regulatory Considerations. *Journal of Agricultural and Food Chemistry*, *67*, 8074–8084. https://doi.org/10.1021/acs.jafc.9b01826

Suman, S.P., & Joseph, P. (2013). Myoglobin chemistry and meat color. *Annual Review of Food Science and Technology*, *4*, 79–99.

Tapp, 3rd W.N., Yancey, J.W.S., & Apple, J.K. (2011). How is the instrumental color of meat measured? *Meat Science*, *89*, 1–5.

Trinderup, C.H., Dahl, A., Jensen, K., Carstensen, J.M., & Conradsen, K. (2015). Comparison of a multispectral vision system and a colorimeter for the assessment of meat color. *Meat Science*, *102*, 1–7. https://doi.org/10.1016/j.meatsci.2014.11.012

Wojciak, K.M., & Dolatowski, Z.J. (2015). Effect of acid whey on nitrosylmyoglobin concentration in uncured fermented sausage. *LWT – Food Science and Technology*, *64*, 713–719. https://doi.org/10.1016/j.lwt.2015.06.009

Yancey, J.W.S., & Kropf, D.H. (2008). Instrumental reflectance values of fresh pork are dependent on aperture size. *Meat Science*, *79*, 734–739. https://doi.org/10.1016/j.meatsci.2007.11.006

Applied Computer Science, vol. 16, no. 3, pp. 80–87
doi:10.23743/acs-2020-23

Submitted: 2020-06-06
Revised: 2020-08-25
Accepted: 2020-09-07

WSN, routing protocol, energy efficient

Muaayed F. AL-RAWI[0000-0003-1841-1222]*

CONVENTIONAL ENERGY EFFICIENT ROUTING PROTOCOLS IN WIRELESS SENSOR NETWORKS

Abstract

Wireless sensor network is a significant piece of wireless communication. It is a gathering of an enormous number of sensor nodes that are set in remote spots. The sensors have ability to do a typical undertaking. So energy exhaustion plays a significant job in keeping up a stable network. To build the system lifetime, a different energy effective algorithm is required which expands the network lifetime and makes the network more energy productive. For the augmenting, the lifetime of the network diverse routing technique has been utilized which help in expanding the lifetime of the network. This article portrays the diverse routing protocol which helps in energy efficient routing in a wireless sensor network.

1. INTRODUCTION

Wireless sensor network (WSN) comprises of a few sensors that are scattered spatially and are utilized to monitor the sensation in environment, for the computation of the conditions occurring in the environment identified with temperature, pollution levels, and humidity. The sink or base station gets data when these sensors collaborate and interface with one another and pass their data in the network. In the course of the most recent decade, there is quick advancement in WSN on account of its properties of having low power battery, wireless communication, and little size. They are generally utilized in numerous applications that are executed in a real environment. The network is basely made out of a few of sensors and gathering of sensor which are conveyed near ready to play out the quantity of

* Mustansiryia University, Computer Engineering Department, Palestine Street, P.O. Box: 14022, Baghdad, Iraq, muaayed@uomustansiriyah.edu.iq

exercises which imply sensing, monitoring, processing and communication abilities implying the chronicle of data about the occasions which are occurring in the environment. The essential components which are attached in the sensors are micro-processors, transceivers, external memory, and processing unit. Some additional components, for example, mobilizer, and power generator are also attached to it. Processing unit which is comprises of analog-digital converter and deals with the methodology through which coordinated effort of one sensor node to another sensor node. Transceiver unit keeps up the foundation of the node to the network. The microprocessor plays out the capacity which incorporates the administration and assortment of data from sensors node, interfacing of physical radio layer to data which is sent by the user (Shuang, 2015). Figure 1 shows the component of wireless sensor networks (WSN).

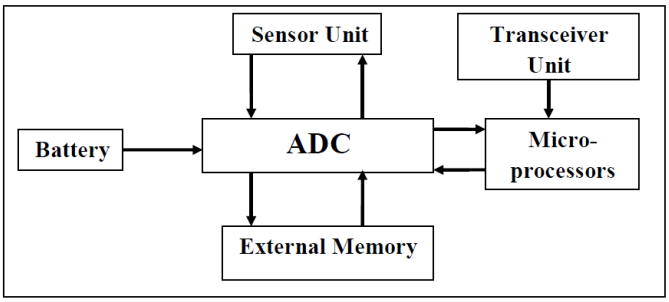

Fig. 1. Wireless sensor component (Shuang, 2015)

2. DIFFICULTIES IN WIRELESS SENSORS

Wireless sensors are sent at remote spots, to get the full limit of sensors networks, some constraint of these networks which causes technical issues in the network must be expelled. A few difficulties which hinder the performance of the network are identified with adaptation to fault tolerance, communication, low latency, scalability, transmission media, and coverage issue. To take care of the above issues diverse routing protocol is utilized. Diverse routing strategies are utilized for transmitting the data from the sensor node to the base station. Routing procedure is very not quite the same as should be expected IP network routing which comprises of various unique characteristics in a manner to unreasonable for a global addressing procedure for different quantities of sensor nodes, requirement for a method that can be applied to a system for appropriate linkage of a sensor node to a base station. For working the system to accomplish the ideal, it must require routing protocol (Swetha, Santhosh Amarnath & Anitha Sofia, 2019). These protocols are characterized into the accompanying ways and to make the system (Wireless Sensor Network) more energy efficient some energy efficient protocols are explained in the following section.

3. ENERGY EFFICIENT PROTOCOLS

Energy efficiency performs a significant job in WSN. These days the size, shape of the network is increasing. Because of it, the huge most measure of energy of a node is utilized which expands the early death of a node. Thus unique effective routing protocol is created to increment the lifetime of the network. Following are known and most common energy-efficient routing protocol.

3.1. Track Sector Clustering (TSC)

Track sector clustering dependent on the clustering algorithm in which each cluster one cluster head is chosen. The entire network is partitioned into triangular sectors and concentric circular tracks. The partition of network right now in energy saving. The procedure of TSC for its execution is partitioned into phases. Track setup, Sector setup, Cluster heads selection, chain construction, and data transmission. Sensor nodes energy is not squandered by the calculation of tracks by the base station. Energy dissipation is additionally decreased by redundancy distance between a head node to the base station. The focal point of these concentric circles is a base station. Random choice of the head node is done at the primary level. At the point when the base station decides the area of the head node it computes the transmission slope. In a specific cluster, the arrangement of the head node happens when nodes that are at a higher level have a similar transmission slope. The methodology utilized assists with decreasing the redundancy level in the data which is transmitted by breaking the long chain of nodes into a littler one. In a specific cluster, the formation of the head node happens when nodes that are at a greater level have a same transmission slope. The benefit of utilizing TSC is to diminish in data for transmission in the network (Gautam, Lee & Pyun, 2009). Figure 2 shows data gathering at head nodes in TSC protocol.

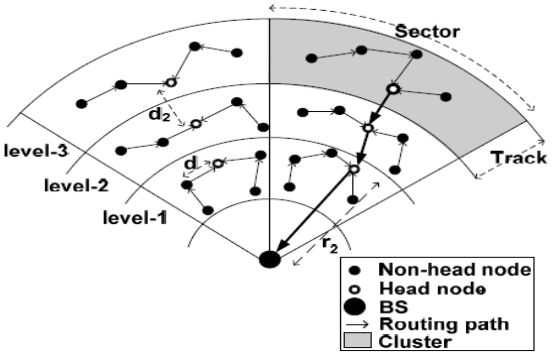

Fig. 2. Data gathering at head nodes in TSC protocol (Gautam, Lee & Pyun, 2009)

3.2. Low Energy Adaptive Clustering Hierarchy (LEACH)

The working of LEACH is partitioned into two phases

1. Set up phase which partitions the network into clusters, CH makes notice for a timetable of transmission.
2. The steady phase involves data aggregation, compression, and transmission to the sink.

The benefit of employments of LEACH is its direct communication by each cluster head for sending the information to sink. The utilization of the cluster is increment the lifetime of the network. It aggregates the original information which is sent by the detected sensor into a littler size for simple transmission of information. In LEACH protocol each node is allowed to turn into a cluster head which assists with diminishing the likelihood of passing on the sensor nodes (Xiangning & Yulin, 2007). Figure 3 shows data gathering at head nodes in LEACH protocol.

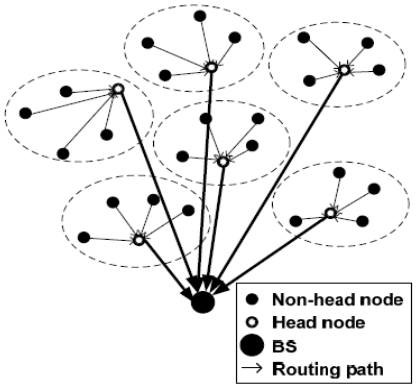

Fig. 3. Data gathering at head nodes in LEACH protocol (Xiangning & Yulin, 2007)

3.3. Power-Efficient Gathering in Sensor Information Systems (PEGASIS)

This PEGASIS protocol was acquired after modification in LEACH was finished. A chain-like structure of nodes is done and every node sets up communication just with its neighbor which is close in distance. The transmission of data happens through one node to another node just with the assistance through one node which is assigned can send data to the base station. The leader node is altered turn by turn during transmission of information. The base station decides if it is chain formation or the chain structure by the nodes themselves utilizing a algorithm (greedy). It needed a global knowledge (network knowledge). At the point when information is move every node assembles its information from its neighboring node. At random areas, to make system powerful sensor nodes die. This entire

procedure is accomplished by changing the transmission leader in each communication round. To take care of above issue, nodes that are permitted, so they can form leaders, by making a limit to a distance for neighbors (Jung, Han & Chung, 2007). The benefit of the PEGASIS is the transmission number is less which helps in less loss of energy by the sensor nodes. Figure 4 shows data gathering at head nodes in PEGASIS protocol.

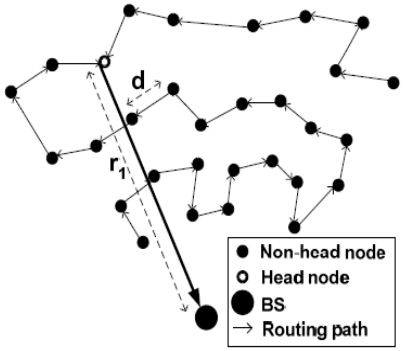

Fig. 4. Data gathering at head nodes in PEGASIS protocol (Jung, Han & Chung, 2007)

3.4. Threshold Sensitive Energy-Efficient Sensor Network Protocol (TEEN)

It is particularly made for reactive networks. The reactive network is the network that comprises of those sensor nodes which embrace the adjustments in themselves as indicated by the progressions which happen in environment. To expand energy efficiency, the transmission number is decreased in the network. There is a particular range of utility when information value falls, at exactly that point information transmission happens. Each cluster in the network has a cluster head that sets properties.

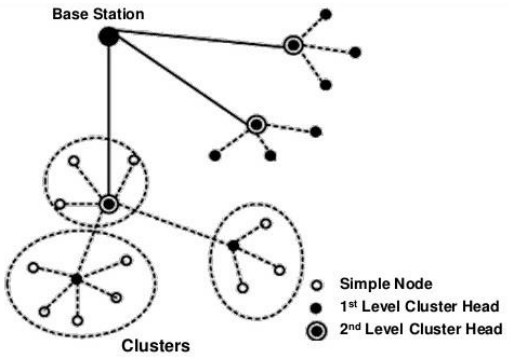

Fig. 5. TEEN protocol (Bria, Wahb & Alaydrus, 2019)

In the (hard and soft) threshold, these thresholds are of its part nodes. The transmission of information occurred when its value is larger than soft threshold value along the estimation of the contrast between the older and new one, on account of the above methodology, certain transmission (TEEN) are wiped out and that conserves the energy of those sensors which are available in the network (Bria, Wahb & Alaydrus, 2019). Figure 5 describes TEEN protocol.

3.5. Hybrid Energy-Efficient Distributed Clustering (HEED)

The reason for this strategy was the formation of a cluster that is distributed and energy efficient. In notice for the choice of cluster head, two parameters must take into account:

1. The residual energy of every node.
2. Node degree.

For the chosen of CH, the residual energy of the node along with some likelihood is taken thought. The procedure of formation of cluster head happens for the situation when the various nodes which are available in the network discovered their CH to keep up less expense of communication benefit. The benefit of utilizing HEED is help in keeping up long network lifetime, shore scalable information aggregation (Younis & Fahmy, 2004). Figure 6 describes HEED protocol.

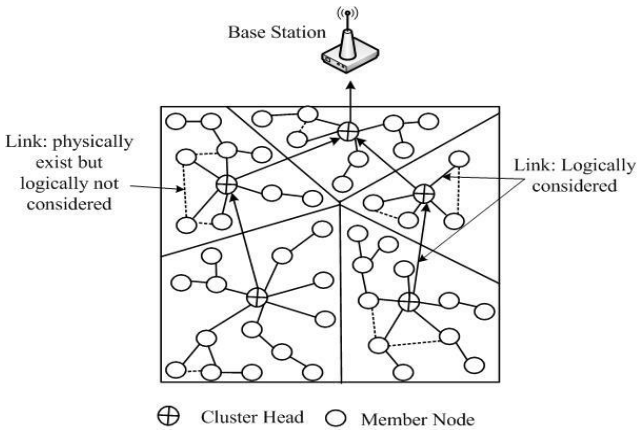

Fig. 6. HEED protocol (Younis & Fahmy, 2004)

3.6. Stable Electron Protocol (SEP)

In the clustered heterogeneous WSN, which has a few benefits over LEACH? The two-level of heterogeneity of sensor node is deemed. They are characterized into two sorts:

1. Normal node.
2. Advanced node.

Advanced node when contrasted with normal node they have greater likelihood of turning into a cluster head when contrasted with other sensor nodes. In the sensor field, this protocol is more scalable, in light of the fact that it needn't the position of nodes (Ayoob, Zhen, Adnan & Gull, 2016). Figure 7 describes SEP protocol.

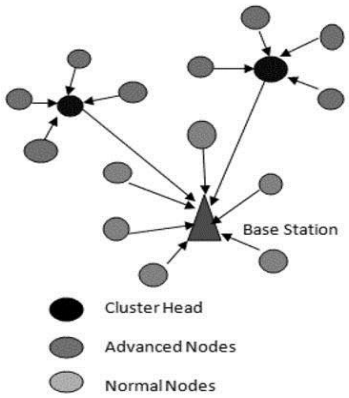

Fig. 7. SEP protocol (Ayoob, Zhen, Adnan & Gull, 2016).

3.7. WSN Routing Protocols Comparison

Right now routing protocols comparison is finished. Table 1 reveals the comparison of various routing protocols in WSN those were studied in this article with the parameters, power efficiency, network stability, cluster head formation, and network scalability.

Tab. 1. Comparison of WSN routing protocols

Energy-efficient routing protocol	Power efficiency	Network stability	Cluster head formation	Network scalability
TSC	moderate	moderate	yes	moderate
LEACH	low	moderate	yes	low
PEGASIS	low	low	no	very low
TEEN	very high	high	yes	low
HEED	moderate	high	yes	moderate
SEP	high	high	yes	high

4. CONCLUSION

In this article short survey on energy efficient routing protocols in WSN and their comparison is introduced. From above comparison a perception is done that cluster based protocols are more energy efficient. WSN which have gain consideration in the course of the most recent couple of years are broadly utilized in both civil and military. There is different difficulties task for viable structure of these WSN. Routing protocols are extraordinary answer for handle the difficulties which happens in WSN. Future work can be reached out on growing new routing protocol which manages issue of node mobility applications.

Acknowledgment

The author thanks Mustansiriyah University for its full support of this work. It is one of the Iraqi public universities named after Mustansiriyah School, which was founded in the time of the Abbasidsin Baghdad in 1233 by the Caliph Al-Mustansir Billah. It was an important scientific and cultural center located in the capital Baghdad. Includes 13 faculties. Founded in 1963.

WWW: http://www.uomustansiriyah.edu.iq

REFERENCES

Ayoob, M., Zhen, Q., Adnan, S., & Gull, G. (2016). Research of Improvement on LEACH and SEP Routing Protocols in Wireless Sensor Networks. *2016 IEEE International Conference on Control and Robotics Engineering* (pp. 1–5). Singapore. http://doi.org/10.1109/ICCRE.2016.7476141

Bria, R., Wahb, A., & Alaydrus, M. (2019). Energy Efficiency Analysis of TEEN Routing Protocol with Isolated Nodes. *2019 Fourth International Conference on Informatics and Computing* (pp. 1–5). Semarang, Indonesia. http://doi.org/10.1109/ICIC47613.2019.8985668

Gautam, N., Lee, W., & Pyun, J. (2009). Track-Sector Clustering for Energy Efficient Routing in Wireless Sensor Networks. *2009 Ninth IEEE International Conference on Computer and Information Technology* (pp. 116–121). Xiamen. http://doi.org/10.1109/CIT.2009.130

Jung, S., Han, Y., & Chung, T. (2007). The Concentric Clustering Scheme for Efficient Energy Consumption in the PEGASIS. *International Conference on Advanced Communication Technology* (pp. 260–265). Okamoto, Kobe. http://doi.org/10.1109/ICACT.2007.358351

Shuang-Hua, Y. (2015). *Wireless Sensor Netwoks*. Springer-Verlag.

Swetha, R., Santhosh Amarnath, V., & Anitha Sofia, V. S. (2019). Wireless Sensor Network: A Survey. *International Journal of Advanced Research in Computer and Communication Engineering*, *7*(11), 144–117.

Xiangning, F., & Yulin, S. (2007). Improvement on LEACH Protocol of Wireless Sensor Network. In *Proceedings of the 2007 International Conference on Sensor Technologies and Applications (SENSORCOMM '07)* (pp. 260–264). IEEE Computer Society.

Younis, O., & Fahmy, S. (2004). Heed. A hybrid, Energy-Efficient, Distributed Clustering Approach for Ad-hoc Networks. *IEEE Transactions on Mobile Computing*, *3*(4), 366–369. http://doi.org/10.1109/TMC.2004.41

Applied Computer Science, vol. 16, no. 3, pp. 88–101
doi:10.23743/acs-2020-24

Submitted: 2020-07-31
Revised: 2020-08-30
Accepted: 2020-09-22

artificial neural networks, mathematical modelling, biomaterials, bone cement,

Anna MACHROWSKA[0000-0003-3289-2421]*,
Robert KARPIŃSKI[0000-0003-4063-8503]*,
Józef JONAK[0000-0003-4658-4569]*,
Jakub SZABELSKI[0000-0003-0917-1693]**,
Przemysław KRAKOWSKI[0000-0001-7137-7145]***

NUMERICAL PREDICTION OF THE COMPONENT-RATIO-DEPENDENT COMPRESSIVE STRENGTH OF BONE CEMENT

Abstract

Changes in the compression strength of the PMMA bone cement with a variable powder/liquid component mix ratio were investigated. The strength test data served to develop basic mathematical models and an artificial neural network was employed for strength predictions. The empirical and numerical results were compared to determine modelling errors and assess the effectiveness of the proposed methods and models. The advantages and disadvantages of mathematical modelling are discussed.

1. INTRODUCTION

The use of polymer biomaterials has become a common standard in a range of medical applications, including orthopaedic surgery and dentistry, where they are referred to as cements (Balin, 2004, 2016). In orthopaedics, they are predominantly found in joint arthroplasty and as a filler material in extensive bone defects.

* Lublin University of Technology Faculty of Mechanical Engineering, Department of Machine Design and Mechatronics, Nadbystrzycka 36, 20-618 Lublin, Poland, a.machrowska@pollub.pl, r.karpinski@pollub.pl, j.jonak@pollub.pl
** Lublin University of Technology, Faculty of Mechanical Engineering Department of Computerization and Production Robotization, Section of Biomedical Engineering, Nadbystrzycka 36, 20-618 Lublin, Poland, j.szabelski@pollub.pl
*** Medical University of Lublin Department of Trauma Surgery and Emergency Medicine, Staszica 16, 20-081 Lublin, Poland, przemysław.krakowski@umlub.pl

At present, in total joint replacement, prostheses are commonly fixtured with the PMMA bone cement (polymethyl methacrylate), which has been in use since 1960s (Charnley, 1960). Charnley, an early pioneer in modern arthroplasty, was the first to use the methyl methacrylate resin to bond endoprostheses (Balin, 2016; Matuszewski et al., 2014). Considering the applications of bone cements in medicine, the fundamental factors of their biofunctionality are as follows: carrying static and dynamic loads, dampening vibrations, abrasion resistance and biocompatibility (Balin, 2016; Wekwejt et al., 2019).

Given the aggressive operating environment, it is of great importance that bone cements are described in due detail with respect to their resistance to ageing processes and the resulting deterioration in strength (Lelovics & Liptakova, 2010, 2019; Matuszewski et al., 2014). Early loss of mechanical properties could cause endoprosthesis loosening and, thereby, necessitate revision surgery. These processes, i.e. the rate of ageing and depletion of mechanical parameters, can be contributed to several factors, including the mixing (Dunne & Orr, 2001; Lelovics & Liptakova, 2010; Liptáková, Lelovics & Necas, 2009), porosity (Dunne, Orr, Mushipe & Eveleigh, 2003; Pałubicka, Czubek & Wekwejt, 2019), contamination of cement with bone marrow, blood, Ringer's solution and other biofluids that by enabling micromovements, increase the risk of debonding at the bone-cement interface (Bialoblocka-Juszczyk, et al., 2008; Karpiński, Szabelski & Maksymiuk 2019a, 2019b; Tan, Koh, Ramruttun & Wang, 2016), or adding special-purpose admixtures into the cement structure (Wekwejt, Moritz, Świeczko-Żurek & Pałubicka 2018, Wekwejt et al., 2020).

Experimental investigations of ageing processes and changes in mechanical properties of biomaterials are cost-intensive let alone exceptionally time-consuming. The intrinsic limitations of empirical testing can be overcome using computer-aided methods, which exponentially reduce data collection and processing times and limit the required computational cost. As a result, they may help select or refine the optimal direction of further research. Numerical methods include predictive analytics, whose models enable the determination of relationships between corresponding parameters on the basis of experimental data (Younesi, Bahrololoom & Ahmadzadeh, 2010). Other analytical instruments of established computational prowess that have been put to use in this work, are the finite element method (FEM) (Falkowicz & Debski, 2019, 2020; Falkowicz, Debski & Wysmulski, 2020) and the boundary element method (BEM).

2. PREDICTIVE ANALYSIS

The performance of the selected analytical methods and tools was verified using statistical analysis and artificial neural network (ANN) modelling. The testing data were obtained from the results of the strength of bone cements in compression. The test specimens had been prepared with a variable amount of the liquid monomer

– one of the two components of bone cement – to evaluate how the changes in the PMMA cement composition by mass correlate with its strength performance (Karpinski, Szabelski & Maksymiuk, 2018, 2019a, 2019b). Two learning datasets were used for predictions and verification against the actual data (Fig. 1):

– the data from the range -30 % to +25 % served to predict the +35 % variant,
– the data from the range -20 % to +35 % served to predict the -35 % variant.

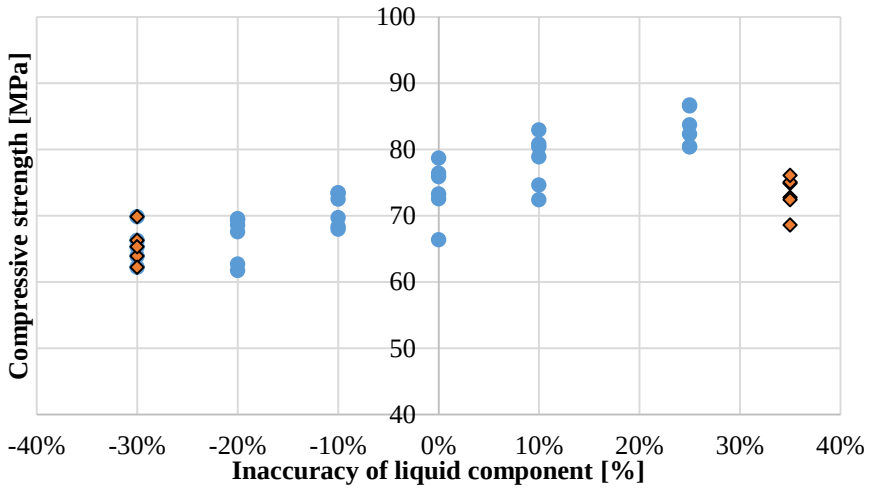

Fig. 1. Result from experimental research on compressive strength

Due to the physical nature of the investigated changes, it was resolved that polynomial models including linear would be most suitable to carry out the calculations, specifically, to determine the relationship accounting for the course of changes in the compressive strength in the specified range. The selected range is a slice of the entire hypothetical range from -100 % (no liquid component) to +∞ (only liquid component). From the logical analysis of the boundary conditions, it seems that, globally, the most appropriate is the quadratic polynomial model. In the model, which is a concave downward parabola, the maximum parameters are recorded in the middle of the range, and towards the edges, they decrease to the minimum (zero). However, in the tested range, it may emerge that one of the other models will perform with higher precision, both in terms of goodness of fit and prediction results.

2.1. Mathematical modelling of compressive strength

Statistical modelling was carried out using Microsoft Excel and Tibco Statistica software. It consisted in the analysis of relationships between variables, the determination of its linearity (regression) and approximation by means of the linear function and polynomials.

2.1.1. Excess of the liquid component (+35 %)

The generated mathematical models are as follows:

$$\sigma_{+35\_1} = 34.349x + 74.494$$
$$\sigma_{+35\_2} = 14.443x^2 + 34.963x + 74.026$$
$$\sigma_{+35\_3} = -108.11x^3 + 7.3284x^2 + 41.435x + 74.213$$
$$\sigma_{+35\_4} = 300.64x^4 - 71.069x^3 - 15.498x^2 + 39.628x + 74.376$$
$$\sigma_{+35\_5} = -8803.6x^5 - 1357.4x^4 + 634.85x^3 + 88.061x^2 + 31.816x + 73.878$$

where: σ – a modelled compressive strength of the cement sample, x – the liquid component excess (wt. %).

The model accuracy is assessed by the coefficient of determination R^2, and it displays a good correlation with the empirical results, which is confirmed by the following:

$$R^2(\sigma_{+35\_1}) = 0.7911$$
$$R^2(\sigma_{+35\_2}) = 0.7951$$
$$R^2(\sigma_{+35\_3}) = 0.7995$$
$$R^2(\sigma_{+35\_4}) = 0.7999$$
$$R^2(\sigma_{+35\_5}) = 0.8022$$

Having established that the models were of adequate predictive capacity, they performed the compressive strength simulations for the material with a +35% excess of the liquid part. The numerical data were subsequently verified using the mean results from the experimental tests:

$$\sigma_{+35\_1\_model} = 86.52\ MPa$$
$$\sigma_{+35\_2\_model} = 88.03\ MPa$$
$$\sigma_{+35\_3\_model} = 84.94\ MPa$$
$$\sigma_{+35\_4\_model} = 87.81\ MPa$$
$$\sigma_{+35\_5\_model} = 56.41\ MPa$$

while

$$\bar{\sigma}_{+35\_experimental} = 73.30\ MPa.$$

The root-mean-square error (RMSE) and its coefficient of variation (CV (RMSE)), accounting for the discrepancies between the predicted and observed values, were shown to attain notably higher values compared to the liquid component deficiency variant:

$$RMSE_{+35\_1} = 13.45, CV(RMSE_{+35\_1}) = 15.5\%$$
$$RMSE_{+35\_2} = 14.94, CV(RMSE_{+35\_2}) = 17.0\%$$
$$RMSE_{+35\_3} = 11.94, CV(RMSE_{+35\_3}) = 14.0\%$$
$$RMSE_{+35\_4} = 14.72, CV(RMSE_{+35\_4}) = 16.8\%$$
$$RMSE_{+35\_5} = 17.07, CV(RMSE_{+35\_5}) = 30.3\%$$

The models generated from the experimental data in the range from -30 % to approx. +25 % of the liquid component can be compared with the actual values for the predicted range of +35 % in Fig. 2.

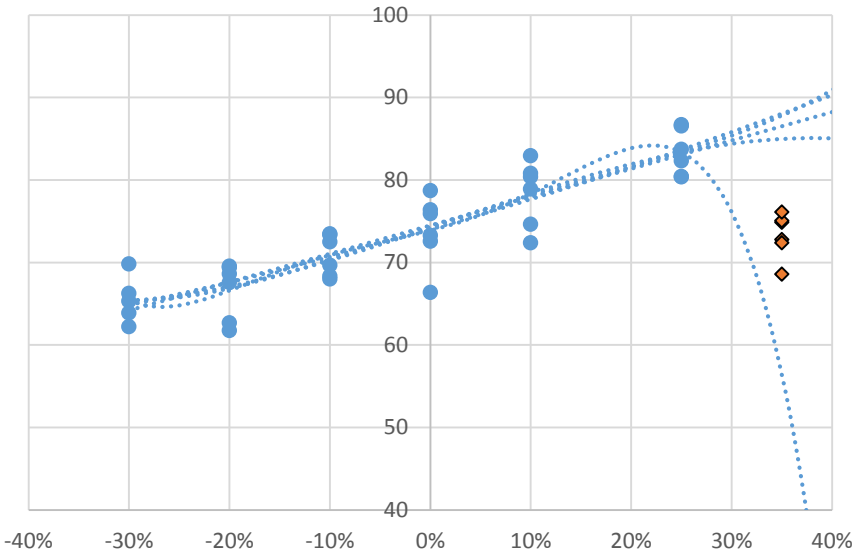

Fig. 2. Compressive strength of bone cement with a +35 % excess of the liquid component: comparison of mathematical models and experimental data

2.1.2. Deficiency of the liquid component (-30 %)

The methodology of computations is the same as in the former case. The following models were generated:

$$\sigma_{-30\_1} = 20.66x + 72.86$$
$$\sigma_{-30_2} = -57.226x^2 + 24.45x + 75.457$$
$$\sigma_{-30\_3} = -377.13x^3 - 30.207x^2 + 54.631x + 75.075$$
$$\sigma_{-30\_4} = -1015.5x^4 - 281.68x^3 + 77.675x^2 + 49.915x + 73.816$$
$$\sigma_{-30\_5} = -4304.9x^5 - 433.68x^4 + 286.35x^3 + 29.73x^2 + 35.211x + 74.165.$$

The goodness of fit of forecasted data with the actual results, assessed by the coefficient of determination, is not as high as in the previous case:

$$R^2(\sigma_{-30\_1}) = 0.4654$$
$$R^2(\sigma_{-30\_2}) = 0.5904$$
$$R^2(\sigma_{-30\_3}) = 0.7414$$
$$R^2(\sigma_{-30\_4}) = 0.7738$$
$$R^2(\sigma_{-30\_5}) = 0.7846$$

Compressive strength forecasting results:

$$\sigma_{-30\_1\_model} = 66.66\ MPa$$
$$\sigma_{-30\_2\_model} = 62.97\ MPa$$
$$\sigma_{-30\_3\_model} = 66.15\ MPa$$
$$\sigma_{-30\_4\_model} = 65.21\ MPa$$
$$\sigma_{-30\_5\_model} = 65.49\ MPa$$

while

$$\bar{\sigma}_{-30\_experimental} = 65.52\ MPa.$$

The RMSE and its coefficient of variation CV (RMSE), provide the description of the difference between predictions and actual strength of bone cement in compression:

$$RMSE_{-30\_1} = 2.81, CV(RMSE_{-30\_1}) = 4.2\%$$
$$RMSE_{-30\_2} = 3.61, CV(RMSE_{-30\_2}) = 5.7\%$$
$$RMSE_{-30\_3} = 2.64, CV(RMSE_{-30\_3}) = 4.0\%$$
$$RMSE_{-30\_4} = 2.58, CV(RMSE_{-30\_4}) = 4.0\%$$
$$RMSE_{-30\_5} = 2.57, CV(RMSE_{-30\_5}) = 3.9\%$$

Fig. 3 presents the results from the simulations, i.e. models generated from the empirical data limited to the range from -20 % to approx. +35 % of the liquid component content, along with the actual values for the predicted range of -30 %.

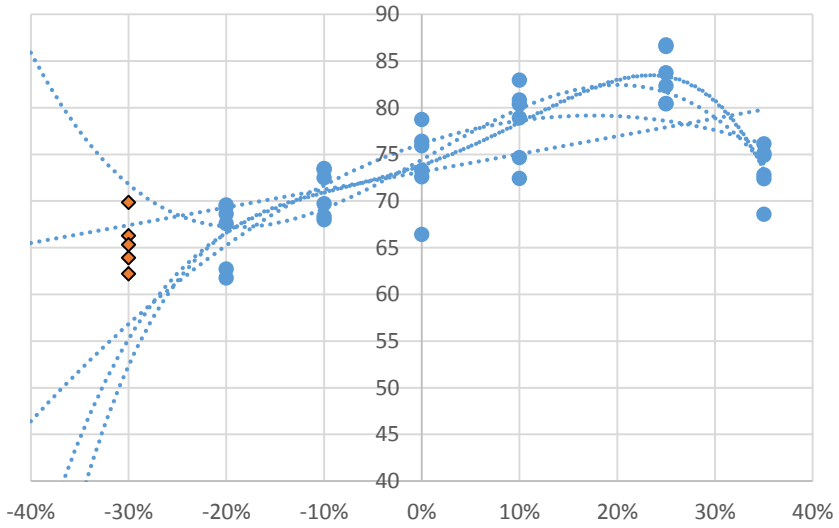

Fig. 3. Compressive strength of bone cement with a -35 % deficiency of the liquid component: comparison of mathematical models and experimental data

2.2. Artificial neural network forecasting

Deep learning neural networks (DLN) have been steadily becoming the standard among machine learning algorithms. Their advantages are demonstrated by their great capacity for capturing existing relationships between particular data – including performing calculations on extensive quantities of data, on numerous levels of abstraction. What distinguishes them from conventional NNs (Neural Networks) is that DLNs' operation is fully automated and does not require supervision or additional generalisation of features by human operators. DLNs are found in a range of applications, including speech recognition (Tu, Du & Lee, 2019; Zhang et al., 2019), image processing (Chen, Zhang, Liu & Kamruzzaman, 2019; de Haan, Rivenson, Wu & Ozcan, 2020; Hatt, Parmar, Qi & El Naga, 2019) or medical diagnosis (Hosseini, Hosseini & Ahi, 2020; Jiménez & Racoceanu, 2019; Lee et al., 2019).

In the works reported in this paper, the performance of DLN algorithms was compared with mathematical modelling. The procedure for analysing the effect of powder/liquid components mix ratio on the compressive strength of bone cements using DLN was the following:

- preliminary data preparation (alignment of the input data length),
- arranging data in the strings: -35 %, -25 %, -10 %, 0 %, +10 %, +20 % and +30 % of the cement mix component disproportion,
- inserting data into MATLAB (Deep Learning package with the Adam optimiser),

– testing in two variants: testing the predictive performance for a series of data from random samples and training the network on mean results (Fig. 4),
– the network architecture was: 50 hidden neurons and 150 iterations; to prevent overfitting, the dropout technique was employed and a gradient threshold was introduced.

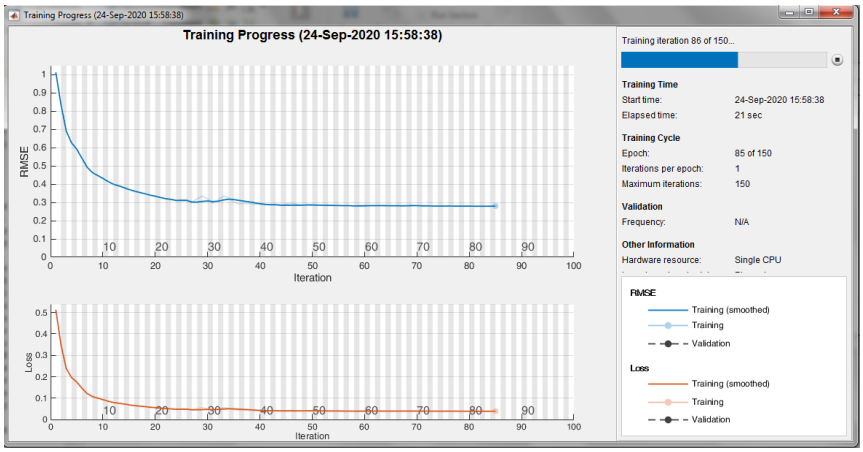

Fig. 4. Network training progress in MATLAB – RMSE reduction as a function of iteration

The compressive strength values predicted by the DLN network are presented below.

2.2.1. Excess of the liquid component (+35 %)

$$\sigma_{+35\_dln1} = 72.73\ MPa$$
$$\sigma_{+35\_dln2} = 69.83\ MPa$$
$$\sigma_{+35\_dln3} = 68.42\ MPa$$
$$\sigma_{+35\_dln4} = 69.56\ MPa$$
$$\sigma_{+35\_dln5} = 54.53\ MPa$$
$$\sigma_{+35\_dln6} = 64.00\ MPa$$

$$\bar{\sigma}_{+35\_dln} = 76.71\ MPa$$

$$SD\left(\sigma_{+35\_dln}\right) = 3.76\ MPa$$
$$CV\left(\sigma_{+35\_dln}\right) = 4.9\%$$

while

$$\bar{\sigma}_{+35\_experimental} = 73.30\ MPa.$$

2.2.2. Deficiency of the liquid component (-30 %)

$$\sigma_{-30\_dln2} = 77.67\ MPa$$
$$\sigma_{-30\_dln3} = 74.97\ MPa$$
$$\sigma_{-30\_dln4} = 78.49\ MPa$$
$$\sigma_{-30\_dln5} = 79.08\ MPa$$
$$\sigma_{-30\_dln6} = 80.10\ MPa$$

$$\bar{\sigma}_{-30\_dln} = 66.50\ MPa$$

$$SD(\sigma_{-30\_dln}) = 7.20\ MPa$$
$$CV(\sigma_{-30\_dln}) = 10.8\%$$

while

$$\bar{\sigma}_{-30_{experimental}} = 65.52\ MPa.$$

Subsequently, the results were analysed statistically and verified against the experimental data from the strength tests. Having proven the normality of data distribution, the analysis of variance confirmed their homogeneity and the Student's t-test, carried out at a confidence level $\alpha = 0.05$, indicated that the results from the neural network modelling were of good quality, that is regardless of the liquid component deficiency/excess variant. Therefore, given the lack of statistically significant differences, in the subsequent analyses mean network results were used.

3. DISCUSSION

Figures 5 and 6 display differences between mean values obtained from analytical investigations (DLN, mathematical modelling with polynomials) and values obtained from destructive physical analysis for both investigated variants of deviation from the correct powder/liquid component mix ratio.

From the comparison of Figures 5 and 6, a notable discrepancy emerges between the accuracy of predictions with respect to particular bone cement composition disproportions. Up to the level of +35 %, the excess of the liquid component is shown to have a positive effect on the material strength; after reaching the threshold limit, there is a steep drop in its resistance to loading in compression.

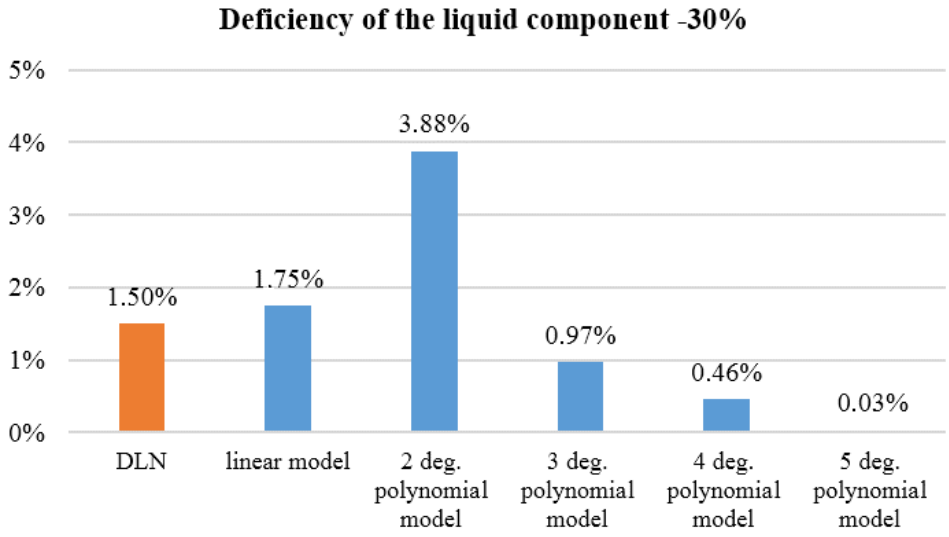

Fig. 5. Differences between modelled and actual compressive strength values for -30 %

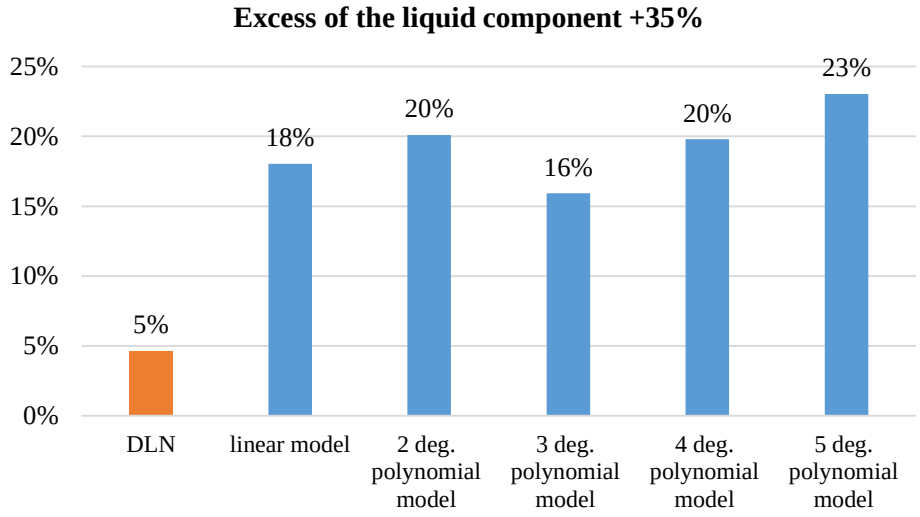

Fig. 6. Differences between modelled and actual compressive strength values for +35 %

Not entirely unexpectedly, the mathematical models have failed to forecast these tendencies, i.e. the differences between the predicted and the actual values were always in the excess of 15 %, regardless of the model (15–23 %) – Fig. 6. The result of mathematical computations can be thus merely treated as a useful forecast. However, these results may not be universally applicable to all situations, since the testing conditions were rather coincidental and perhaps non-replicable.

On the other hand, it is worth noting the exceptional predictive performance of the deep learning network, which displayed a slight, 5 %, error when correlated with the results from the strength tests. Thereby, the DLN outperformed the mathematical models and confirmed that the parameter change predictions from the latter are burdened with limitations, despite their good fit with the learning data. Furthermore, our findings appear to indicate that striving for the best fit is in itself insufficient to guarantee satisfactory predictive accuracy of the model. This is exemplified by Fig. 7, which compares the R^2 values (the coefficient of determination) of the subsequent models and the coefficient of variation of the root-mean-square deviation (CV (RMSD)), which describes the difference between the predicted and the observed values (with respect to the mean value).

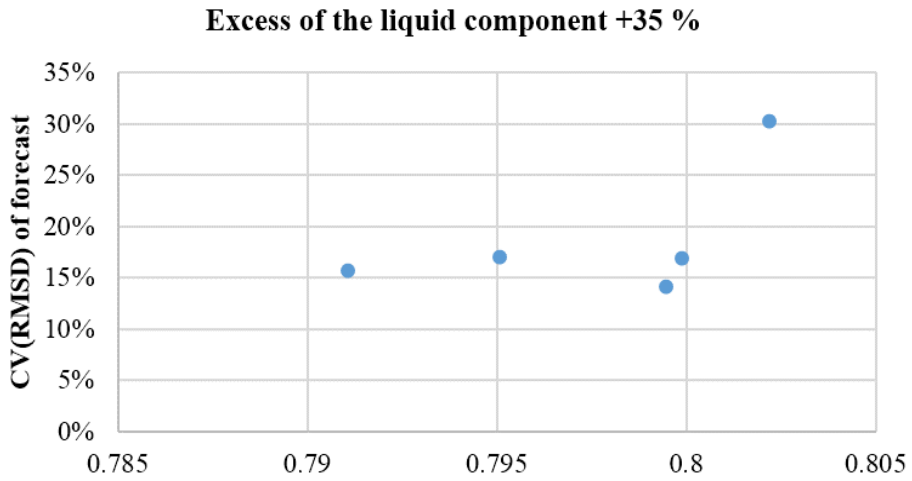

Fig. 7. CV(RMSD) vs R2 for +35 % forecasting

A notable increase in the quality of predictions was observed in the case when the -30 % variant of the liquid component deficiency was considered. The compressive strength values generated by the mathematical models did not exhibit a marked difference from the average values obtained experimentally (0.03–3.88% – within the margin of error), and the models can be, thus, considered as reliable predictors of the compressive strength of cement. As in the prior case, the DLN displayed good predictive capacity (a statistically insignificant difference of 1.5 % from the experimental value). Considering the deficiency of the liquid part, the strength parameter is shown to change in a more predictable way along with the decrease in the proportion of the liquid part. Similarly to the + 30 % variant, the model's goodness of fit was strongly correlated with the increase with each degree of polynomial approximating the results from the empirical tests. However, this correlation did not translate into more accurate results (Fig. 8).

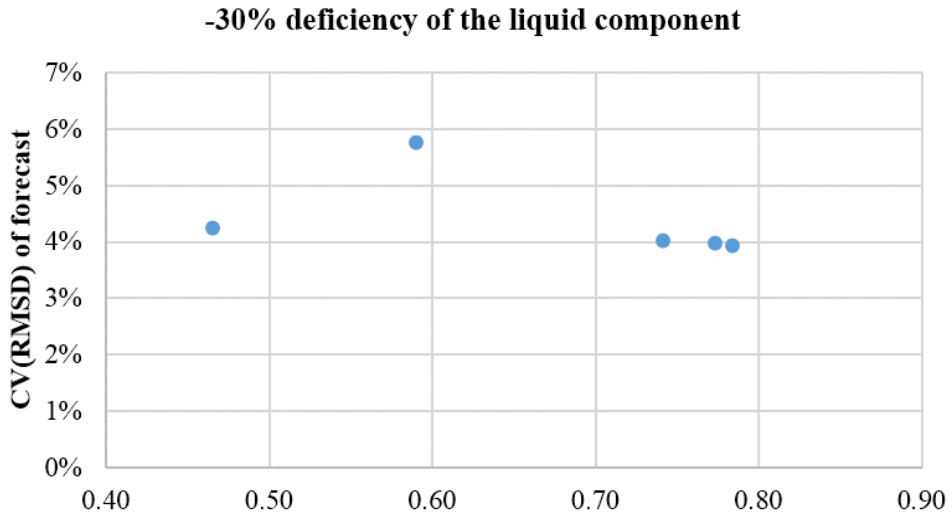

Fig. 8. CV(RMSD) vs R^2 for -30 % forecasting

5. CONCLUSIONS

The results of this investigation have shown that, in general terms, there is no consistent association between increasing the model/learning datasets' goodness of fit and an enhancement in the predictive accuracy of models. Furthermore, in spite of the improved values of coefficient of determination (with each degree of polynomial), the decrease in the root mean square error for the predicted values was negligible, or otherwise remained largely unchanged, except for rare cases of a slight increase. Therefore, based on our findings, there are no grounds to claim that even the best fit of the modelled and input data should guarantee a comparable level of predictive accuracy for values outside the range of the input data. Moreover, the learning data on the basis of which the models were generated, displayed a sharp change in the rising trend (considering the excess of the liquid component) above the +35 % level. This occurrence was found to severely hamper forecasting, as such a sudden drop is in principle impossible to predict when creating a mathematical model. This results in high uncertainty of the compressive strength values predicted with the use of the mathematical method. Interestingly, the artificial neural network exhibited a fairly high precision of compressive strength predictions despite the aforementioned problems. This may be indicative of an important capability of deep learning ANNs (DLN) to define relationships without the need to generalise their features. It is likely that the dropout technique (preventing overfitting) may have also played a significant role. From the point of view of their practical implementation, the choice of either of the described methods requires prior consideration and selection of the optimal modelling solution. What

needs to be considered is that although the network may provide a better fit, the use of DLN may incur a high computational cost. That is why, in some applications, a simple linear model is a sufficient tool that will provide an acceptable level of predictive capacity.

REFERENCES

Balin, A. (2004). *Materiałowo uwarunkowane procesy adaptacyjne i trwałość cementów stosowanych w chirurgii kostnej*. Wydawnictwo Politechniki Śląskiej.

Balin, A. (2016). *Cementy w chirurgii kostnej*. Wydawnictwo Politechniki Śląskiej.

Bialoblocka-Juszczyk, E., Baleani, M., Cristofolini, L., & Viceconti, M. (2008). Fracture Properties of an Acrylic Bone Cement. *Acta of Bioengineering and Biomechanics*, *10*(1), 21–26.

Charnley, J. (1960). Anchorage of the Femoral Head Prosthesis to the Shaft of the Femur. *The Journal of Bone and Joint Surgery. British Volume*, *42*(1), 28–30. https://doi.org/10.1302/0301-620X.42B1.28

Chen, X., Zhang, L., Liu, T., & Kamruzzaman, M.M. (2019). Research on Deep Learning in the Field of Mechanical Equipment Fault Diagnosis Image Quality. *Journal of Visual Communication and Image Representation*, *62*, 402–409. https://doi.org/10.1016/j.jvcir.2019.06.007

Dunne, N.J., & Orr, J.F. (2001). Influence of Mixing Techniques on the Physical Properties of Acrylic Bone Cement. *Biomaterials*, *22*(13), 1819-1826. https://doi.org/10.1016/S0142-9612(00)00363-X

Dunne, N.J., Orr, J.F., Mushipe, M.T., & Eveleigh, R.J. (2003). The Relationship between Porosity and Fatigue Characteristics of Bone Cements. *Biomaterials*, *24*(2), 239–245. https://doi.org/10.1016/S0142-9612(02)00296-X

Falkowicz, K., & Debski, H. (2019). The Work of a Compressed, Composite Plate in Asymmetrical Arrangement of Layers. *AIP Conference Proceedings*, *2078*, 020005. https://doi.org/10.1063/1.5092008

Falkowicz, K., & Debski, H. (2020). The Post-Critical Behaviour of Compressed Plate with Non-Standard Play Orientation. *Composite Structures*, *252*, 112701. https://doi.org/10.1016/j.compstruct.2020.112701

Falkowicz, K., Debski, H., & Wysmulski, P. (2020). Effect of Extension-Twisting and Extension-Bending Coupling on a Compressed Plate with a Cut-Out. *Composite Structures*, *238*, 111941. https://doi.org/10.1016/j.compstruct.2020.111941

de Haan, K., Rivenson, Y., Wu, Y., & Ozcan, A. (2020). Deep-Learning-Based Image Reconstruction and Enhancement in Optical Microscopy. *Proceedings of the IEEE*, *108*(1), 30–50. https://doi.org/10.1109/JPROC.2019.2949575

Hatt, M., Parmar, Ch., Qi, J., & El Naqa, I. (2019). Machine (Deep) Learning Methods for Image Processing and Radiomics. *IEEE Transactions on Radiation and Plasma Medical Sciences*, *3*(2), 104–108. https://doi.org/10.1109/TRPMS.2019.2899538

Hosseini, M.P., Hosseini, A., & Ahi, K. (2020). A Review on Machine Learning for EEG Signal Processing in Bioengineering. In *IEEE Reviews in Biomedical Engineering* (p. 1–1). IEEE. https://doi.org/10.1109/RBME.2020.2969915

Jiménez, G., & Racoceanu, D. (2019). Deep Learning for Semantic Segmentation vs. Classification in Computational Pathology: Application to Mitosis Analysis in Breast Cancer Grading. *Frontiers in Bioengineering and Biotechnology*, *7*, 145. https://doi.org/10.3389/fbioe.2019.00145

Karpiński, R., Szabelski, J., & Maksymiuk, J. (2018). Analysis of the Properties of Bone Cement with Respect to Its Manufacturing and Typical Service Lifetime Conditions. *MATEC Web of Conferences*, *244*, 01004. https://doi.org/10.1051/matecconf/201824401004

Karpiński, R., Szabelski, J., & Maksymiuk, J. (2019a). Effect of Physiological Fluids Contamination on Selected Mechanical Properties of Acrylate Bone Cement. *Materials*, *12*(23), 3963. https://doi.org/10.3390/ma12233963

Karpiński, R., Szabelski, J., & Maksymiuk, J. (2019b). Seasoning Polymethyl Methacrylate (PMMA) Bone Cements with Incorrect Mix Ratio. *Materials*, *12*(19), 3073. https://doi.org/10.3390/ma12193073

Lee, S.M., Seo, J.B., Yun, J., Cho, Y.-H., Vogel-Claussen, J., Schiebler, M.L., Gefter, W.B., van Beek, E.J.R., Goo, J.M., Lee, K.S., Hatabu, H., Gee, J., & Kim, N. (2019). Deep Learning Applications in Chest Radiography and Computed Tomography: Current State of the Art. *Journal of Thoracic Imaging*, *34*(2), 75–85. https://doi.org/10.1097/RTI.0000000000000387

Lelovics, H., & Liptáková, T. (2019). Comparison of Some Mechanical and Rheological Properties of Bone Cements'. In *5th Danubia – Adria Symposium on Advances in Experimental Mechanics* (pp. 157–158). Czech Republic.

Lelovics, H., & Liptakova, T. (2010). Time and Mixing Techniquedependent Changes in Bone Cement SmartSet (R) HV. *Acta of Bioengineering and Biomechanics*, *12*(4), 63–67.

Liptáková, T., Lelovics, H., & Necas, L. (2009). Variations of Temperature of Acrylic Bone Cements Prepared by Hand and Vacuum Mixing during Their Polymerization. *Acta of Bioengineering and Biomechanics*, *11*(3), 47–51.

Matuszewski, Ł., Olchowik, G., Mazurkiewicz, T., Kowalczyk, B., Zdrojewska, A., Matuszewska, A., Ciszewski, A., Gospodarek, M., & Morawik, I. (2014). Biomechanical Parameters of the BP-Enriched Bone Cement. *European Journal of Orthopaedic Surgery & Traumatology*, *24*(4), 435–441. https://doi.org/10.1007/s00590-013-1230-1

Pałubicka, A., Czubek, J., & Wekwejt, M. (2019). Effect of Aeration of Antibiotic-Loaded Bone Cement on Its Properties and Bactericidal Effectiveness. *Minerva Ortopedica e Traumatologica*, *70*(2), 78–85. https://doi.org/10.23736/S0394-3410.19.03913-4

Tan, J.H., Koh, B.Th., Ramruttun, A.K., & Wang, W. (2016). Compression and Flexural Strength of Bone Cement Mixed with Blood. *Journal of Orthopaedic Surgery (Hong Kong)*, *24*(2), 240–244. https://doi.org/10.1177/1602400223

Tu, Y.-H., Du, J., & Lee, Ch.-H. (2019). Speech Enhancement Based on Teacher–Student Deep Learning Using Improved Speech Presence Probability for Noise-Robust Speech Recognition. *IEEE/ACM Transactions on Audio, Speech, and Language Processing*, *27*(12), 2080-2091. https://doi.org/10.1109/TASLP.2019.2940662

Wekwejt, M., Michalska-Sionkowska, M., Bartmański, M., Nadolska, M., Łukowicz, K., Pałubicka, A., Osyczka, A.M., & Zieliński, A. (2020). Influence of Several Biodegradable Components Added to Pure and Nanosilver-Doped PMMA Bone Cements on Its Biological and Mechanical Properties. *Materials Science and Engineering: C*, *117*, 111286. https://doi.org/10.1016/j.msec.2020.111286

Wekwejt, M., Moritz, N., Świeczko-Żurek, B., & Pałubicka, A. (2018). Biomechanical Testing of Bioactive Bone Cements – a Comparison of the Impact of Modifiers: Antibiotics and Nanometals. *Polymer Testing*, *70*, 234–243. https://doi.org/10.1016/j.polymertesting.2018.07.014

Wekwejt, M., Michno, A., Truchan, K., Pałubicka, A., Świeczko-Żurek, B., Osyczka, A.M., & Zieliński, A. (2019). Antibacterial Activity and Cytocompatibility of Bone Cement Enriched with Antibiotic, Nanosilver, and Nanocopper for Bone Regeneration. *Nanomaterials*, *9*(8), 1114. doi: https://doi.org/10.3390/nano9081114

Younesi, M., Bahrololoom, M.E., & Ahmadzadeh, M. (2010). Prediction of Wear Behaviors of Nickel Free Stainless Steel–Hydroxyapatite Bio-Composites Using Artificial Neural Network. *Computational Materials Science*, *47*(3), 645–54. https://doi.org/10.1016/j.commatsci.2009.09.019

Zhang, W., Cui, X., Finkler, U., Kingsbury, B., Saon, G., Kung, D., & Picheny, M. (2019). Distributed Deep Learning Strategies for Automatic Speech Recognition. In *ICASSP 2019 - 2019 IEEE International Conference on Acoustics, Speech and Signal Processing (ICASSP)* (pp. 5706–5710). Brighton, United Kingdom: IEEE.